ELM Energy/Particle Plasma Losses and Fluxes on PFCs

Alberto Loarte

European Fusion Development Agreement

Close Support Unit - Garching

Contributions from : G. Saibene, R. Sartori, T. Eich, M. Kempenaars, M. Becoulet, G. Federici, P. Snyder, P. Ghendrih, G. Huysmans, C. Pérez, R. Koslowki, I. Nunes, B. Gonçalves, C. Silva, W. Fundamenski, T. Petrie, A. Leonard, M. Fenstermacher, J. Boedo, J. Stober, N. Oyama, Y. Kamada, N. Asakura, G. Counsell, A. Kirk, S. Saarelma, J Lönnroth, V. Parail, …..

Outline of the Talk

1. Introduction
2. Physics of ELM instability and experimental evidence
3. Main plasma ELM energy/particle losses
4. ELM energy/particle fluxes to PFCs
5. Regimes with high P_{ped} + small/no ELMs
6. Conclusions

Introduction (I)

H ~ 1 at n ~ n_{GW} in Type I ELMy H-modes requires high W_{ped}

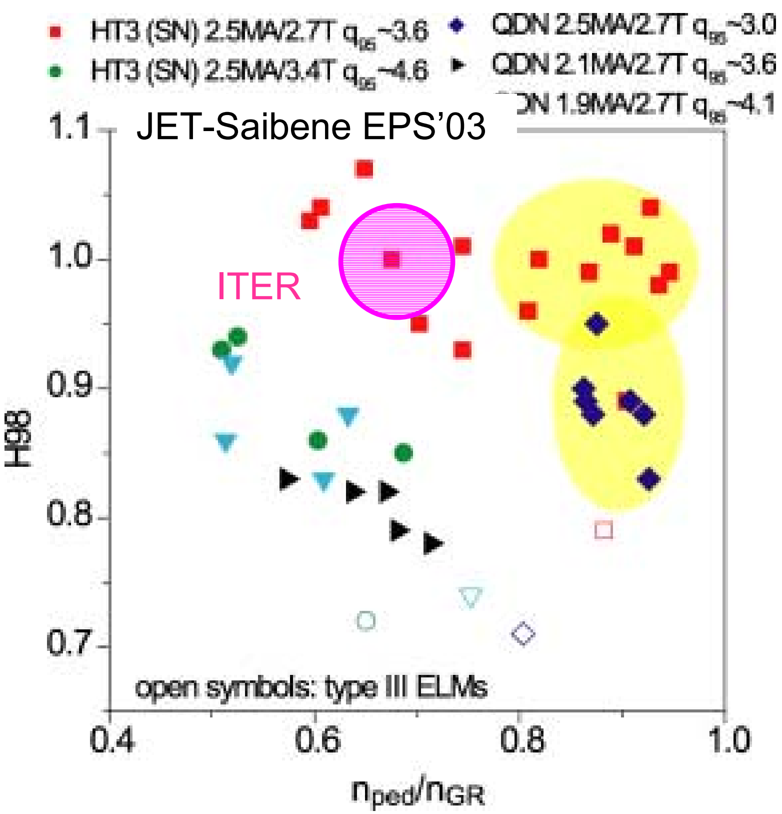

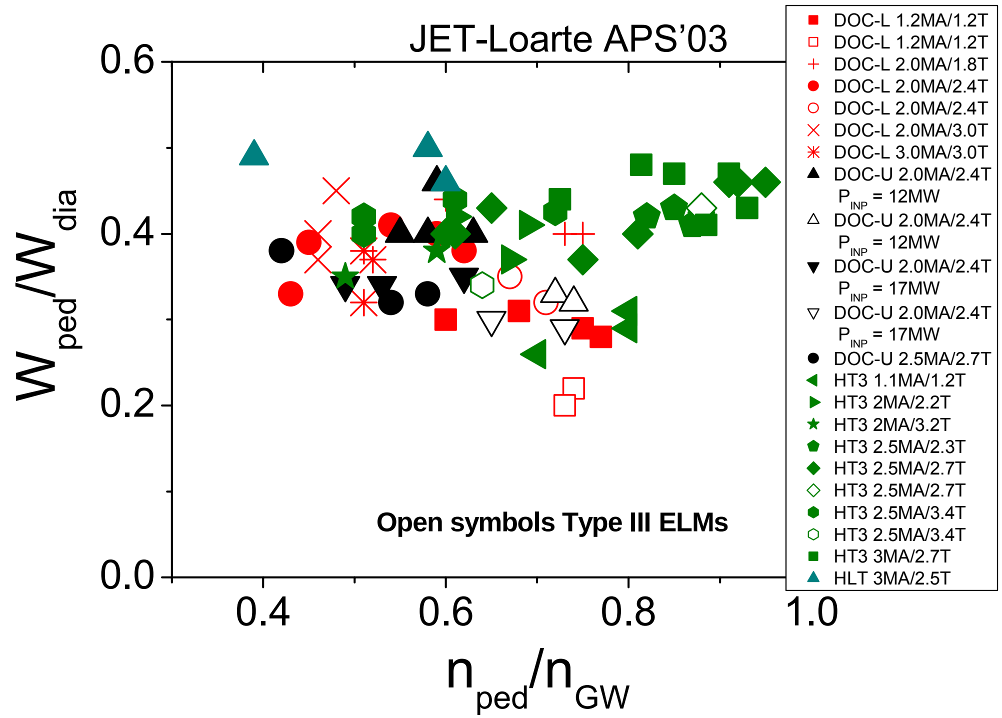

W_{ped}/W_{dia} (JET-Type I ELMs) ~ 0. 4 ± 0.1

general result for Type I ELMy H-modes (ASDEX-U, DIII-D, JET, …)

- weak W_{ped}/W_{dia} dependence on :
  q_{95} ($2.8 < q_{95} < 5.2$), P_{inp} , δ ($\delta > 0.27$)
- lower W_{ped}/W_{dia} @ low I_p & Type III ELMs

Introduction (II)

Pedestal plasma experiences quasi-periodic relaxations → ELMs

ΔW_{ELM} small fraction of W_{plasma} (<10 %) to divertor/wall in ~ 200 μs → Large Energy Flux

JET – Type I ELM - Saibene

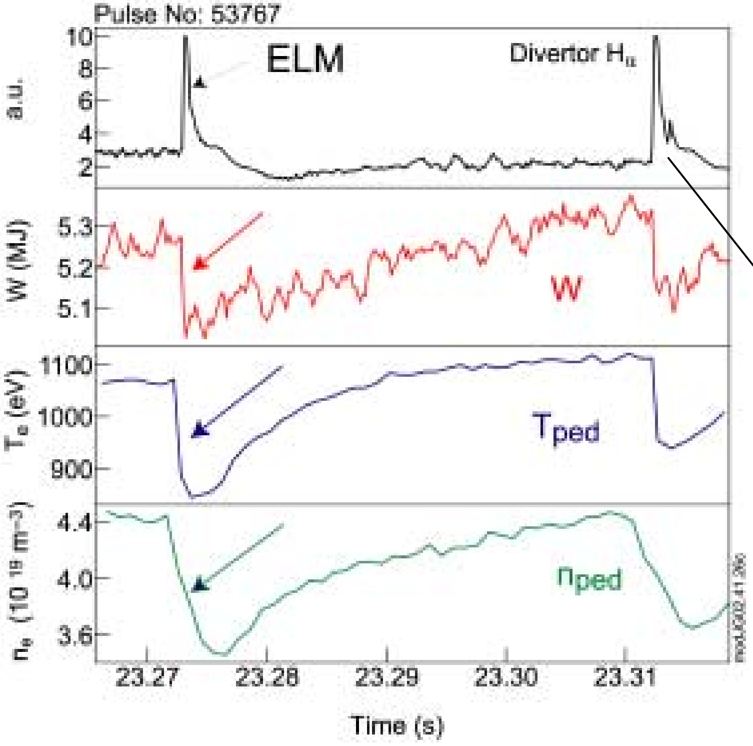

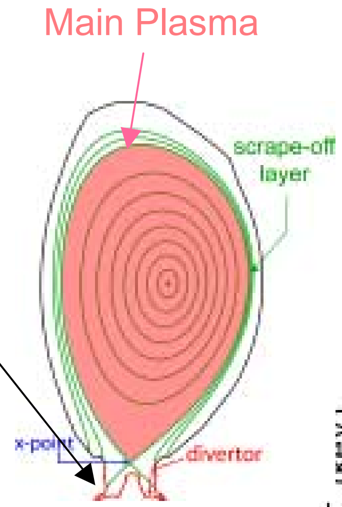

Only Pedestal Region of Plasma Affected by ELMs

JET – Type I ELM - Saibene

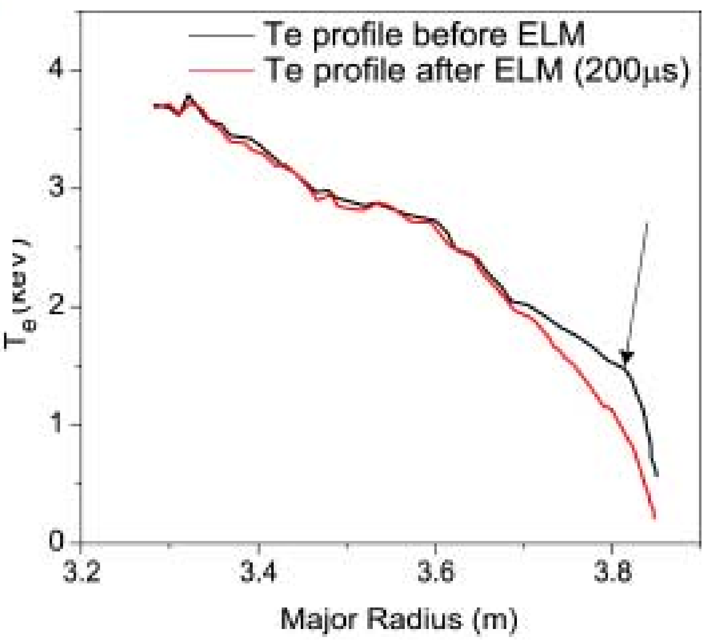

Introduction (III)

ITER rough estimates

W_{dia} = 350 MJ → W_{ped} = 90 – 150 MJ, ΔW_{ELM} = 10 - 30 MJ

(A_{div} = 3 m^2, τ_{ELM}= 300 μs)

$T_{max}^{ELM} > T_{ev,melt}^{C,W}$ → ELM Erosion

ITER-Federici PPCF'03

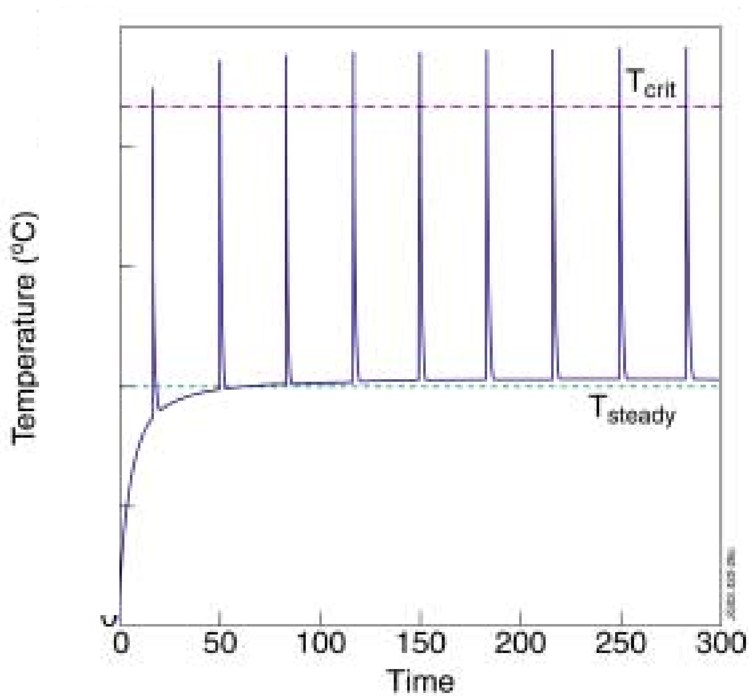

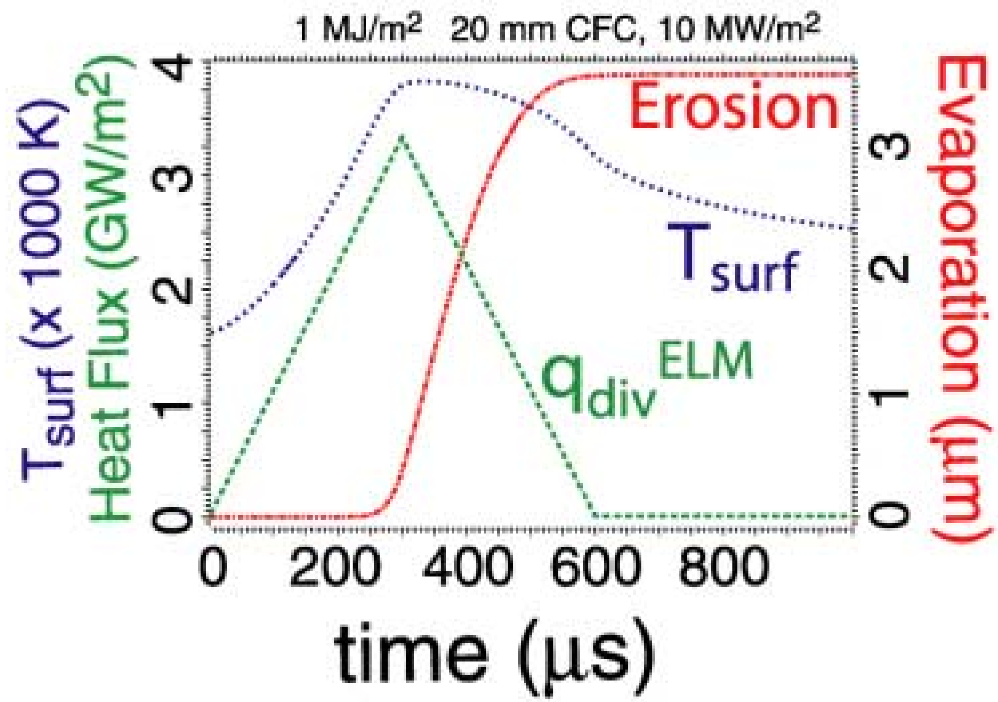

$\Phi_{ELM}^{C,W}$(MJm^{-2}s$^{-1/2}$) ≤ 50 for small ELM erosion ~ 3.5 μm/ELM + C-target = 2 cm → 6000 ELMs !!

Physics of ELM instability (I)

Peeling-Ballooning model of the ELMs (Connor PPCF'98)

- Ballooning modes driven by grad P_{ped}
- Kink (peeling) modes driven by edge current (large $J_{bootstrap}$)
- Coupled peeling-ballooning modes

JET-Huysmans '01

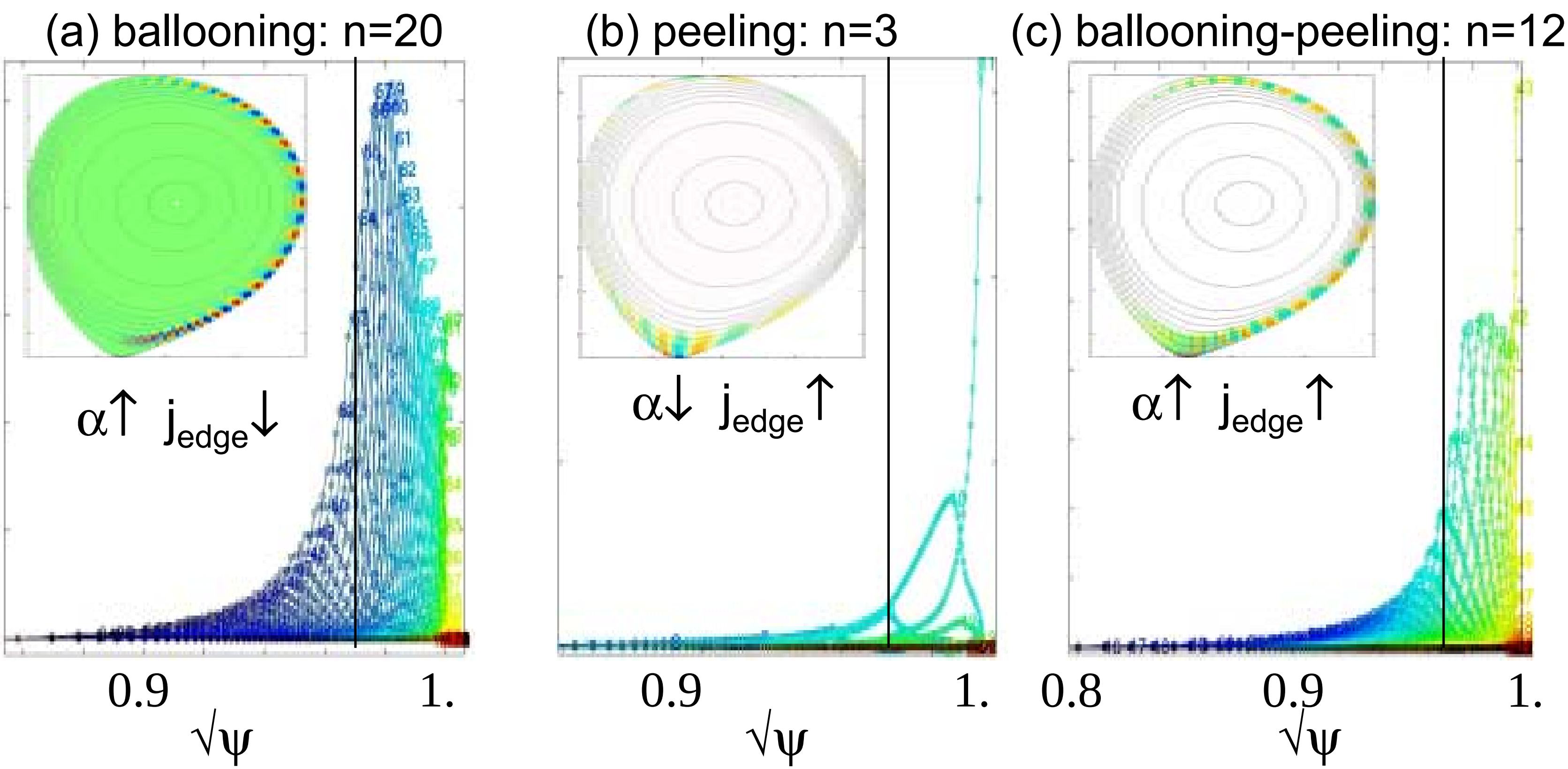

Physics of ELM instability (II)

Peeling-Ballooning calculations-experiment comparison

DIII-D-Snyder NF'04

- P_{ped} matched with model
- Change of mode instability analysed
- Role of $j_{bootstrap}$ evaluated (+ measured)

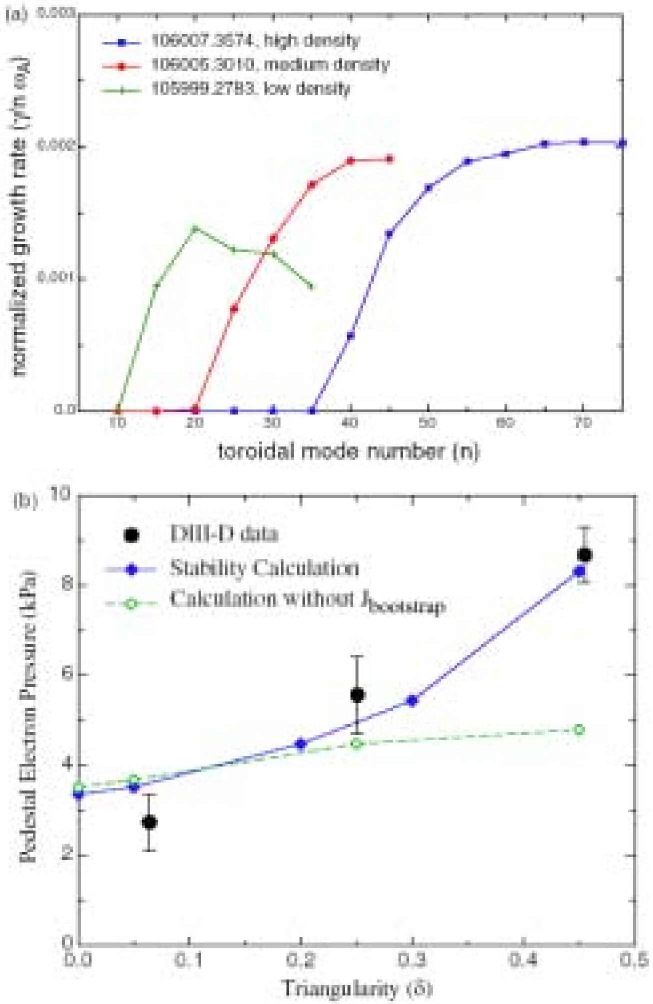

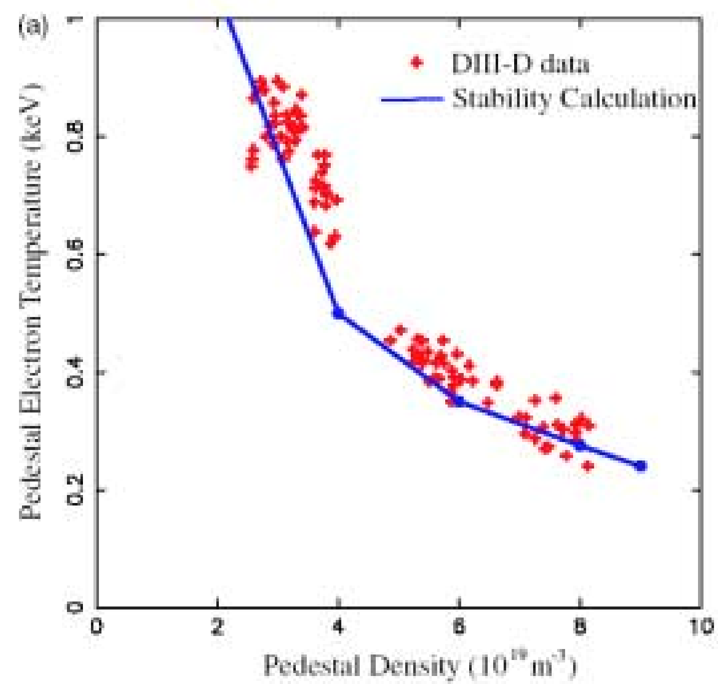

Physics of ELM instability (III)

Role of edge current on ELM triggering demonstrated

JET-Becoulet EPS'03

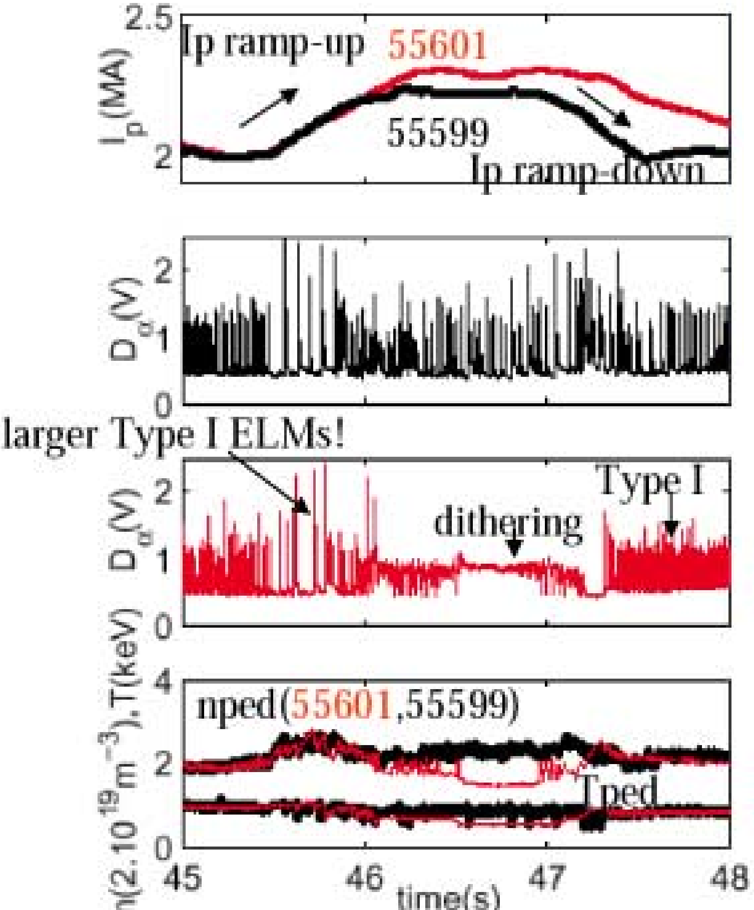

JET-JETTO-Lönnroth-Parail '04

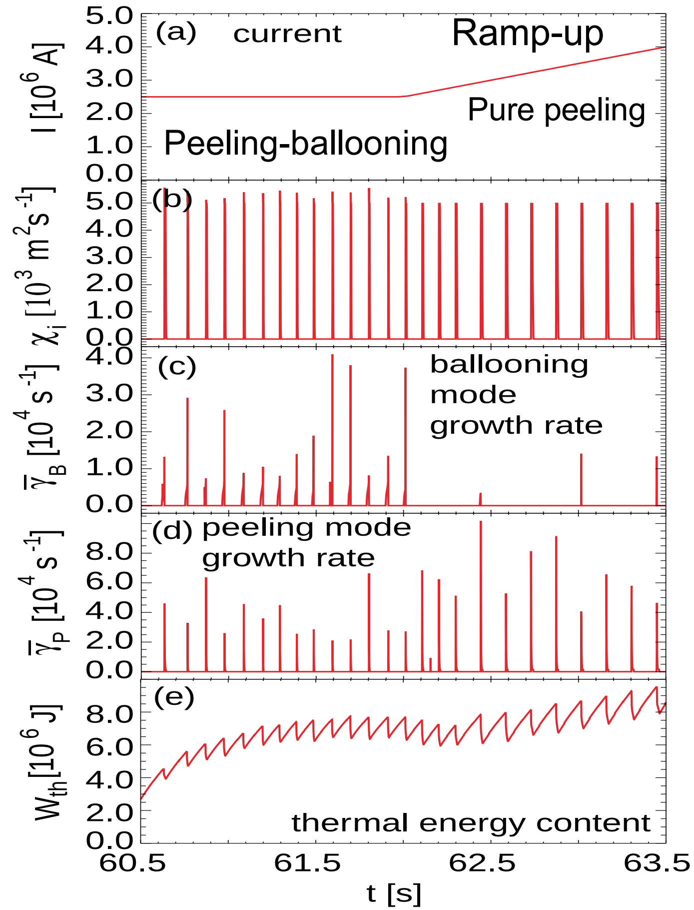

seen in COMPASS-D, MAST, JET

Physics of ELM instability (IV)

Scaling of pedestal pressure and peeling-ballooning model

DIII-D-Snyder NF'04

$P_{ped}^{Type\ I} \sim I_p$

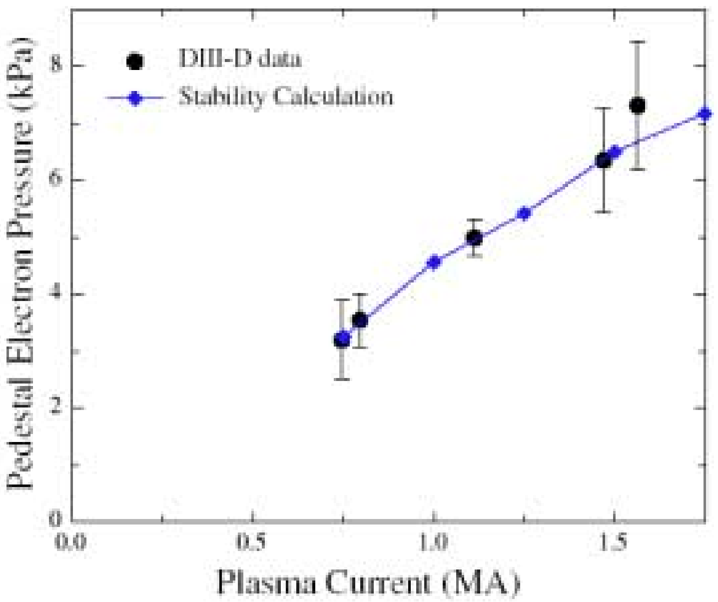

JET-Loarte APS'03

$P_{ped}^{Type\ I} \sim I_p^2$(ballooning-like)

P_{ped} depends weakly on : q_{95} and $n_{e,ped}/n_{GW}$

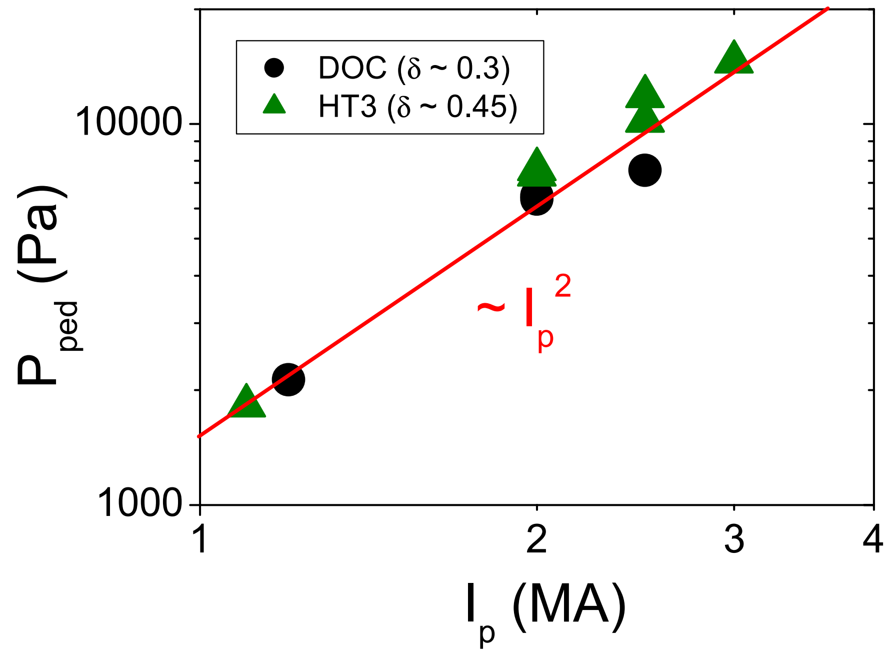

comparison of model with various experiments required to identify physics processes

Physics of ELM instability (VI)

precursors seen before ELMs in many experiments with n = 1-10

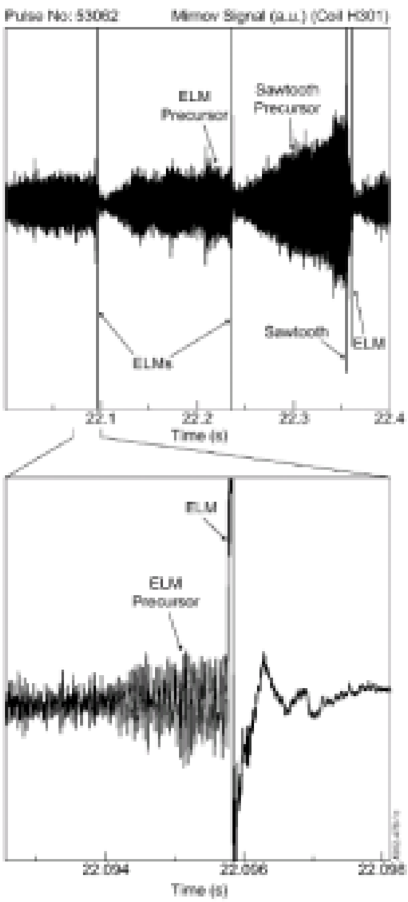

JET-Pérez NF'04

- ➢ precursors' n as expected from P-B
- ➢ precursors do not grow as linearly unstable modes $e^{t/\tau}$
- ➢ role of precursor on ELM trigger is unclear

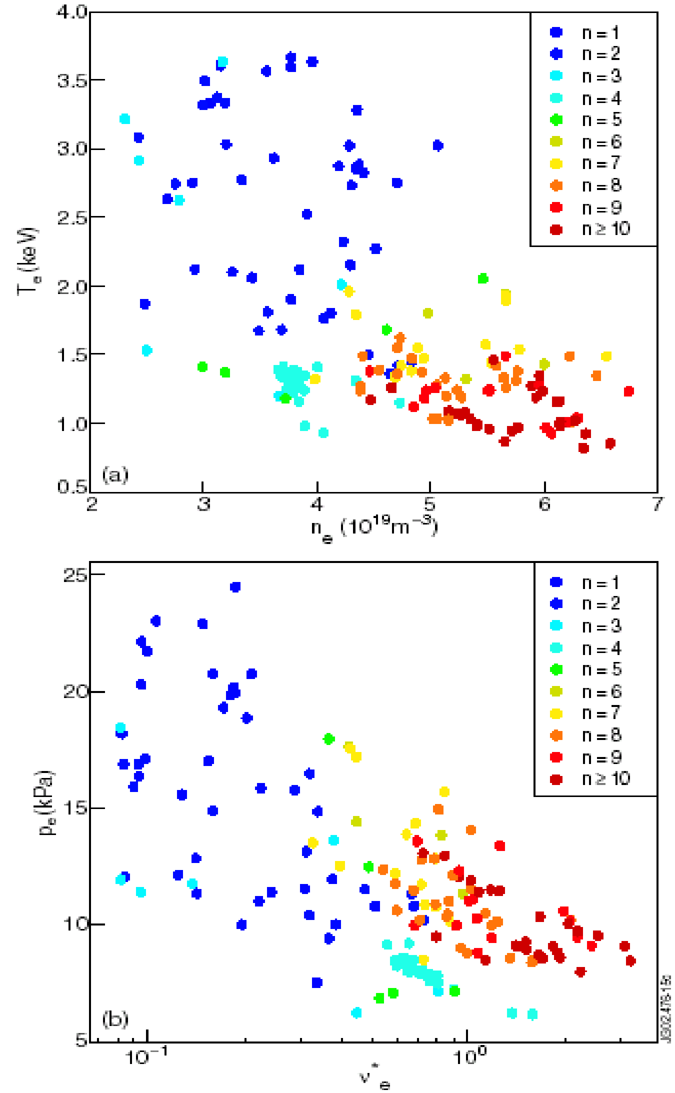

Physics of ELM instability (VII)

Filaments are seen to appear in the plasma boundary prior to ELMs (n = 10, q =4)

MAST-Akers PPCF'03

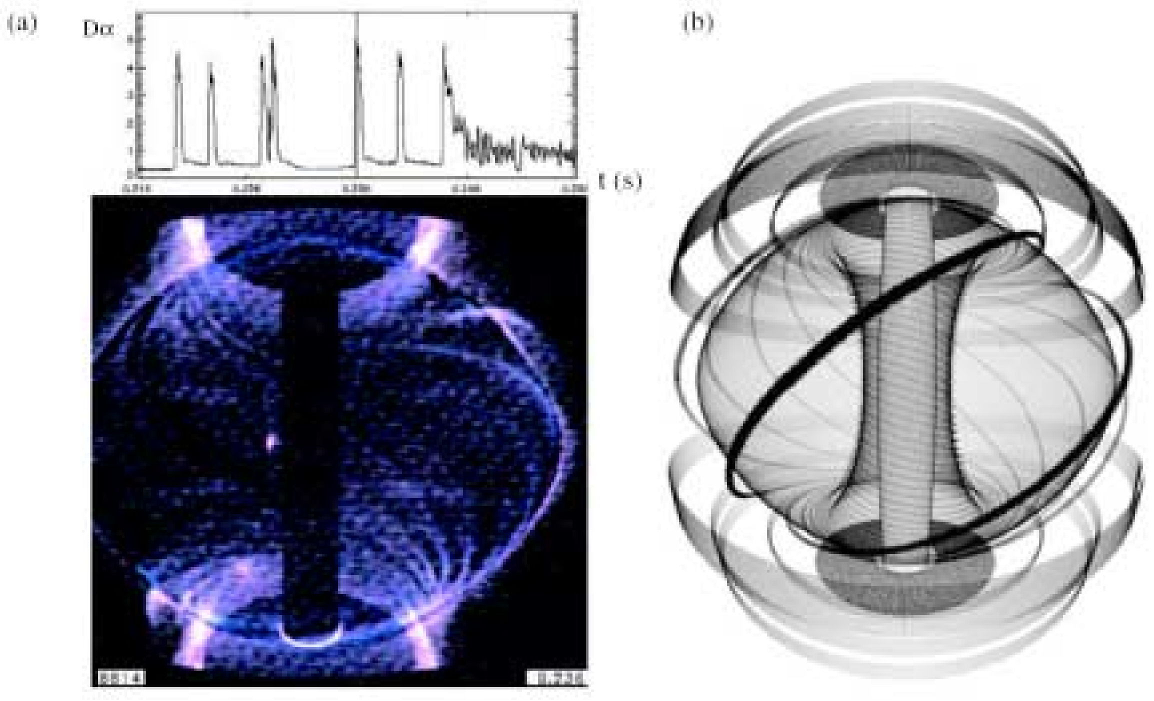

how much energy flows in the filaments?

Physics of ELM instability (VIII)

Analyses of energy fluxes far from strike point in ASDEX Upgrade are consistent with n = 8 – 24 modes

ASDEX Upgrade-Eich PRL'04

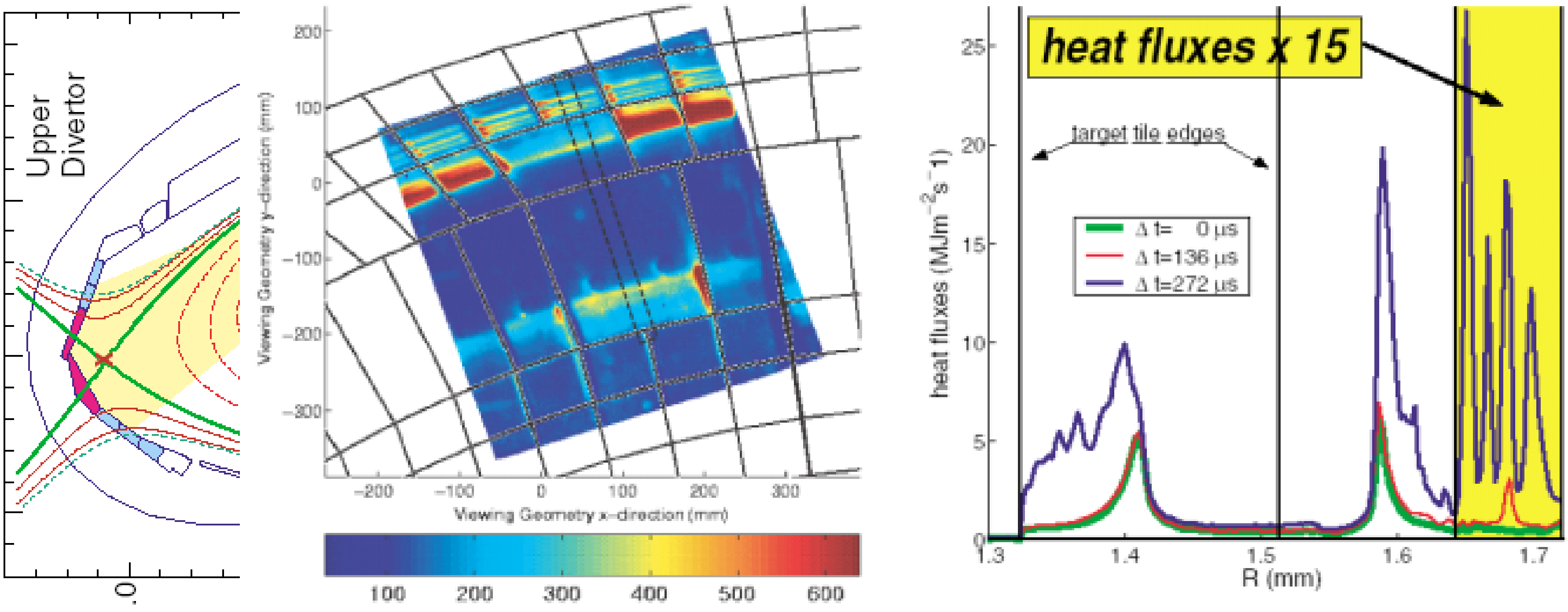

energy content in stripes less than 3% of ΔW_{ELM}^{div} !!

Physics of ELM instability (X)

ELM spatial and temporal ballooning character

DIII-D-Petrie NF'03

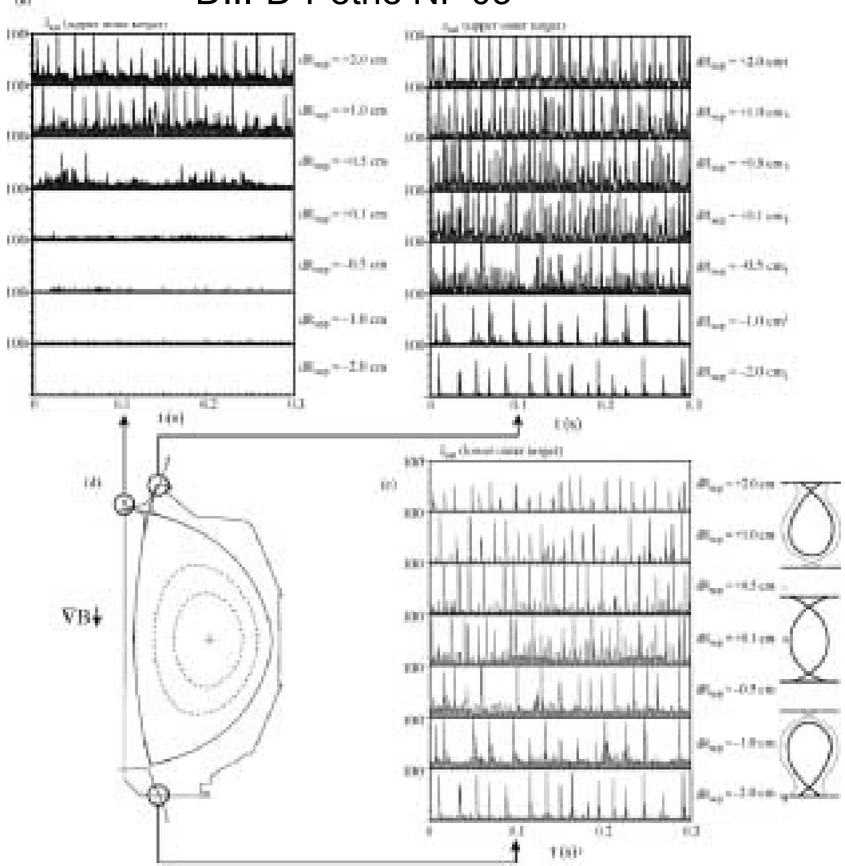

ASDEX Upgrade-Nunes EPS'03 subm. NF'04

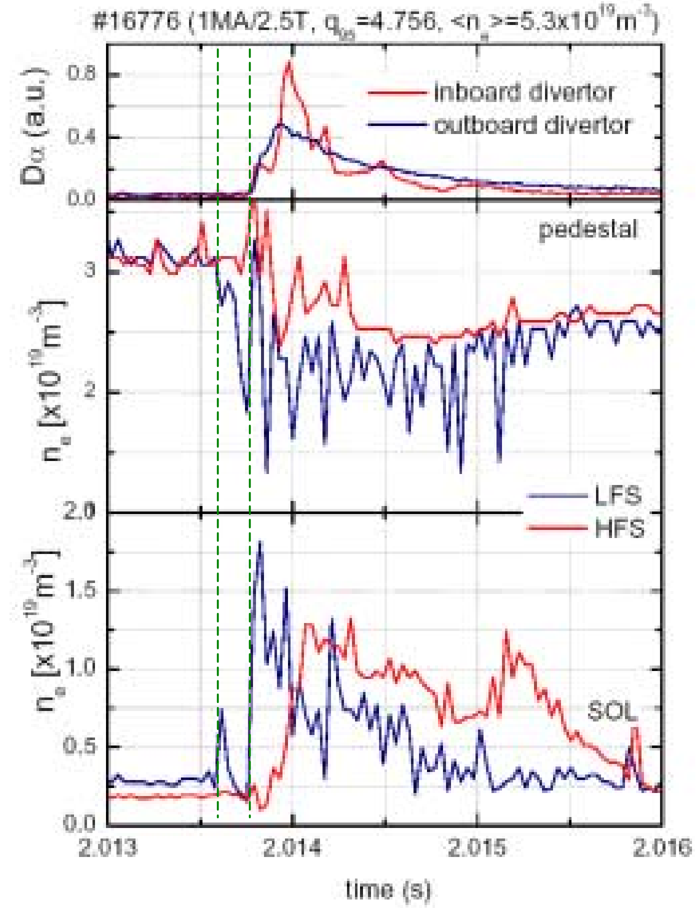

similar results on divertor fluxes from ASDEX Upgrade, MAST, JET

Physics of ELM instability (XI)

Timescale of ELM pedestal collapse/MHD phase timescale :
collapse of pedestal - hot e⁻ impact on divertor - MHD

JET-Loarte APS'03

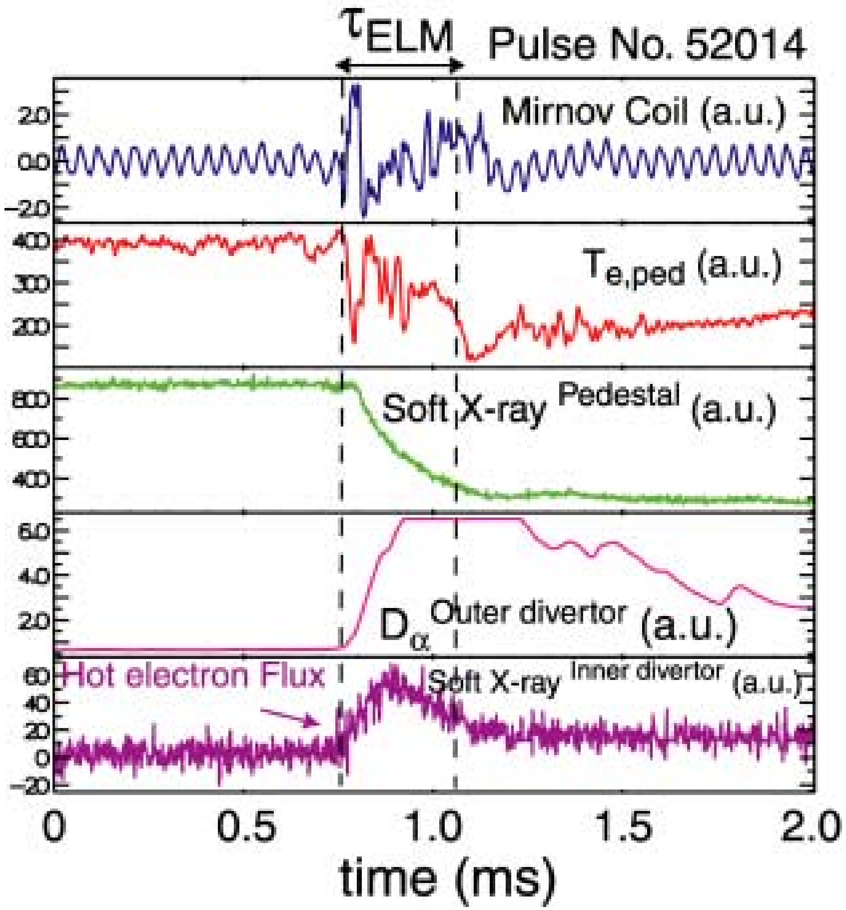

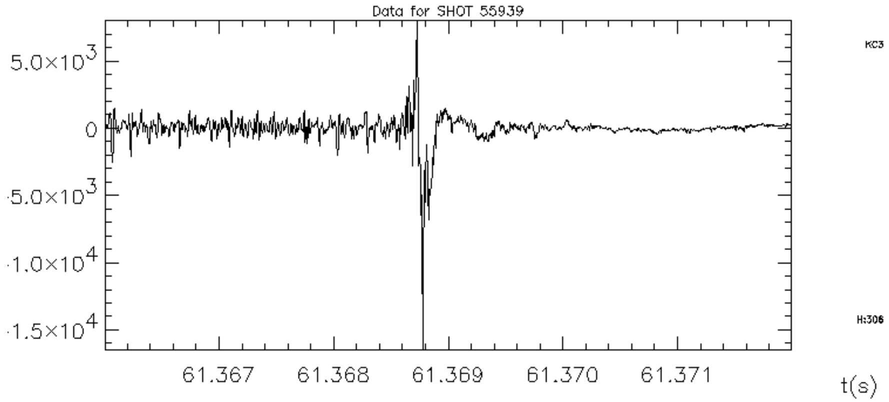

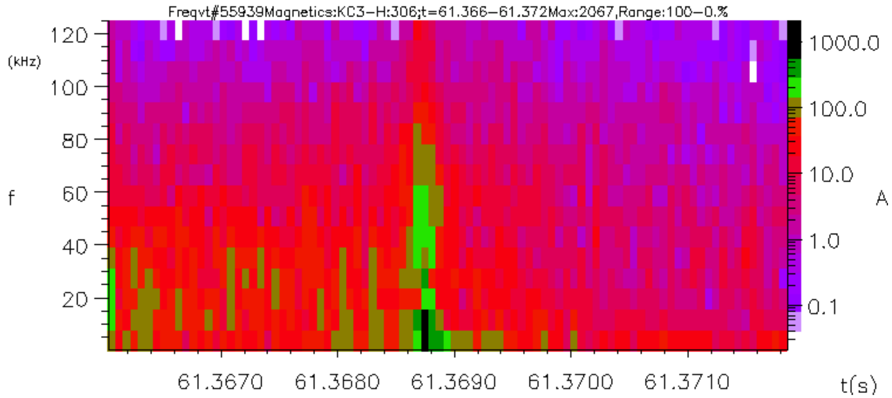

Physics of ELM instability (XII)

Timescale of ELM pedestal collapse ~ 200 - 300 μs for JET Type I ELMs

JET-Loarte APS'03

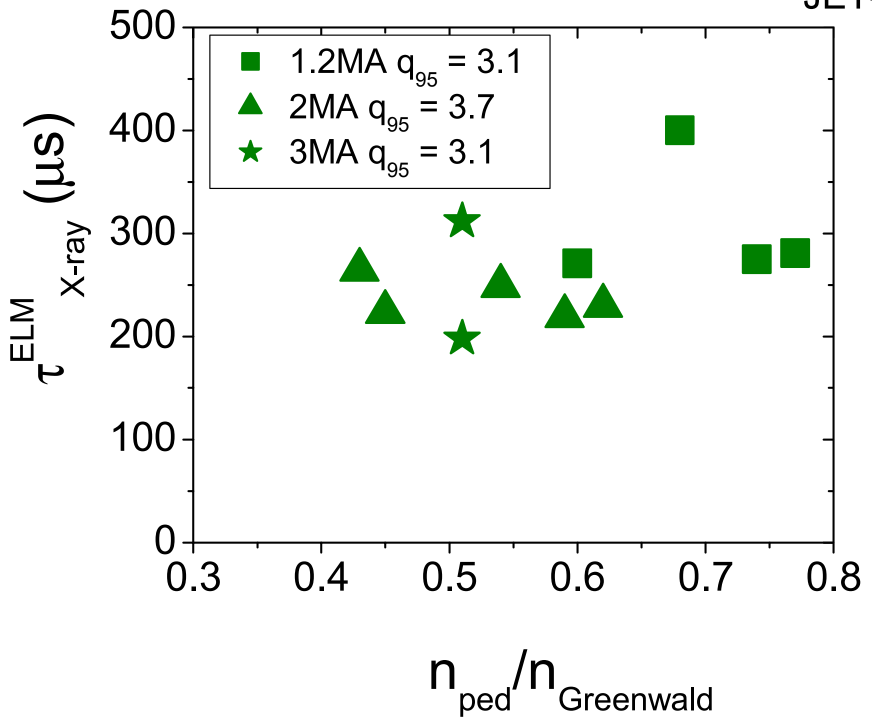

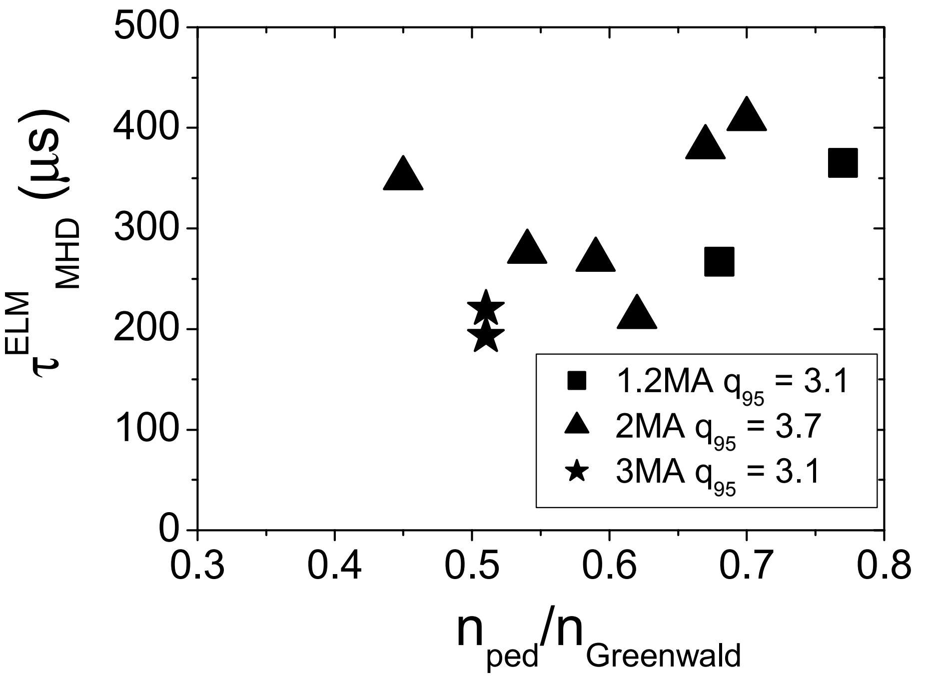

Similar timescales in JT-60U, DIII-D, ASDEX Upgrade MAST

Physics of ELM instability (XIV)

Physical mechanisms of ELM growth

- Non-linear explosive ballooning (Cowley PPCF'03)

$$\tau_{ELM} \sim (\tau_E\ \tau_A{}^2)^{1/3}$$

$$\tau_A \sim qRn^{1/2}/B,\ \tau_E\ ?$$

JET : τ_{ELM} (τ_E) ~ 50-100 μs but $\tau_{ELM} \sim R^{\alpha}$ with $\alpha \sim 5/3$

$\tau_{ELM} \sim (I_p{}^{-2/3}\ n^{1/3})\ x\ (P^{-2/9}\ n^{1/6}\ I_p{}^{1/3}) \sim I_p{}^{-1/18}$ (if $n \sim I_p$, $P \sim I_p$) !!!

- Edge Reconnection (Igitkahnov EPS'01)

$$\tau_{ELM} \sim \tau_A(\tau_\eta/\tau_A)^{\beta}\ \ (\beta = [1/3,1])$$

τ_{ELM} (β=1/2) ~ $(R^{1/2}\ I_p{}^{-1/2}\ n^{1/4})\ x\ (a^{1/2}\ \ T^{3/4}) \sim R\ I_p{}^{1/2}$ (if $n \sim I_p$, $T \sim I_p$)

More experimental and theoretical work is needed!!!

Physics of ELM instability (XV)

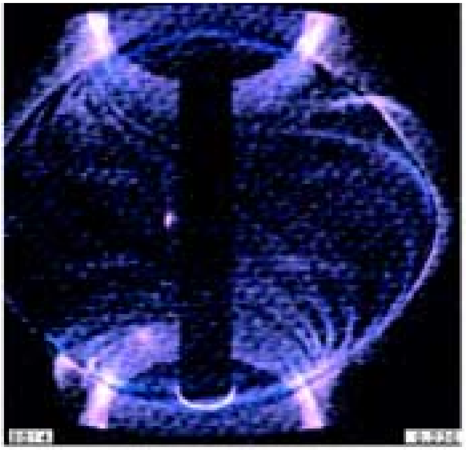

how filaments evolve
to an edge plasma collapse ?

MAST-Kirk PPCF'04

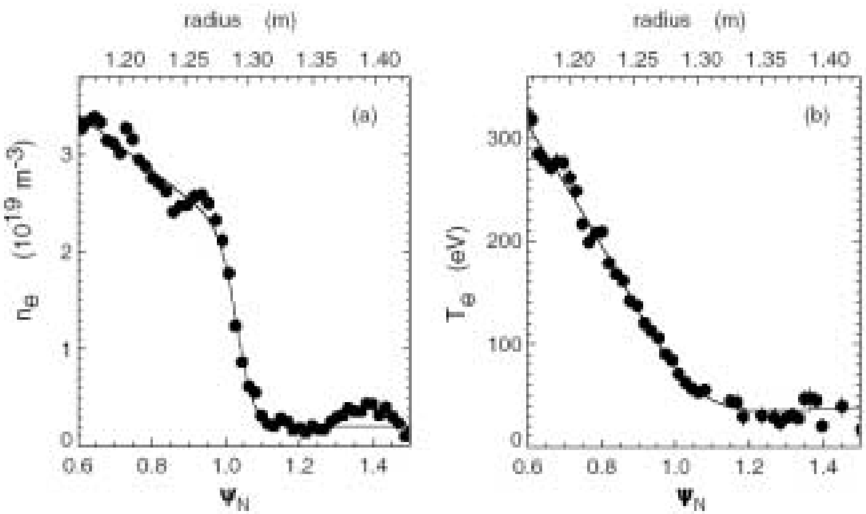

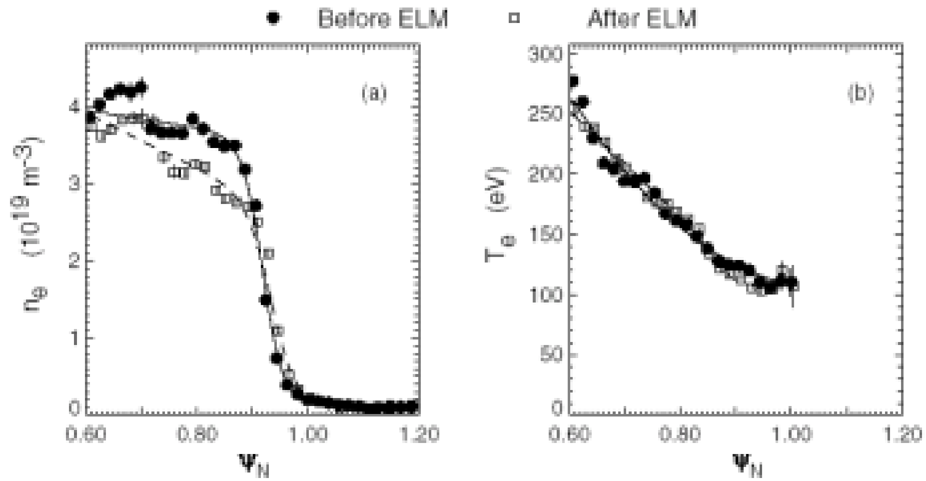

Main plasma ELM energy/particle losses (I)

ELM energy/particle losses depend on pedestal parameters

ITPA-Loarte PPCF'03

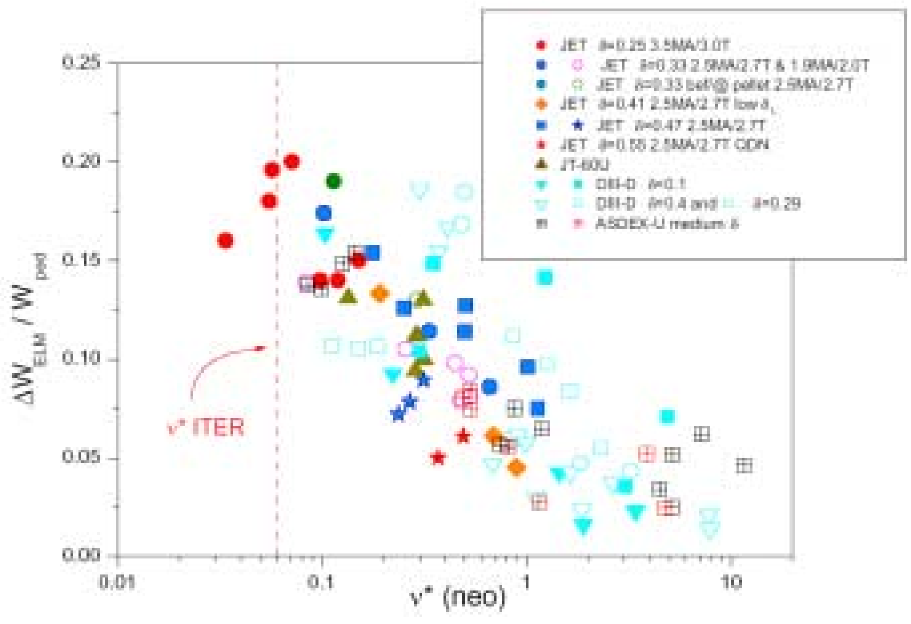

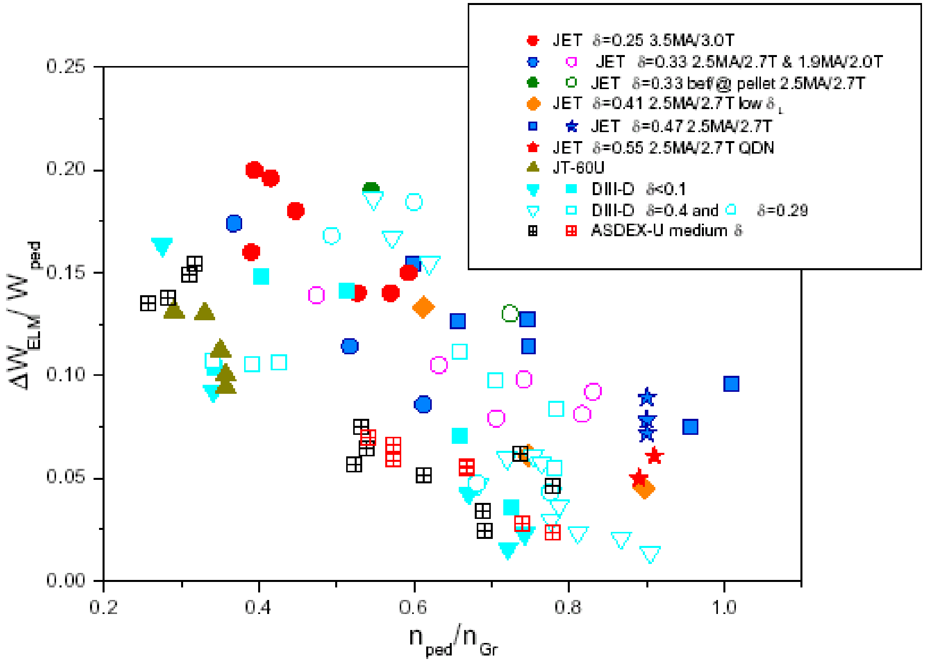

Small $\Delta W_{ELM}/W_{ped}$ seen at high $n_{e,ped}/n_{GW}$ and/or high ν^*_{ped}(neo)

Main plasma ELM energy/particle losses (II)

Simple picture : small ΔW_{ELM} ←→ small volume of plasma affected by ELM

Peeling/Ballooning Picture : increasing n_{ped} - ν^*_{ped}

↓

n of unstable modes increase ←→ poloidal width of modes decrease

↓

ELM affected volume (V_{ELM}) → ΔW_{ELM} decreases

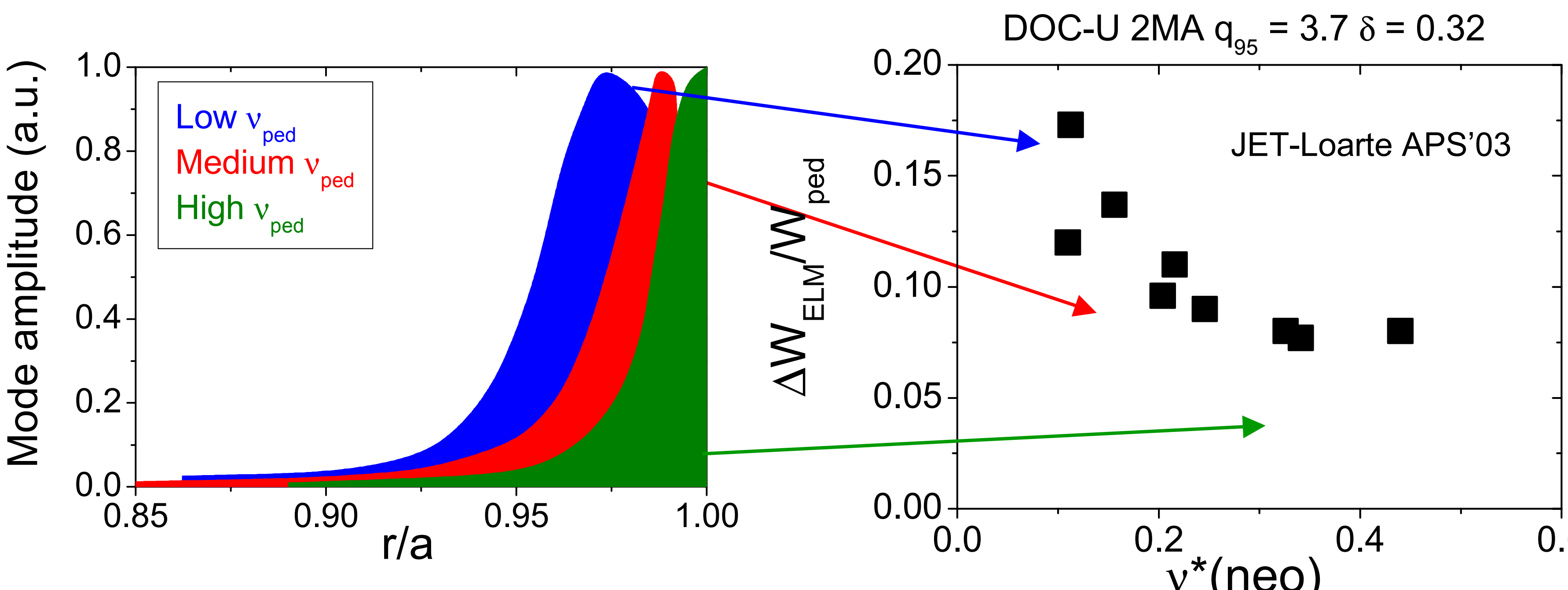

EFDA EUROPEAN FUSION DEVELOPMENT AGREEMENT

Main plasma ELM energy/particle losses (III)

ΔW_{ELM} ⇎ ELM affected Volume

V_{ELM} from fast ECE

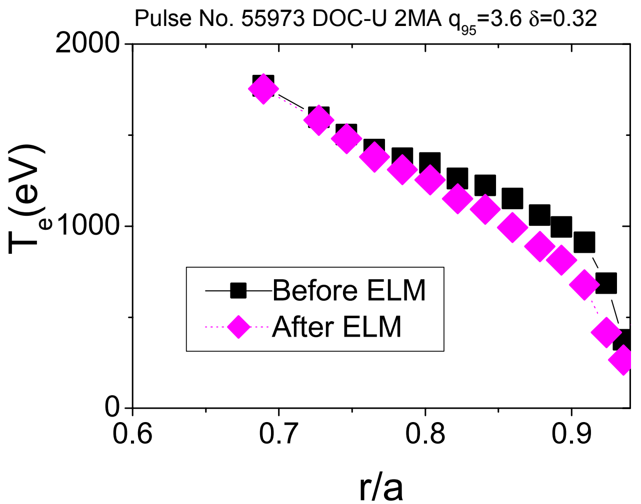

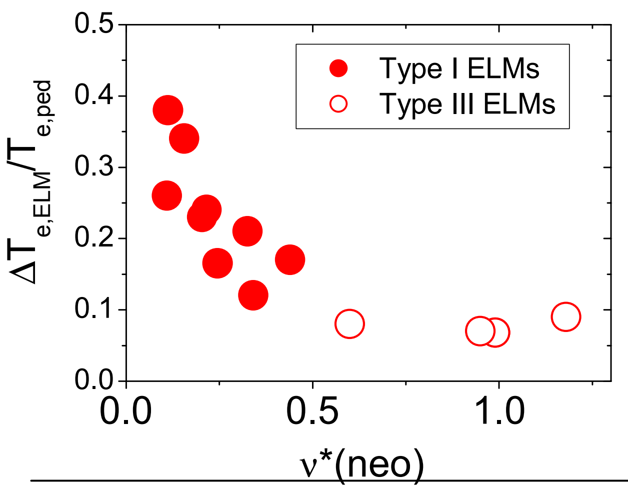

ΔW_{ELM} down by ~ 3 at V_{ELM} ~ constant !!

JET-Loarte APS'03

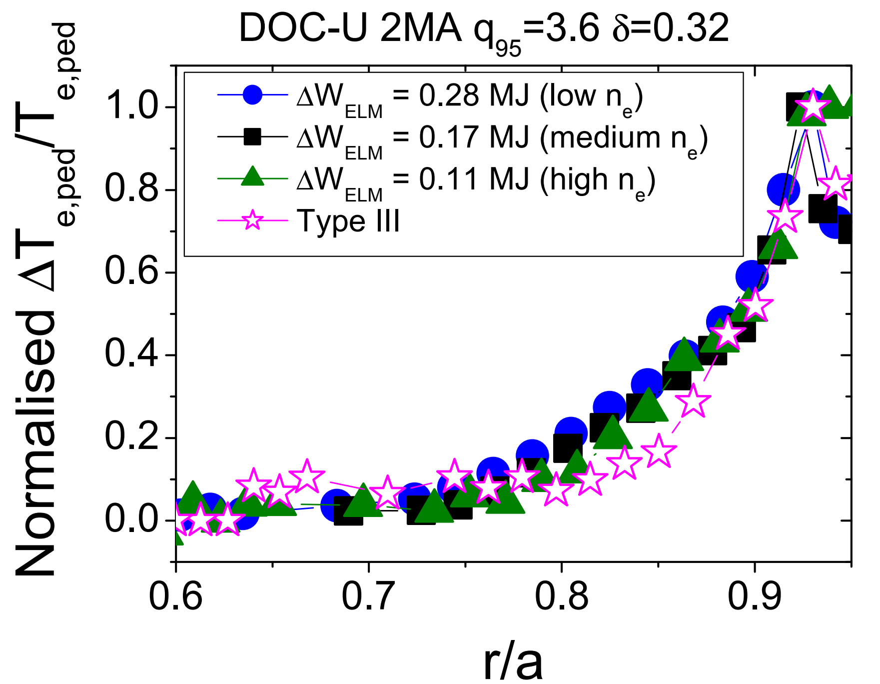

decrease of ΔT_{ELM} <u>not</u> of V_{ELM} → ΔW_{ELM}

similar results in DIII-D (Leonard)

Main plasma ELM energy/particle losses (IV)

Variation of ΔW_{ELM} ←→ ELM energy transport (DIII-D, JET)

DIII-D-Leonard PPCF'02

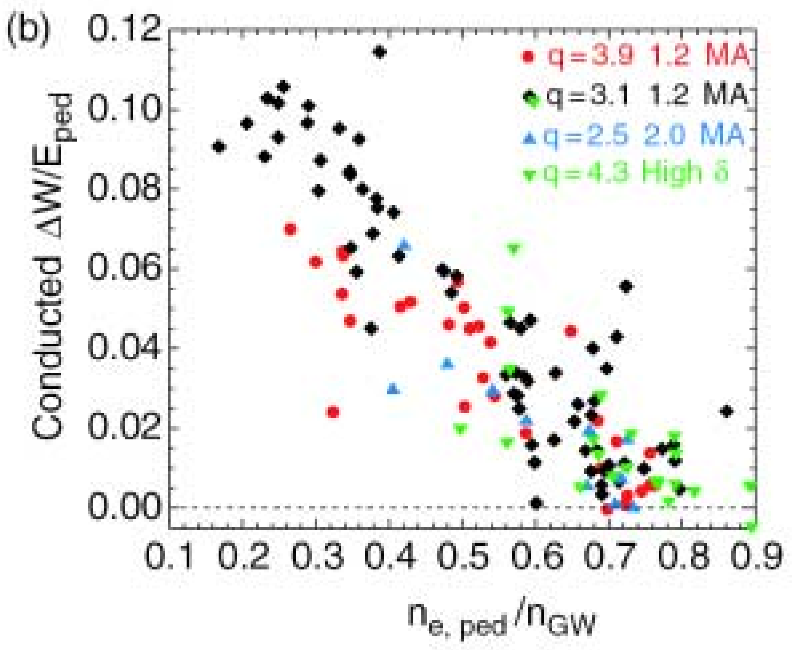

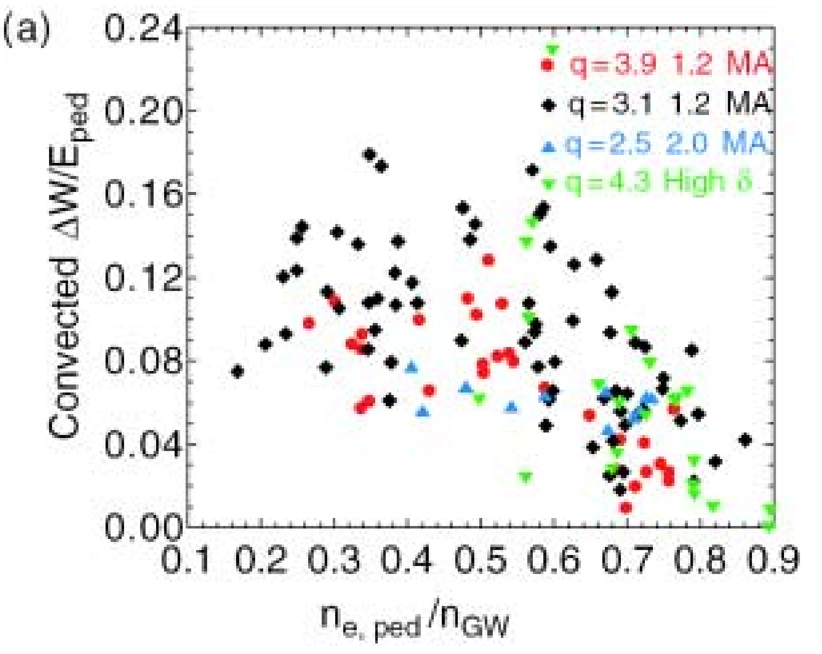

$$\Delta W_{ELM} = \Delta W_{ELM}^{cond}\,(\Delta T_{ELM}) + \Delta W_{ELM}^{conv}\,(\Delta n_{ELM})$$

ΔW_{ELM}^{cond} decreases with $n_{e,ped}$ (or $\nu_{e,ped}$(neo))

Smaller ΔW_{ELM} ←→ convective ELMs

Main plasma ELM energy/particle losses (V)

high q_{95} + δ → small ΔW_{ELM} at low ν^*_{ped} - n_{ped}

JET-Loarte APS'03

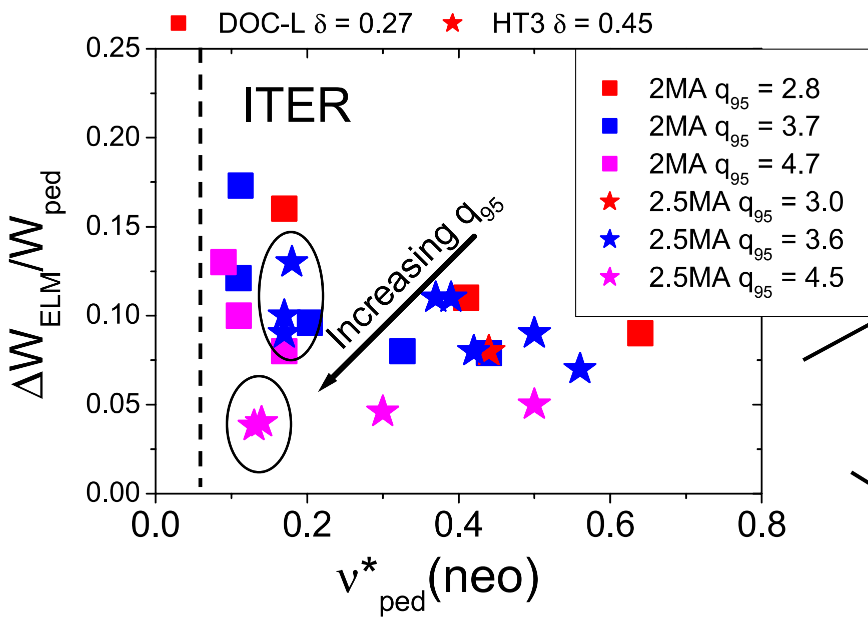

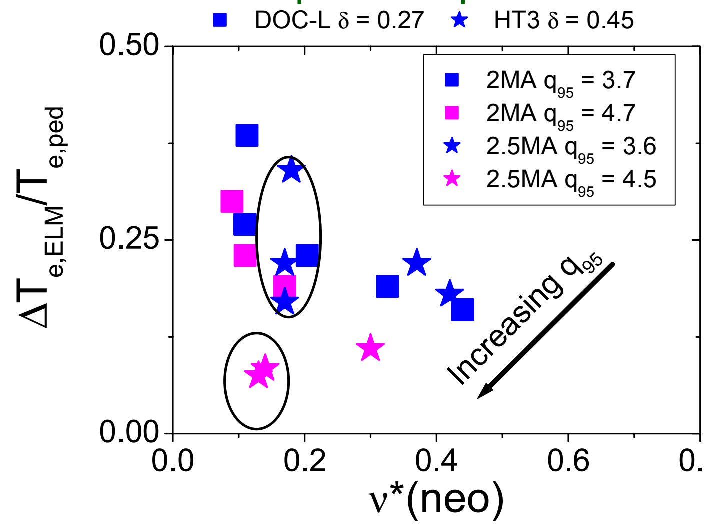

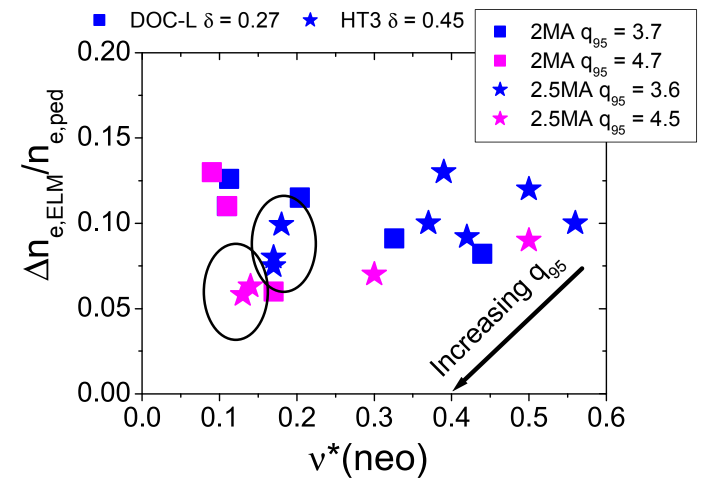

ΔW_{ELM} ↘ ←→ ΔT_{ELM} ↘

MHD pedestal stability affects ΔW_{ELM} through ELM energy conduction

Main plasma ELM energy/particle losses (VI)

effect of high q_{95} on P-B stability largest at high δ

ASDEX Upgrade-Saarelma NF'03

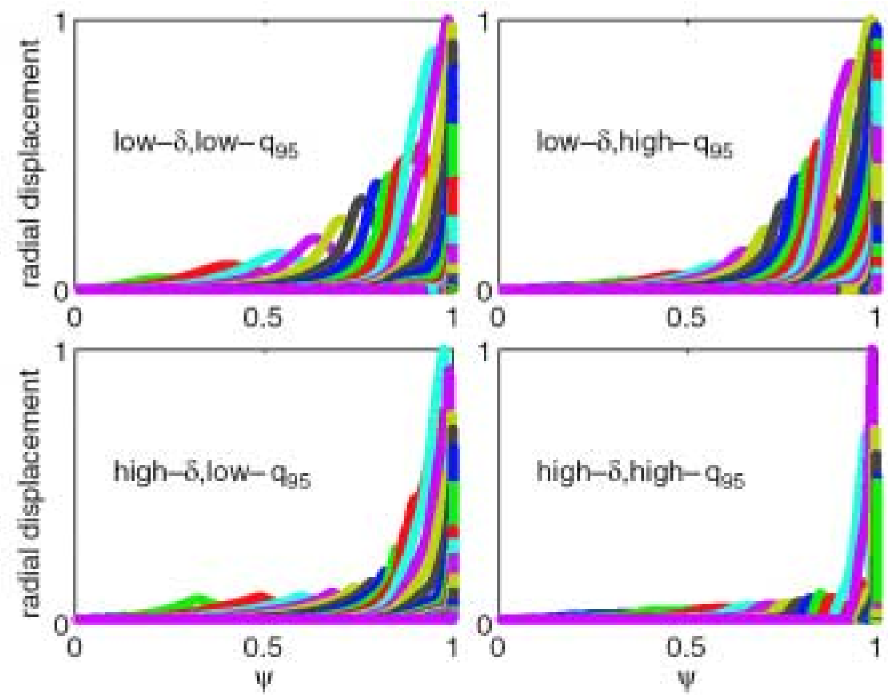

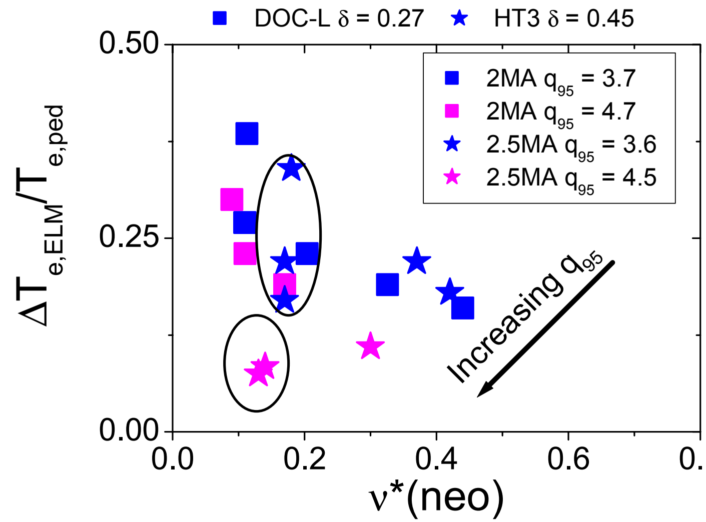

V_{ELM} ~ constant with q_{95}!!

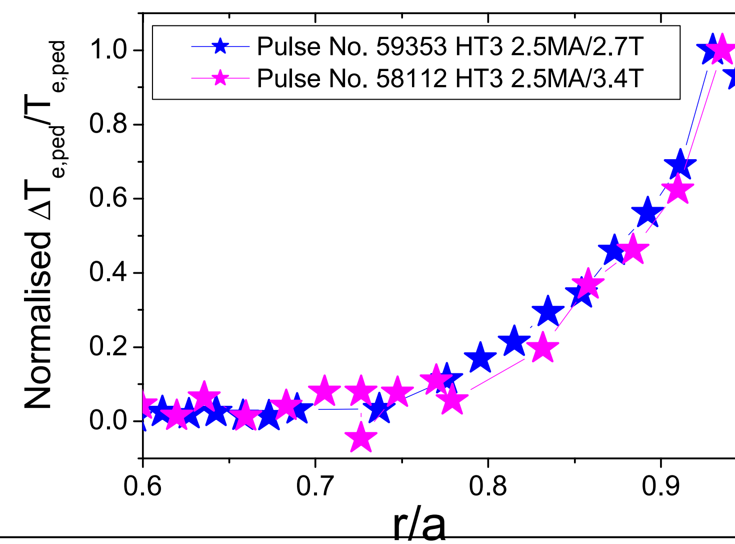

P-B stability effect on ELMs →non-linear evolution

Main plasma ELM energy/particle losses (VII)

Plasma shape (δ, κ, …) changes V_{ELM} as expected from P-B analysis

(JET & DIII-D (TTF'02-Córdoba) not ASDEX Upgrade (Urano PPCF'03))

JET- Loarte PPCF'02

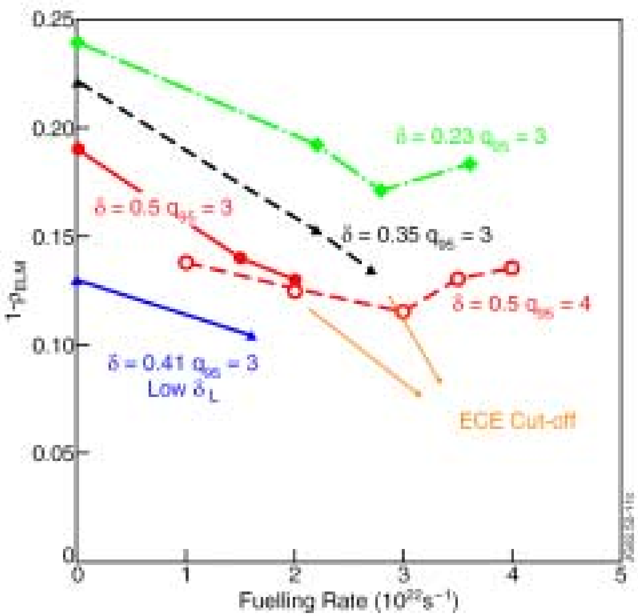

JET- Loarte APS'03

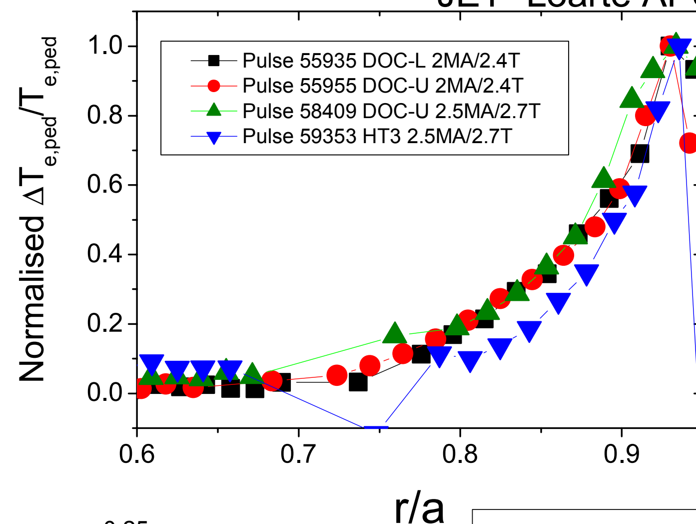

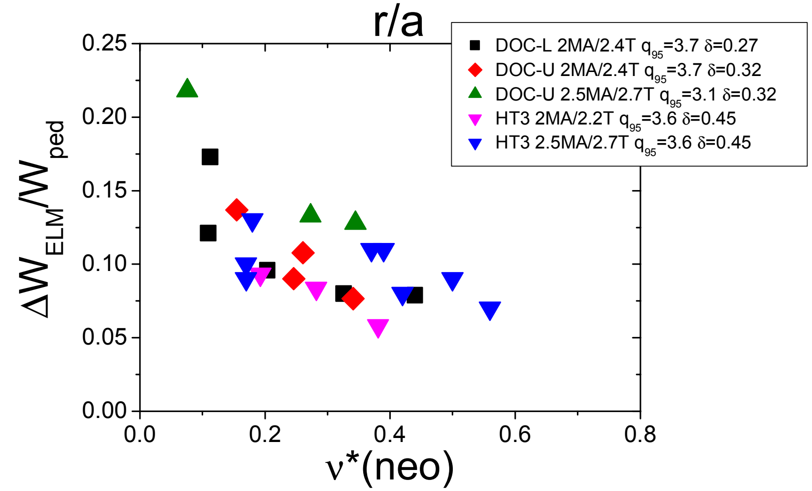

lower $\Delta W_{ELM}/W_{ped}$ for same ν^*_{ped} at high δ

but

ΔW_{ELM} is larger for higher δ (higher W_{ped}) !!!

Main plasma ELM energy/particle losses (VIII)

Collapse of effect of pedestal plasma at ELM is not Θ symmetric

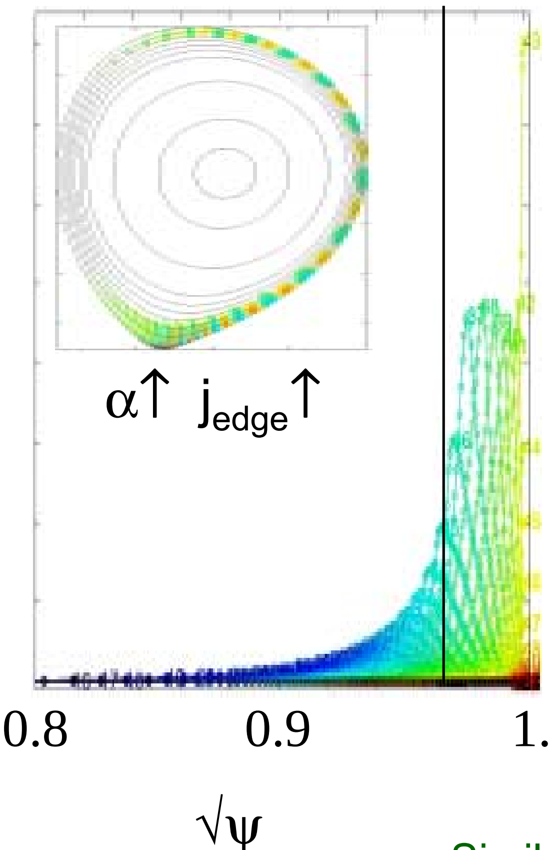

ASDEX Upgrade-Nunes EPS'03 subm. NF'04

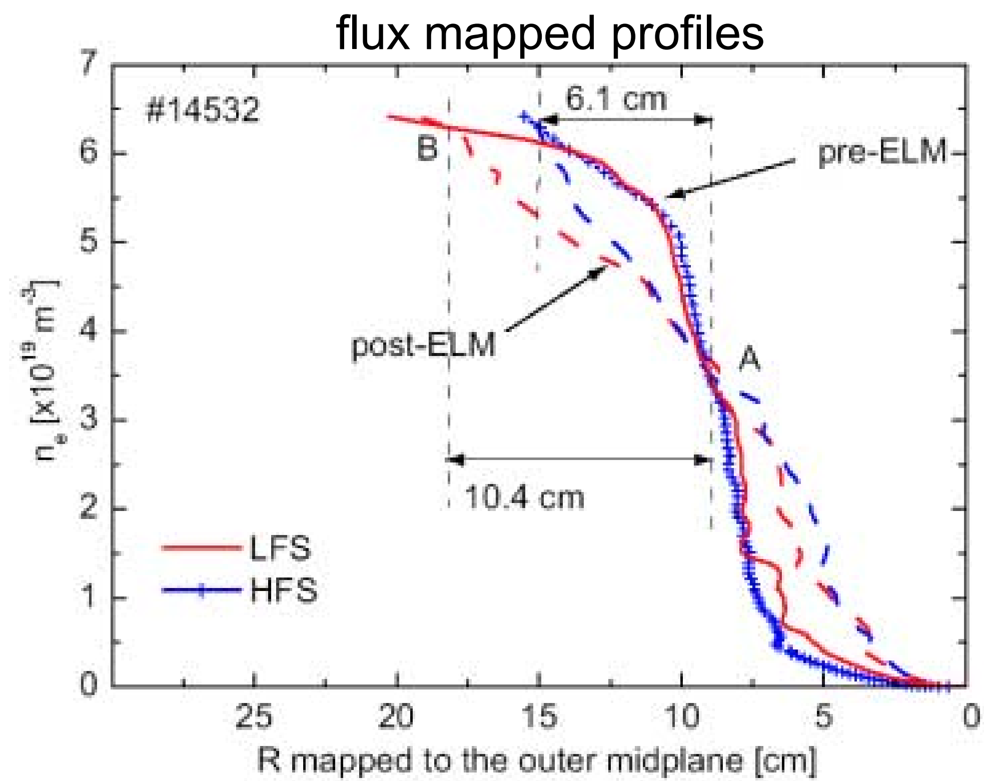

Similar results in JT-60U (Oyama NF'03 & NF'04) & MAST (Kirk PPCF'04)

ballooning structure is maintained to the end of the ELM collapse

Main plasma ELM energy/particle losses (IX)

Collapse of pedestal plasma during ELMs is not simultaneous at all Θ

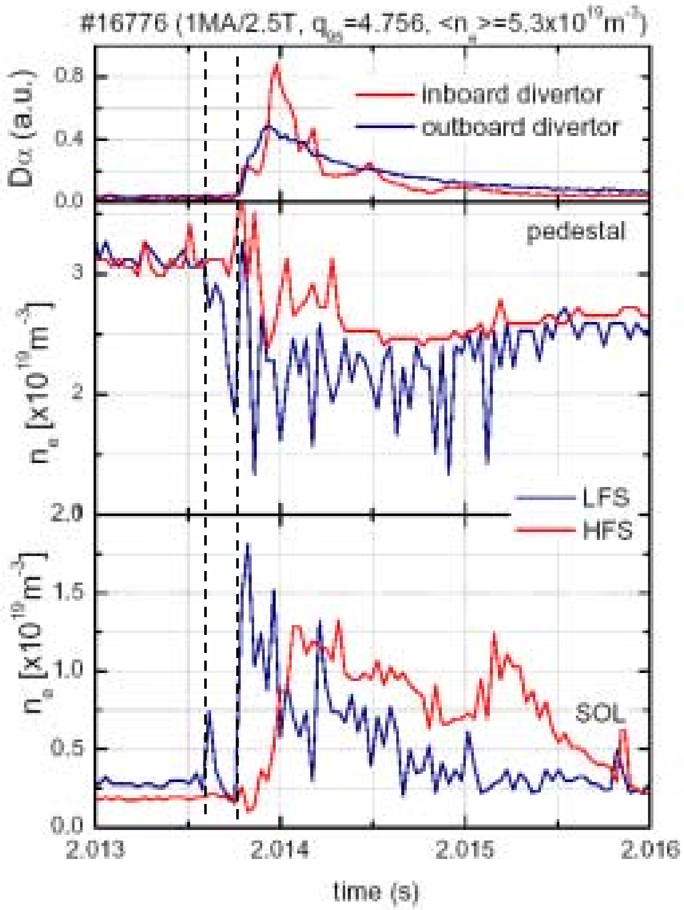

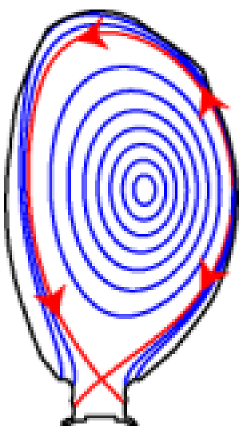

ASDEX Upgrade-Nunes EPS'03 subm. NF'04

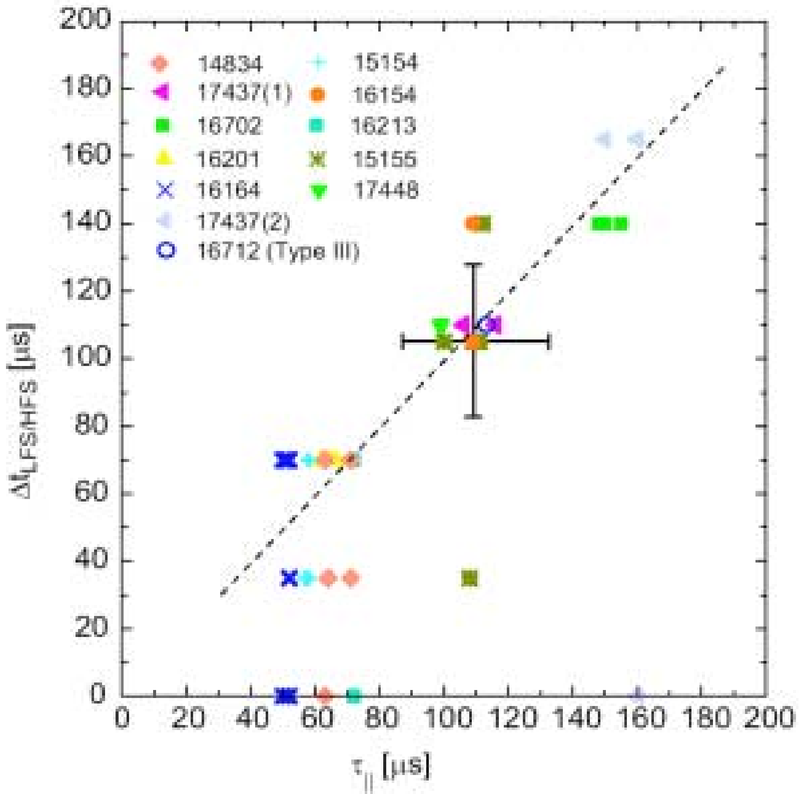

Delay scales with LFS-HFS ion transit time!

Main plasma ELM energy/particle losses (X)

ELMs are triggered at precise values of $n_{e,ped}$ and $T_{e,ped}$

JET-Loarte APS'03

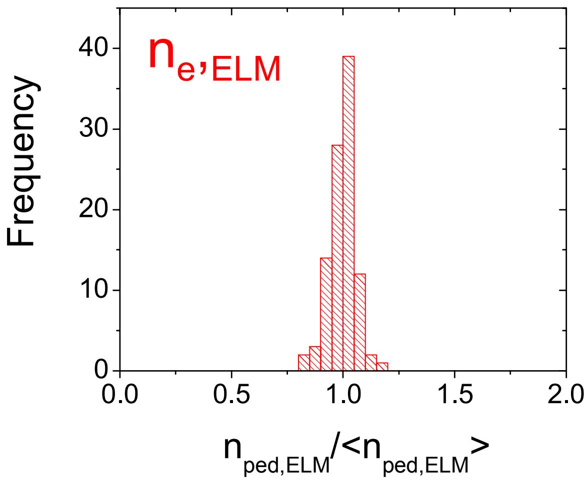

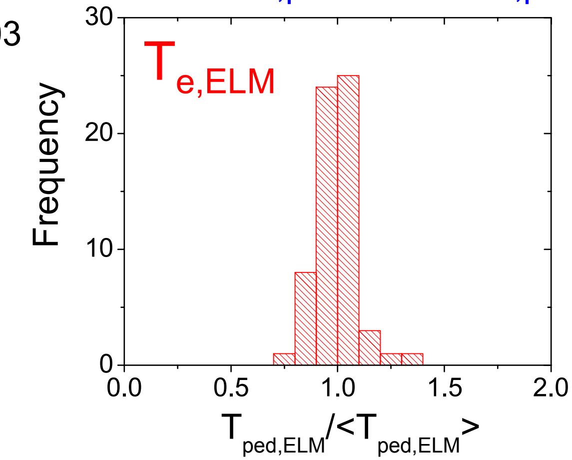

ELM crash has a much wider scatter for same $n_{e,ped}$ and $T_{e,ped}$

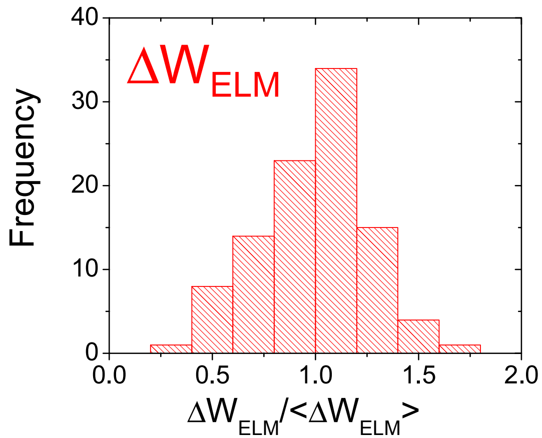

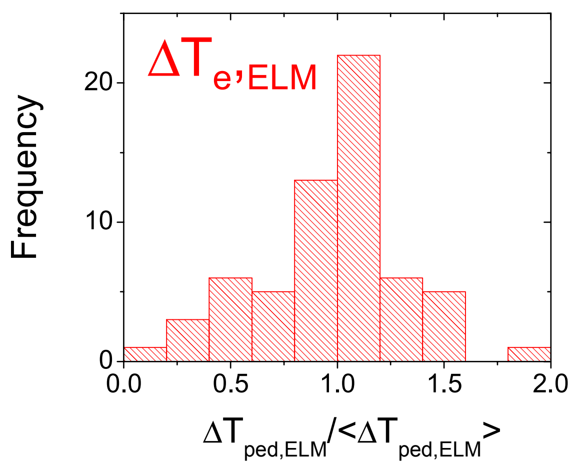

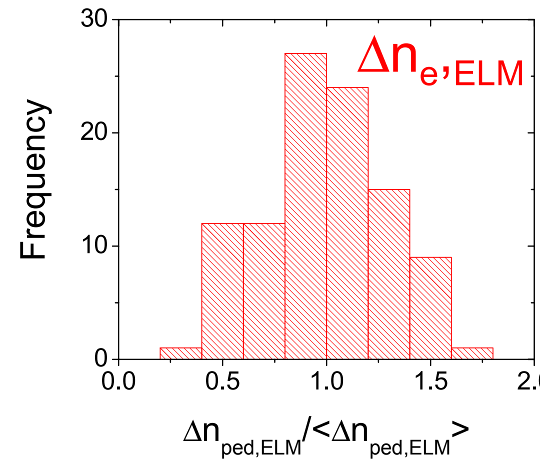

ELM energy/particle fluxes to PFCs (I)

ELMs lead to fluxes both at the divertor and main chamber PFCs

ASDEX Upgrade-Eich PRL'04

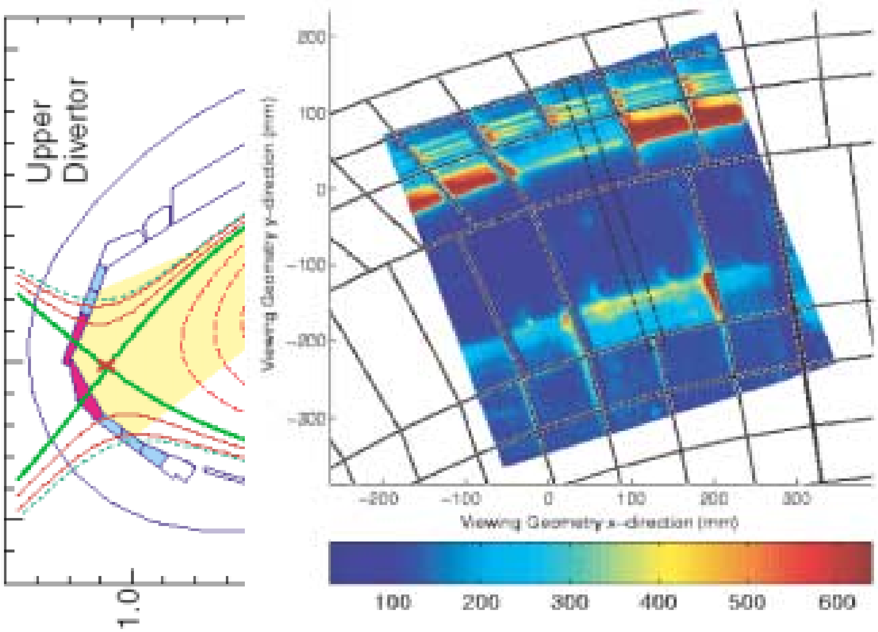

ASDEX Upgrade-Herrmann EPS'03

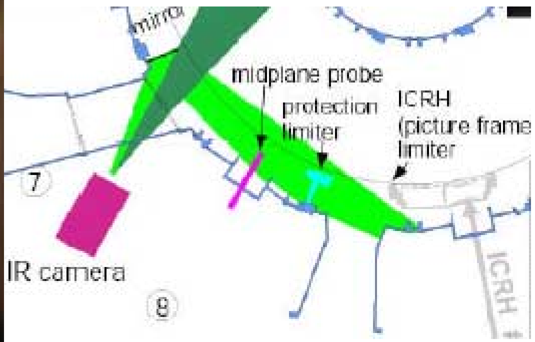

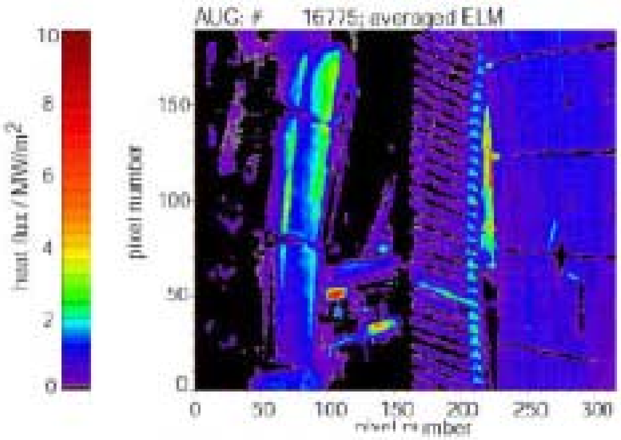

$\Delta W_{ELM} \rightarrow$ divertor and main chamber

Parameters to be determined & understood :

- timescales and areas
- transport mechanisms (extrapolation)

ELM energy/particle fluxes to PFCs (II)

divertor ELM fluxes are toroidally symmetric near separatrix (long L_c/high S)

DIII-D Leonard JNM'97 (Loarte PPCF'03)

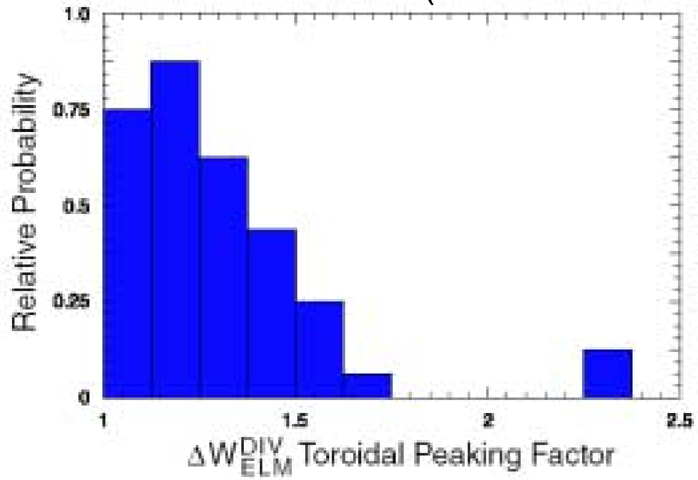

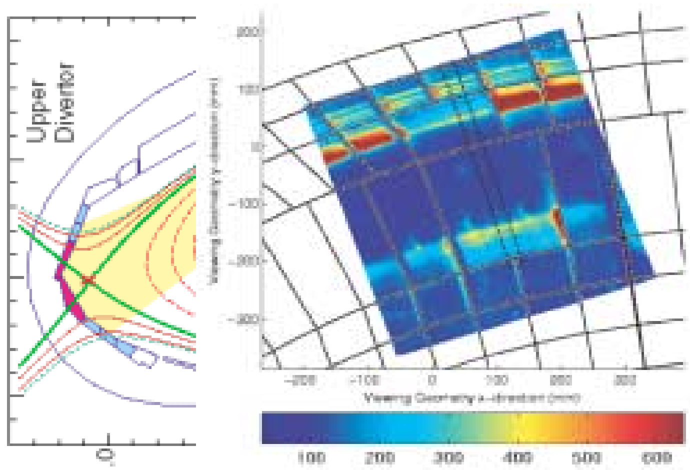

ASDEX Upgrade-Eich PRL'04

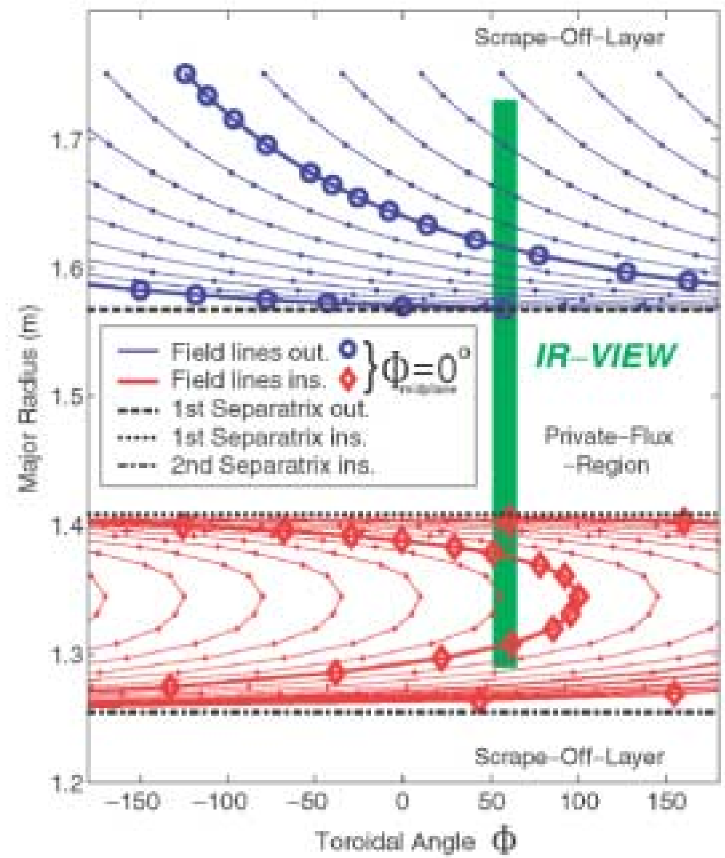

but ELM currents in DIII-D?

ELM energy/particle fluxes to PFCs (III)

divertor ELM energy wetted area ≈ divertor wetted area between ELMs

JET-Eich PSI'04

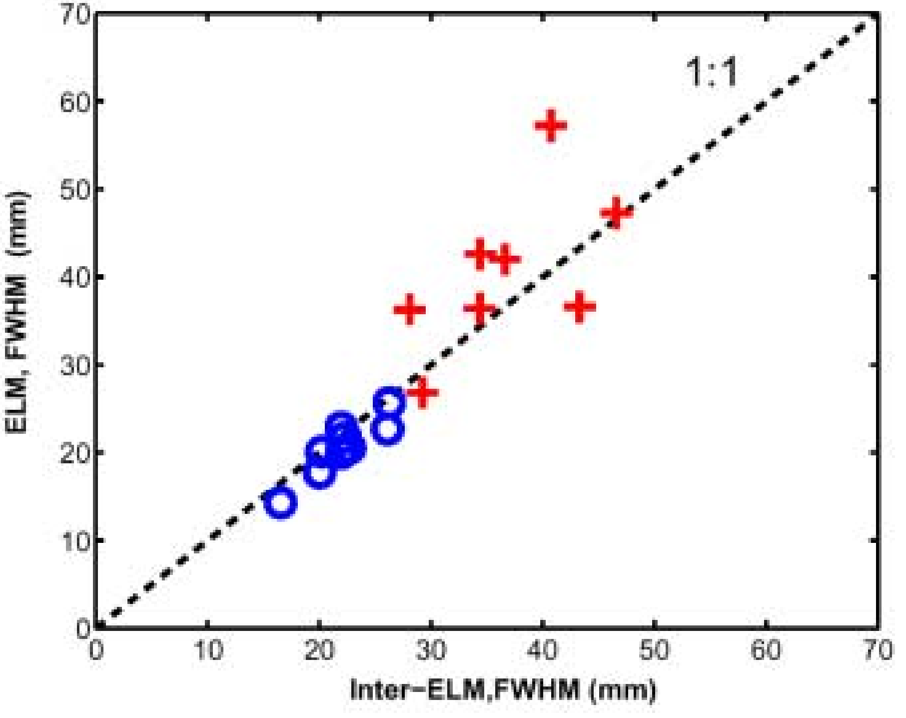

ASDEX Upgrade-Herrmann PPCF'02 (Loarte PPCF'03)

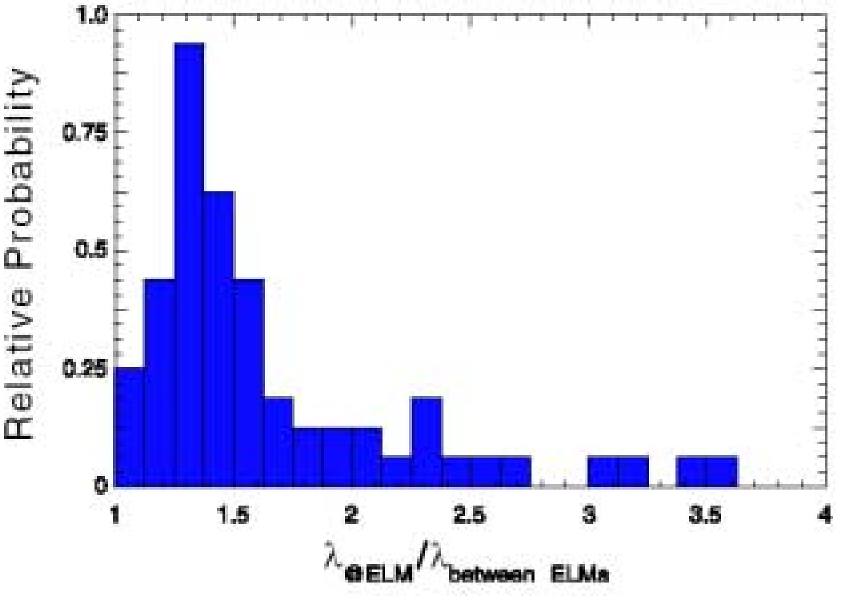

⊥ B & II B are enhanced in a similar way during ELMs

Similar results in MAST (Kirk PPCF'04) and DIII-D (Fenstermacher PPCF'03)

ELM energy/particle fluxes to PFCs (IV)

Time history of divertor ELM energy is complex

T^{max}_{surf}

JET-Eich PSI'02, Matthews NF'03

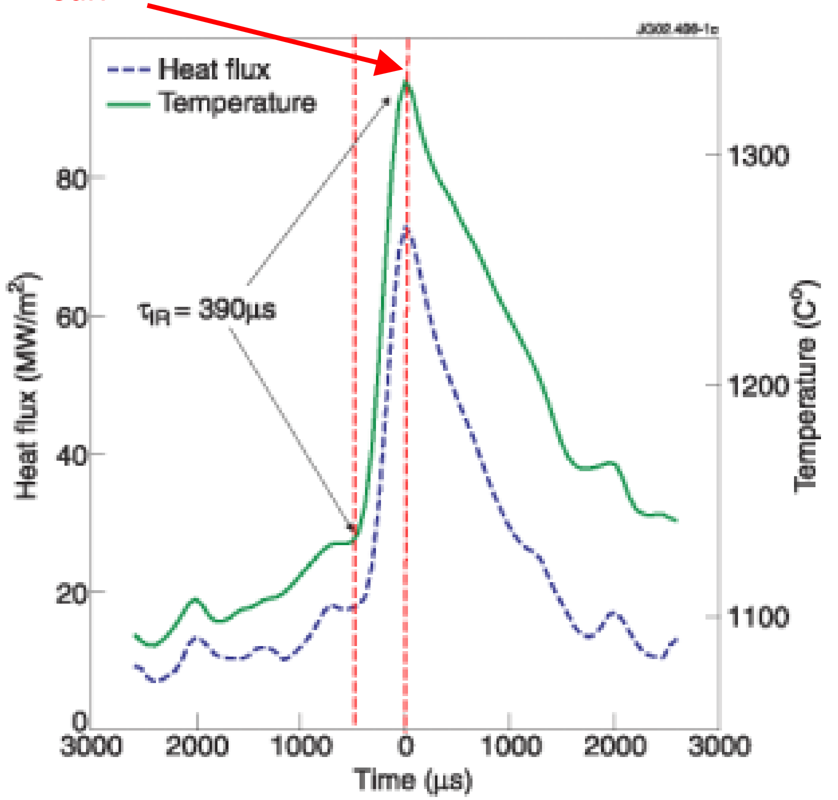

Significant fraction of ΔW_{ELM}^{div} arrives after T^{max}_{surf} !!!!

ELM erosion in ITER determined by $T^{max}_{surf} > T_{evap}^{C}$

ELM energy/particle fluxes to PFCs (V)

n_{ped} or $\nu^*(neo)$ ↗ → ELMs more convective → more of ΔW_{ELM}^{div} after T^{max}_{surf}

JET-Loarte APS'03, Eich PSI'04

DOC-L δ = 0.27

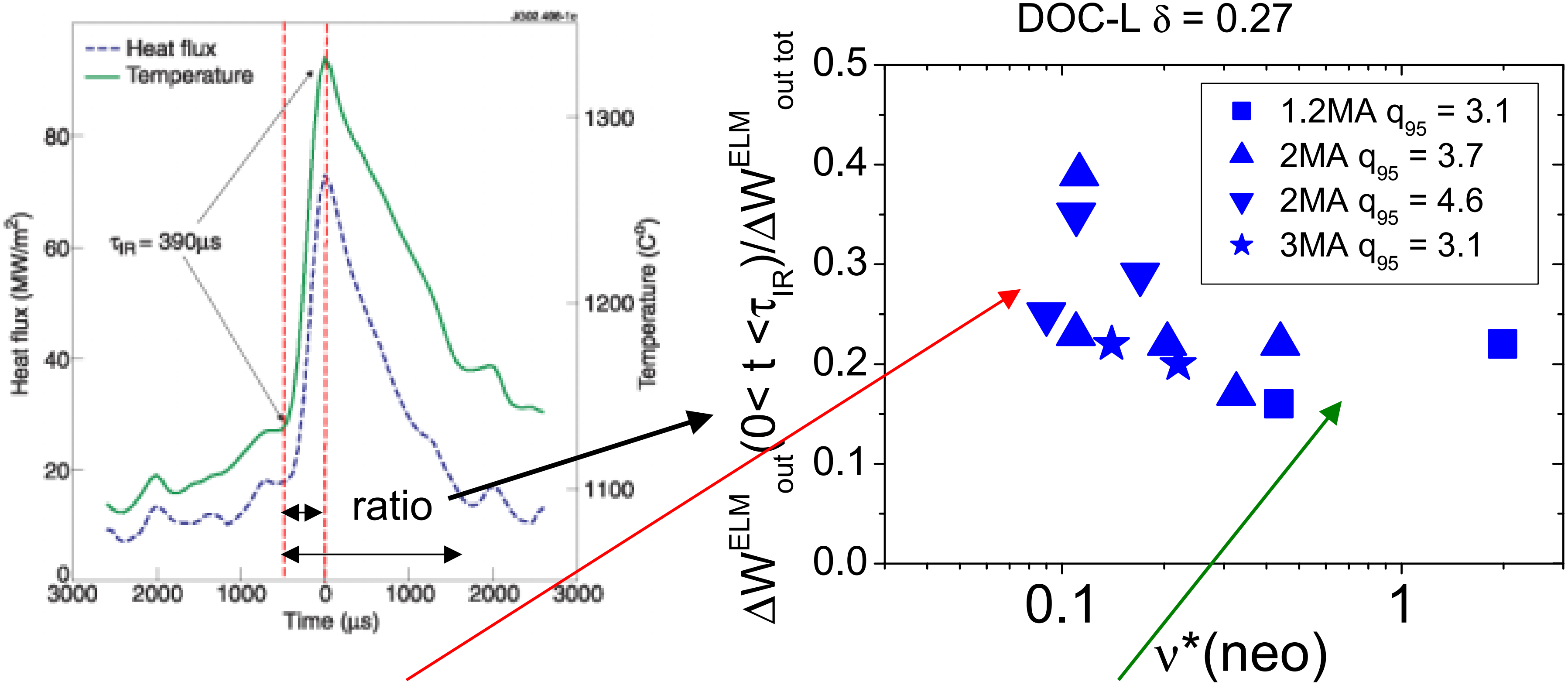

$0.40 > \Delta W_{ELM}^{div} (0<t<\tau_{IR})/ \Delta W_{ELM}^{div}{}_{tot} > 0.15$

conductive ELM — convective ELM

ELM energy/particle fluxes to PFCs (VI)

Timescale of ELM heat flux on divertor correlated with $\tau_{||} \sim L/c_{s,ped}$

JET- Eich, ASDEX Upgrade-Herrmann, JT-60U Asakura, MAST-Kirk

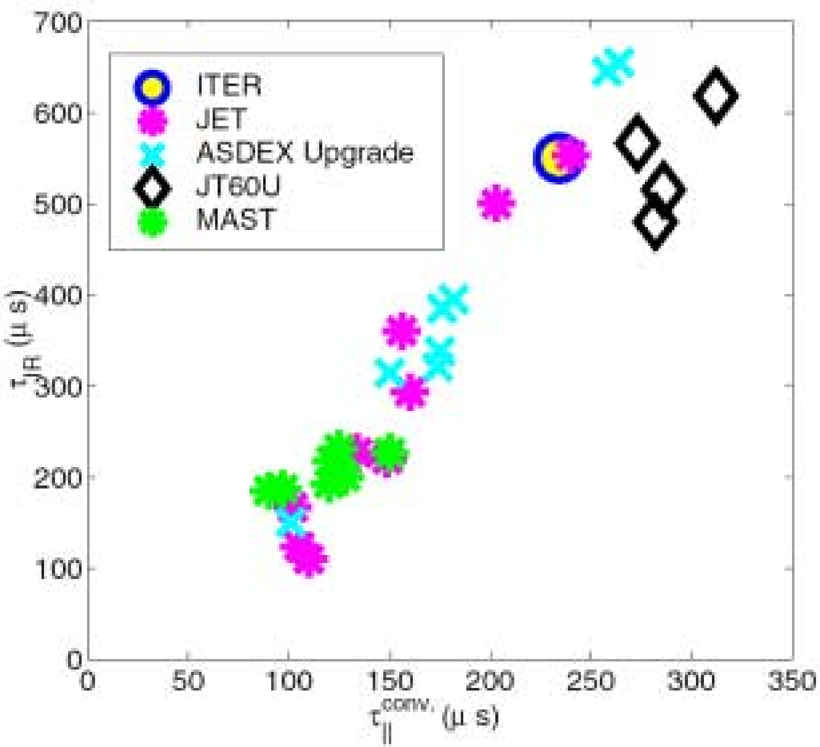

- $\Gamma_{div} = \Gamma_{e,div}(\tau_{ELM}^{MHD}) + \Gamma_{i,div}(\tau_{||})$
- Formation of high energy sheath

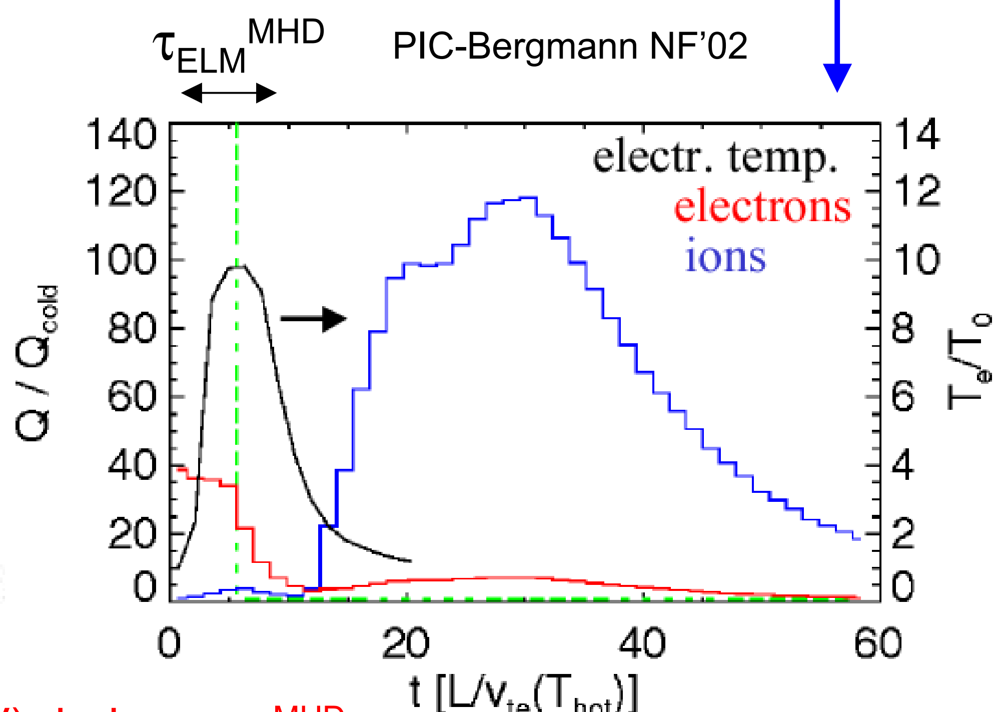

Experiment → high $\Gamma_{x\text{-}ray}$ (electrons ~ keV) during τ_{ELM}^{MHD}

ELM energy/particle fluxes to PFCs (VII)

- $\Delta W_{ELM}/W_{ped}$ decreases with $\tau_{||}$

ITPA-Loarte PPCF'03

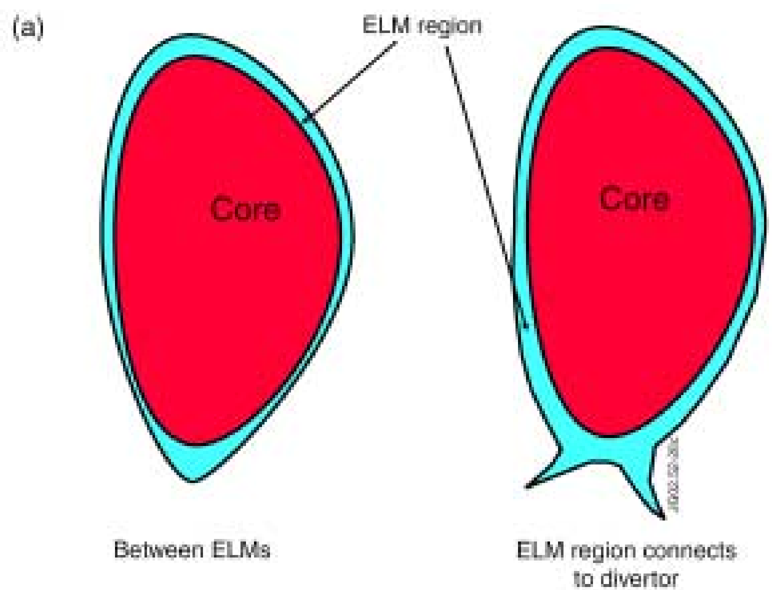

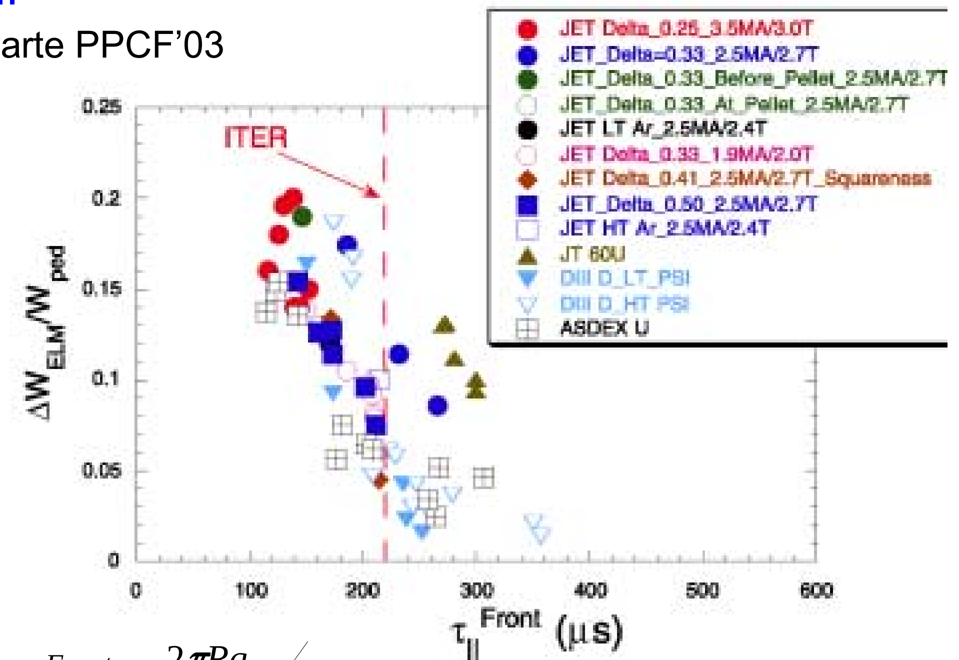

$$\tau_{||}^{Front} = \frac{2\pi R q_{95}}{c_{s,ped}}$$

Physics Model :

1) Pedestal connects to divertor for τ_{ELM}^{MHD}

2) Energy flow restricted by sheath ($\tau_{||}$) → $\Delta W_{ELM}/W_{ped} \sim (1-\exp(-\tau^{ELMMHD}/\tau_{||}))$

ELM energy/particle fluxes to PFCs (VIII)

separation of e^- flux (τ_{ELM}^{MHD}) & ion flux inner divertor

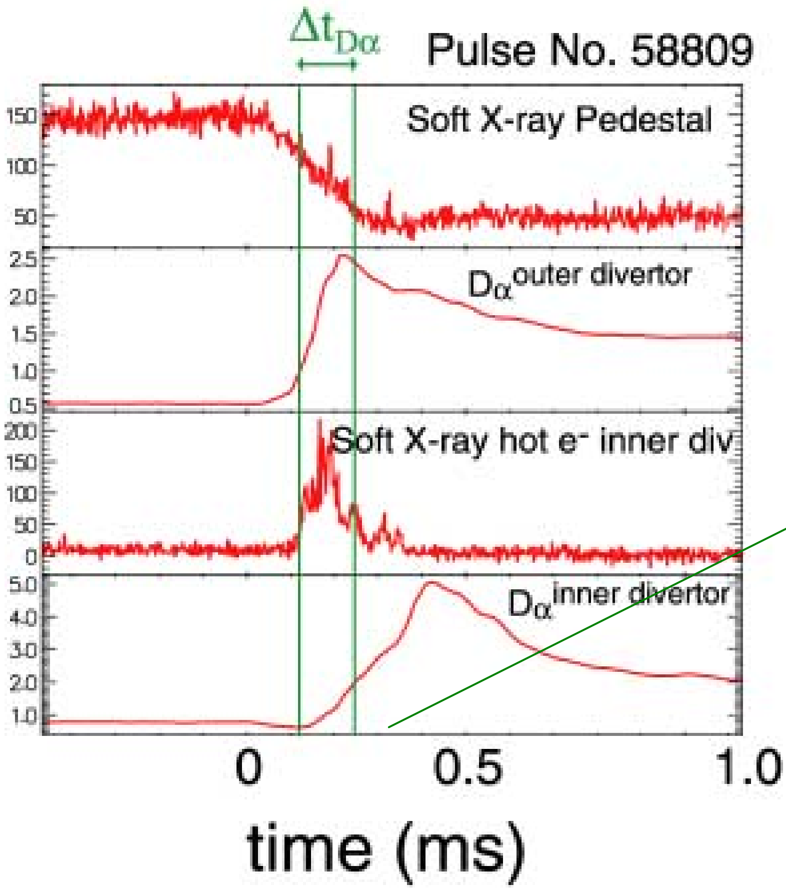

JET-Loarte, PPCF'02, PPCF'03, APS'03

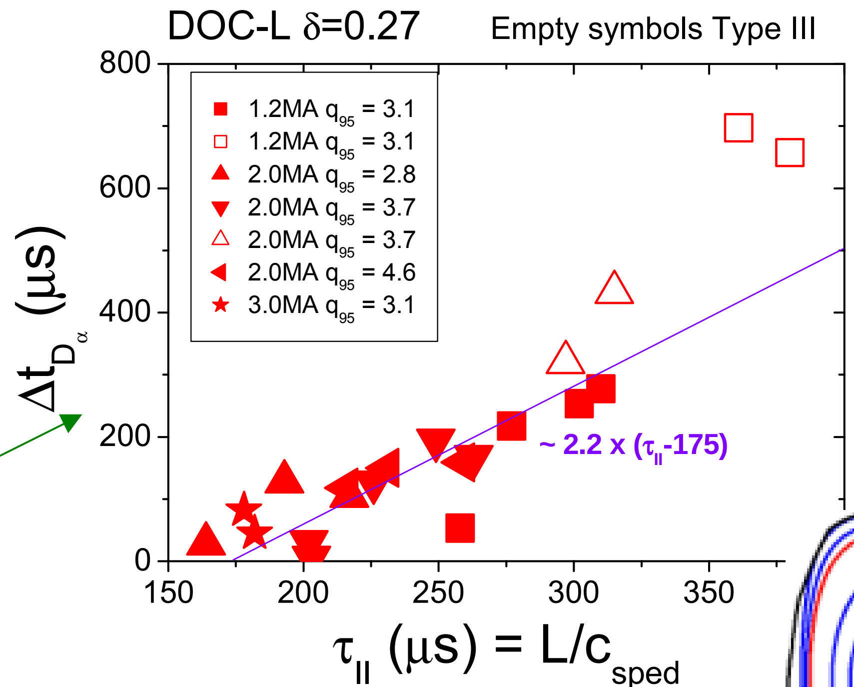

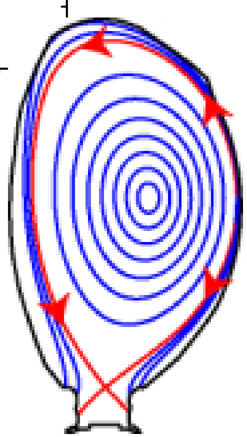

$\Delta t_{D\alpha}$ ~ 0 for finite τ_{II}

Similar results from DIII-D (Fenstermacher PPCF'03, Boedo APS'03)

ELM energy/particle fluxes to PFCs (IX)

$\Delta t_{D\alpha} \sim 0$ for finite τ_{II} : a) main plasma collapse ($\tau_{ELM}^{MHD} \neq 0$) ?

b) change of ELM start X-point → midplane ?

DIII-D-Fenstermacher PPCF'03

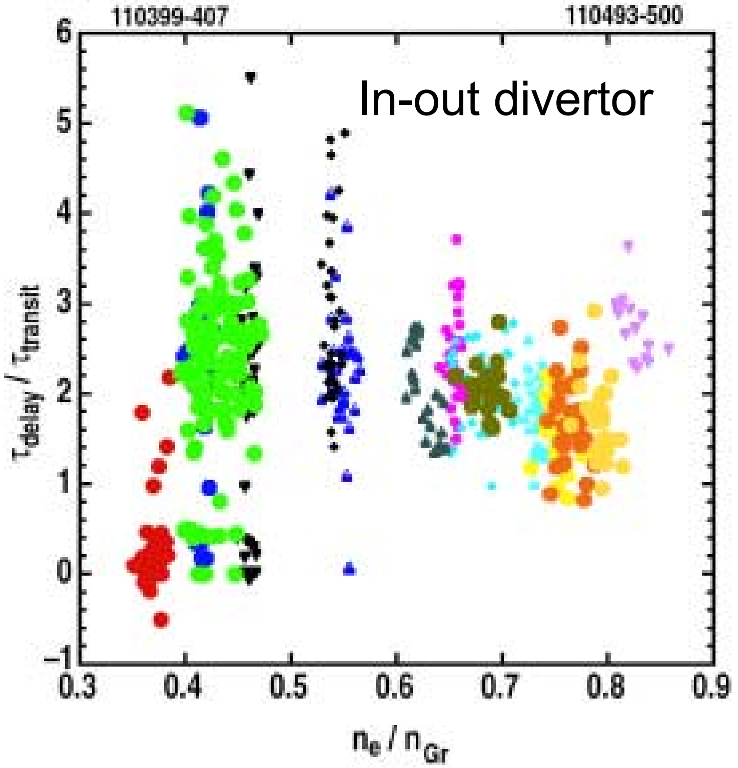

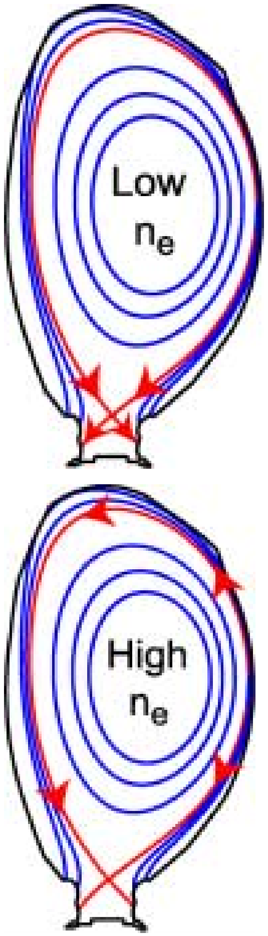

ASDEX Upgrade-Nunes EPS'03 subm. NF'04

HFS-LFS main plasma

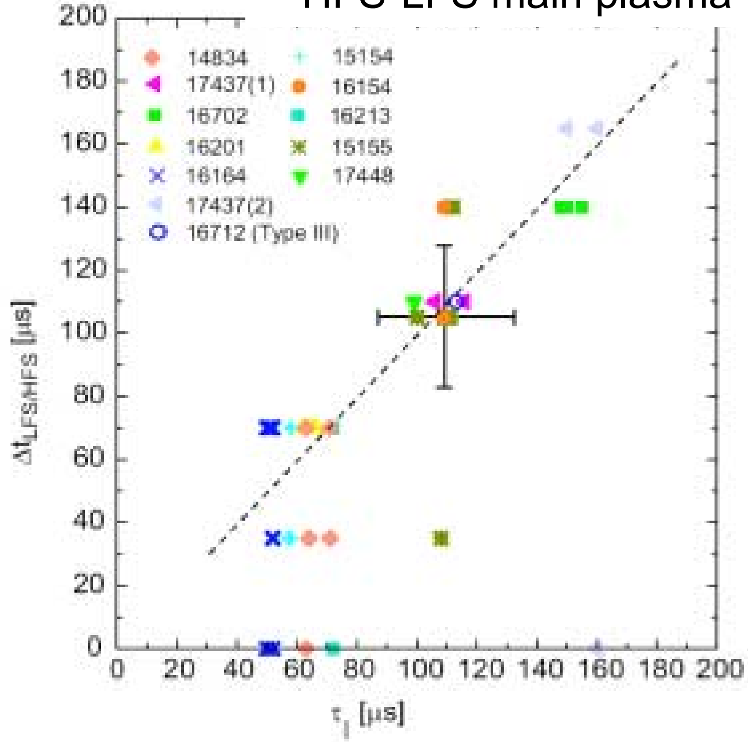

ELM energy/particle fluxes to PFCs (X)

$\Delta W_{ELM}^{div} < \Delta W_{ELM}$ but $\lambda_{ELM}^{div} \sim \lambda_{inter\text{-}ELM}^{div}$

ASDEX Upgrade Herrmann EPS'97 (Loarte PPCF'03)

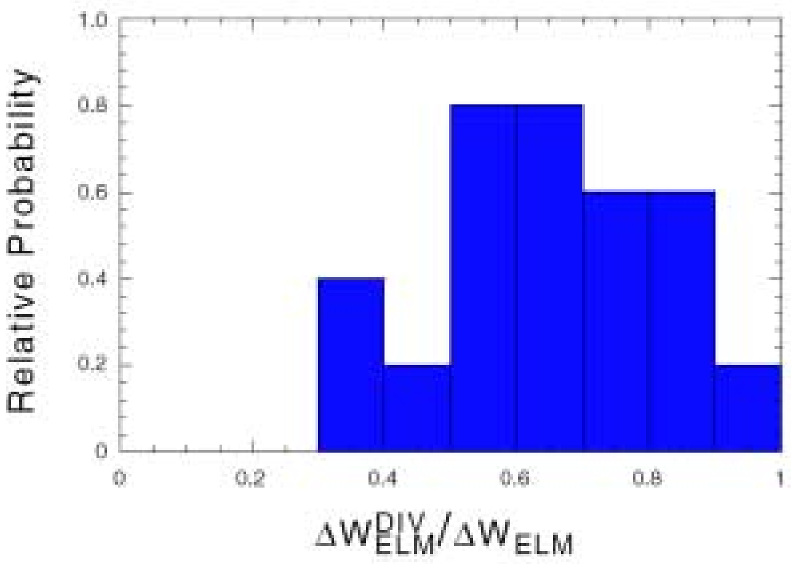

JET-Loarte APS'03, Eich PSI'04

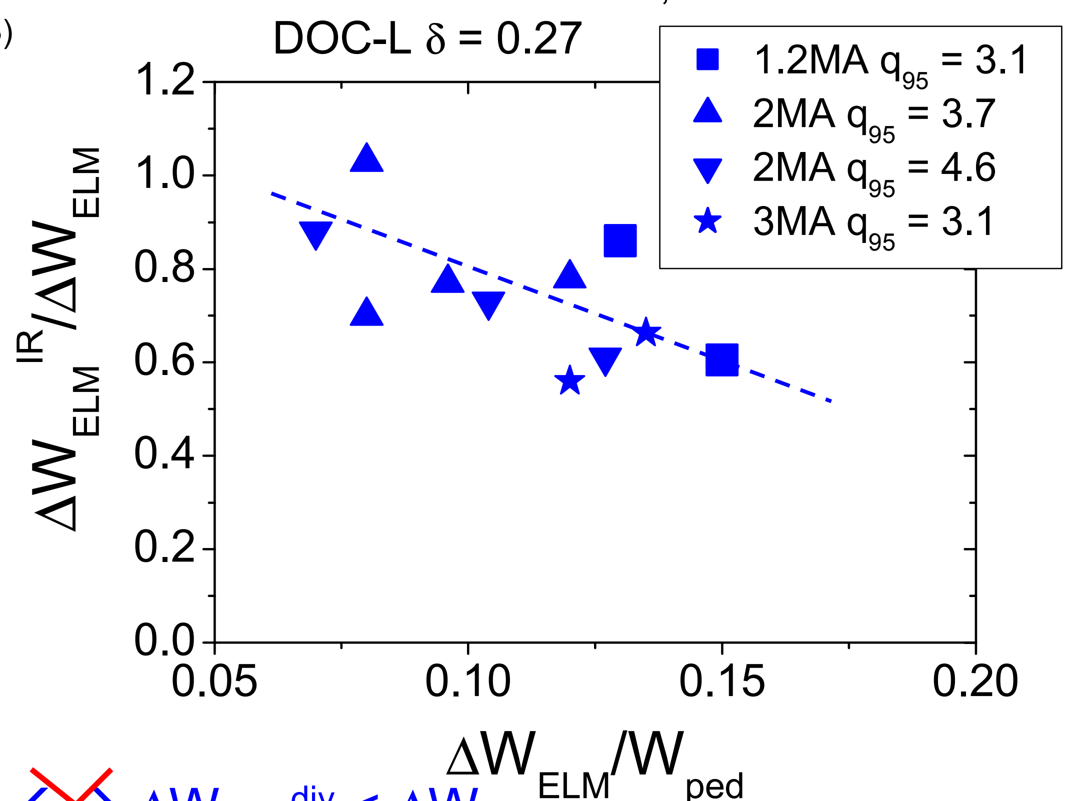

Transient radiation ⇎ $\Delta W_{ELM}^{div} < \Delta W_{ELM}$

larger $\Delta W_{ELM}/W_{ped}$ → smaller $\Delta W_{ELM}^{div} / \Delta W_{ELM}$

ELM energy/particle fluxes to PFCs (XI)

large particle fluxes measured far from separatrix at ELMs

DIII-D-Boedo+Zeng APS'03/PPCF'04

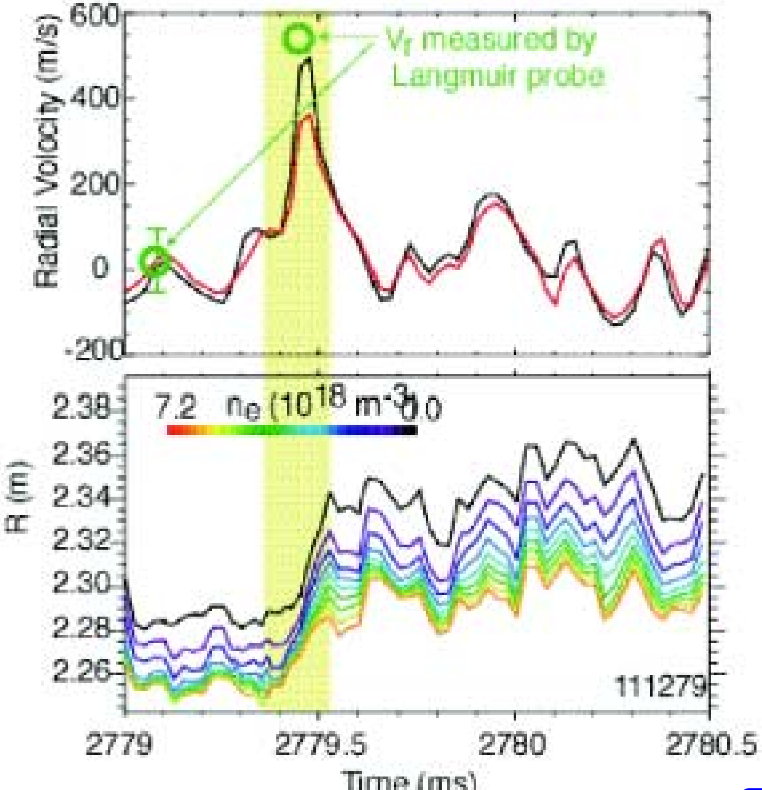

MAST-Counsell PPCF'02

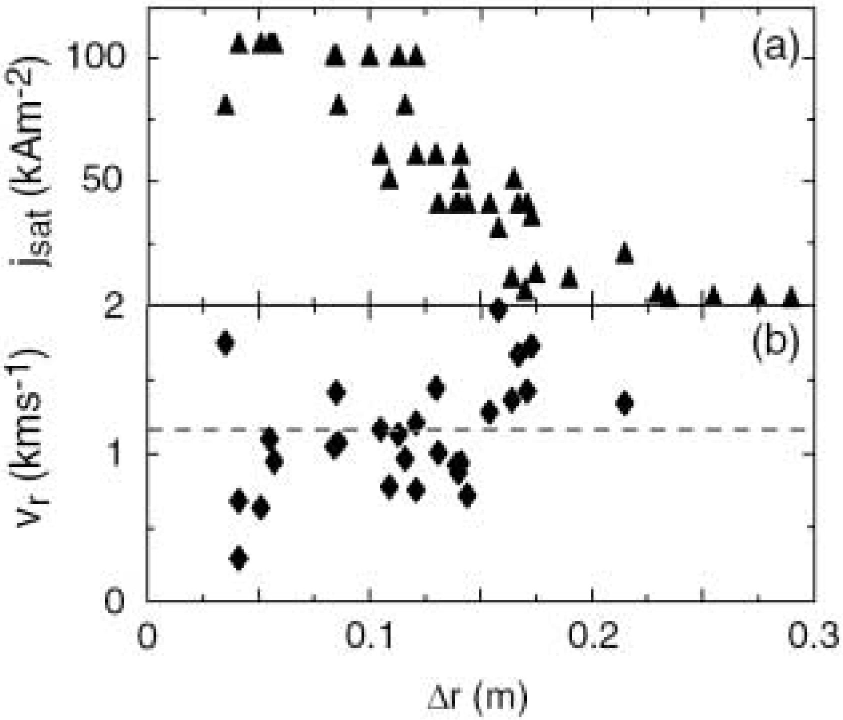

$\tau_{perp,ELM}$~100 μs~τ_{II} → large $\Gamma^{main\ chamber}$

v_r (km/s): JET (0.5-1.2, Gonçalves PPCF'03, Fundamenski'04), MAST (0.2-1.7, Counsell PPCF'02, Kirk PPCF'04), DIII-D (0.2-0.6, Zeng PPCF'03, Boedo APS'3)

ELM energy/particle fluxes to PFCs (XII)

significant energy fluxes measured on main chamber PFCs

ASDEX Upgrade
Herrmann EPS'03

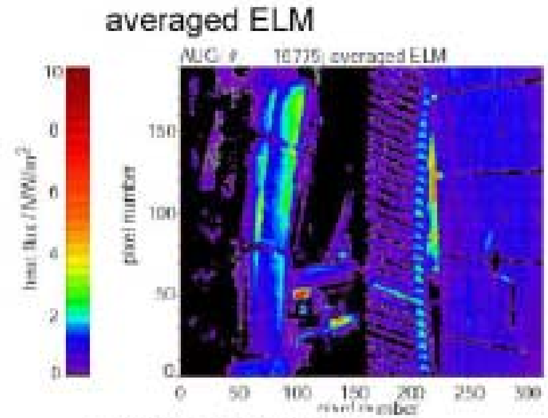

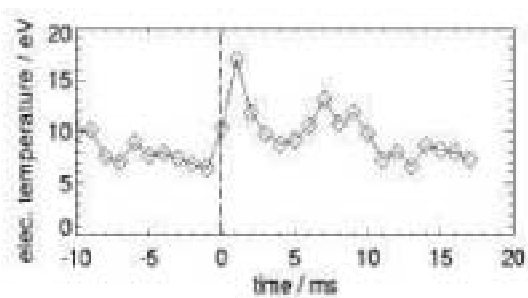

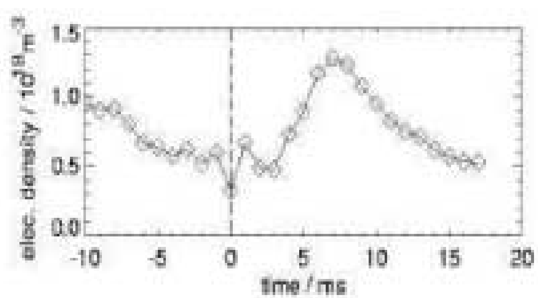

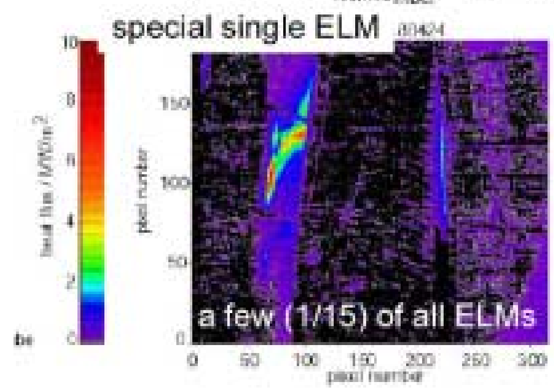

Energy on PFCs on large area of limiter (most ELMs)

$\Delta W_{ELM}{}^{wall} \sim 25$ % of ΔW_{ELM}

$T_{e,ELM}{}^{PFC} << T_{e,ped} \rightarrow T_{i,ELM}{}^{SOL}$

ELM energy/particle fluxes to PFCs (XIII)

What do we know about radial ELM fluxes ?

DIII-D-Boedo-Fenstermacher APS'03 /PPCF'03

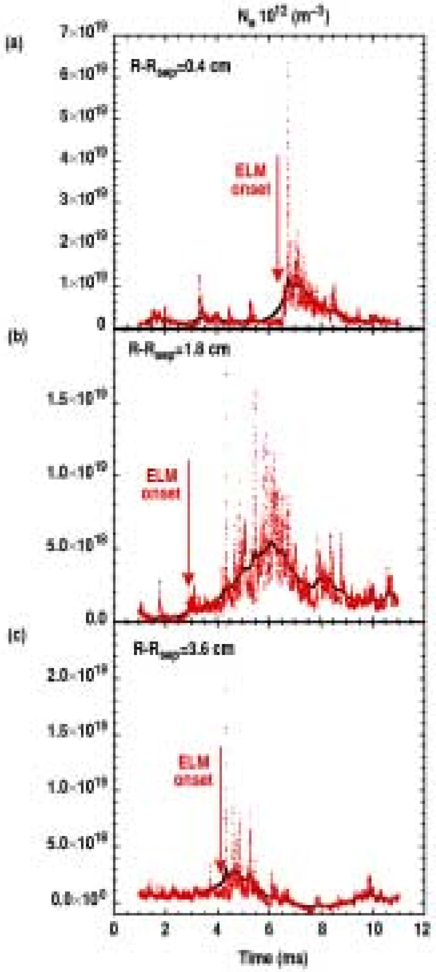

complex filamentary rotating structure

$T_{e,ELM}$ decays radially faster than $n_{e,ELM}$

$\tau_{E\text{-}e,SOL} < \tau_{II}$

$v_{r,ELM}$ decreases with n_e (and r ?)

DIII-D-Boedo APS'03

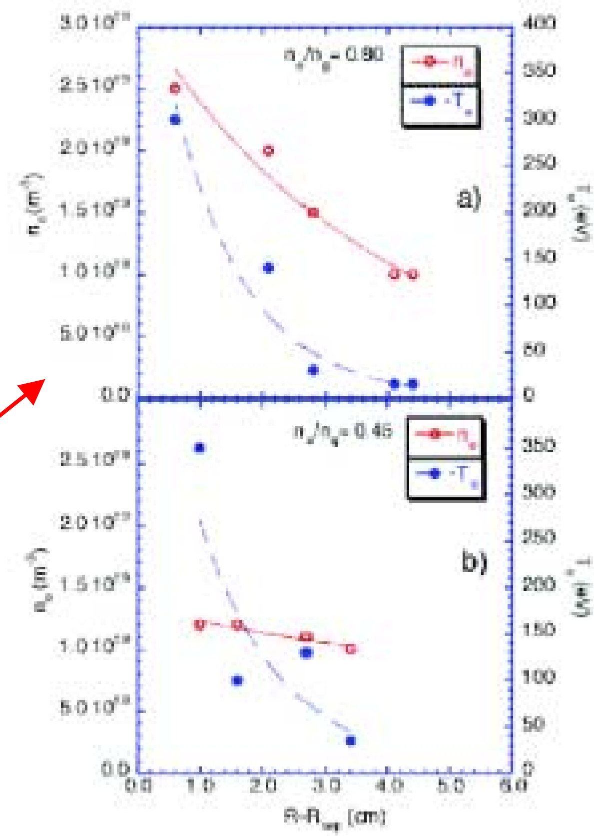

ELM energy/particle fluxes to PFCs (XIV)

decrease of v_r with n_e (and ΔW_{ELM}?) compatible with $\Delta W_{ELM}^{div}/\Delta W_{ELM}$

JET-Loarte APS'03, Eich PSI'04

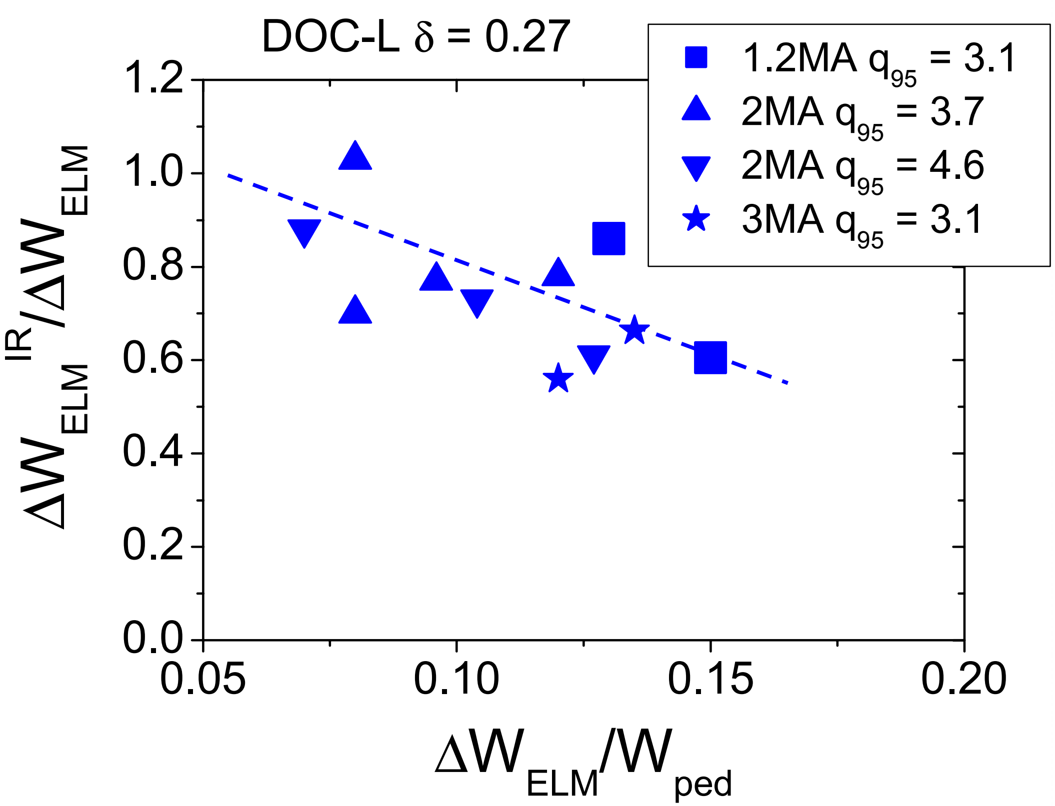

DIII-D-Zeng PPCF'04

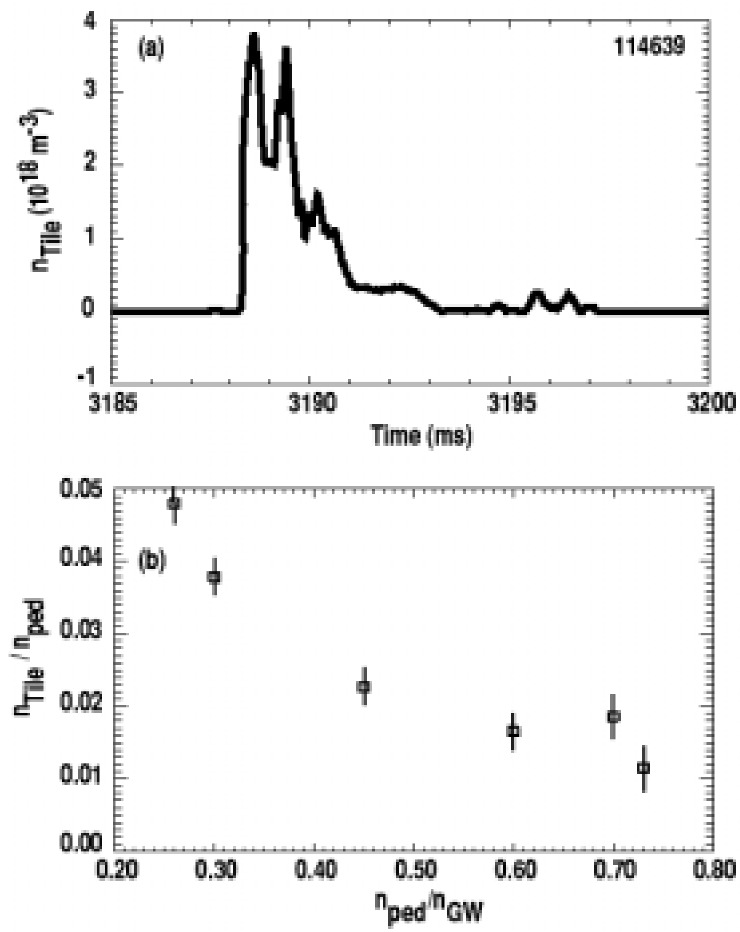

ELM energy/particle fluxes to PFCs (XV)

What determines v_r?

1.Non-linear ballooning explosive mode dependence on (n_e, T_e, ν^*_{ped})

S.Cowley-PPCF'03

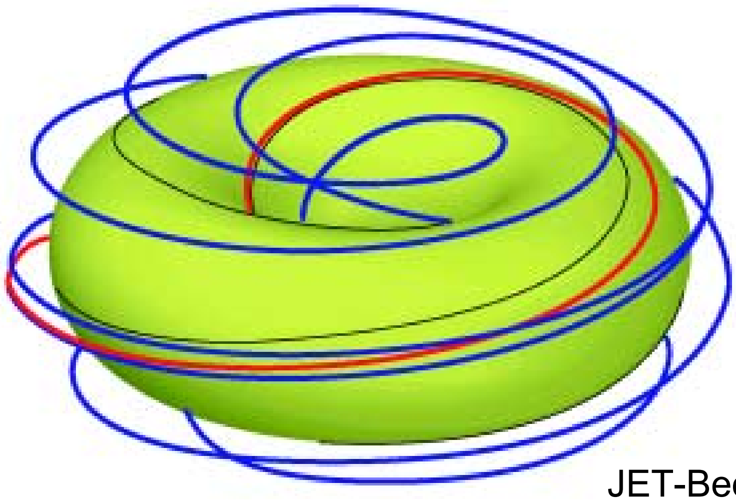

ELM $\tilde{B}_\theta$ "amplitude" decreases with n_{ped}

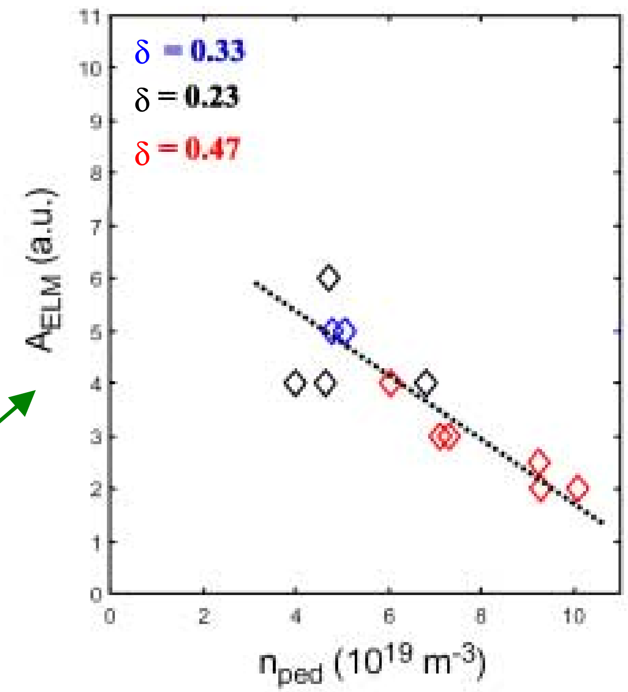

JET-Becoulet-H-mode WS'01

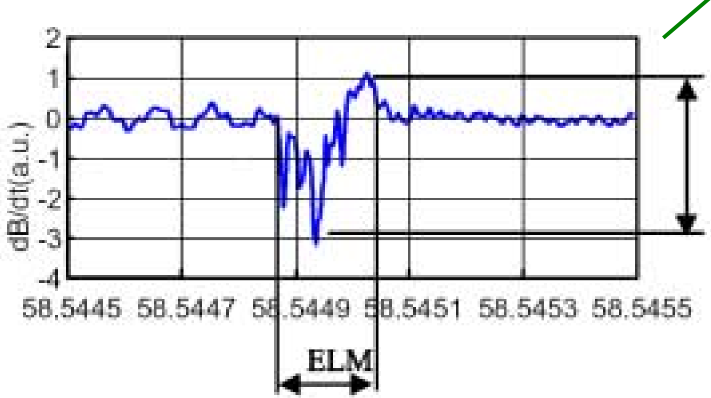

ELM energy/particle fluxes to PFCs (XVI)

2. Dynamics of ELM pressure blob radial transport (Krasheninnikov, D'Ippolito,….)

$v_r = c_s\, 2\rho^2 L / R r_b^{\,2}$

- JET : T_{ped} ~ 1.5 keV, if r_b ~ 20 cm → v_r ~ 1 km/s
- DIII-D : T_{ped} ~ 0.5 keV, if r_b ~ 13 cm → v_r ~ 1 km/s

Scaling of $v_r \sim T_{ped}^{3/2}\, r_b^{-2} \sim n_{ped}^{-3/2}\, r_b^{-2}$

ASDEX Upgrade-Nunes EPS'03 subm. NF'04

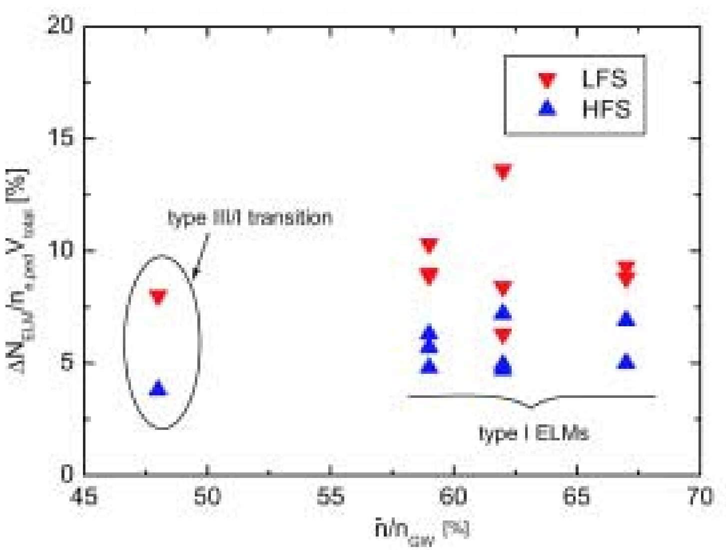

dependence of r_b on n_{ped}, T_{ped} , 2 hypothesis :

- Empirical $\Delta N_{ELM} \sim n_{ped}$ (DIII-D, JET, ASDEX Upgrade)

↓

r_b ~ constant

- r_b ~ P-B mode width → $r_b \sim n_{ped}^{-\alpha}$

Extrapolation of Type I ELMs to ITER

W_{dia}^{ITER} = 350 MJ → W_{ped} < 0.4 W_{dia}^{ITER} =140 MJ (n_{ped}~8 10^{19} m^{-3} T_{ped}~4.3 keV)

$\tau_{IR}^{ELM} \sim 300\ \mu s$

$A_{ELM}^{ITER} = A_{S.S}^{ITER} = 3\ m^2$ ($\lambda_{power}^{midplane}$ = 5 mm)

	Convective ELMs	Conductive ELMs
ΔW_{ELM}^{ITER} (MJ)	10	28
$\Delta W_{ELM}^{ITER,\ div}$(MJ)	80%	50%
$\Delta W_{ELM}^{ITER,div}$ ($0 < t < \tau_{IR}$) (MJ)	20%	40%
Φ_{ELM}^{ITER} ($MJm^{-2}s^{-1/2}$)	20	72

C-ablation in ITER ~ 50 $MJm^{-2}s^{-1/2}$

$\Delta W_{ELM}^{ITER,wall}$ (MJ)	20%	50%

ELM erosion less critical than previously believed even for conservative assumptions

Conclusions (I)

- Peeling-Ballooning model provides a reasonable description of pedestal pressure limitation by Type I ELMs
  - Detailed multi-machine comparison (& pedestal width scaling) in progress
  - Which is the ELM triggering mechanism ?
  - Non-linear evolution of ELM and timescales

- Type I ELM energy losses determined by $n_{e,ped}$ & $T_{e,ped}$, q_{95}, δ

  Small ELMs ←→ Convective ELMs

  - What determines V_{ELM} ?
  - Physical process that produce convective ELMs (ν^*_{ped} and high δ/q_{95}) ?

    (link between MHD stability ←→ ELM energy transport ?)
  - What determines the ELM variability ?

Conclusions (II)

- ELM energy fluxes determined by determined by $n_{e,ped}$ & $T_{e,ped}$
  - timescale of ELM energy flux on divertor by τ_{II} and not τ_{ELM}^{MHD}
    (role of sheath/IIB transport on divertor ELM energy Flux ?)
  - $\Delta W_{ELM}^{div} < \Delta W_{ELM}$ and fluxes to main chamber PFCs
    (convective radial ion transport versus IIB losses ?)
  - spatial distribution of ELM heat loads
    (toroidal symmetry ?, main chamber fluxes ?, in/out divertor balance ?)

Conclusions (II)

- ELM energy fluxes determined by determined by $n_{e,ped}$ & $T_{e,ped}$
  - timescale of ELM energy flux on divertor by τ_{II} and not τ_{ELM}^{MHD} (role of sheath/IIB transport on divertor ELM energy Flux ?)
  - $\Delta W_{ELM}^{div} < \Delta W_{ELM}$ and fluxes to main chamber PFCs (convective radial ion transport versus IIB losses ?)
  - spatial distribution of ELM heat loads (toroidal symmetry ?, main chamber fluxes ?, in/out divertor balance ?)
- Regimes with small/no Type II ELMs/good confinement exist but:
  - operational space is narrow and not well characterised (reproducibility in various experiments ?)
  - extrapolability to next step devices/compatibilty with other requirements ? (low ν^*_{ped}, low q_{95}, high $P_{rad}^{divertor}$, pellet fuelling, He pumping, ….)
  - operation close to double null required ?

Regimes with high P_{ped} + small/no ELMs (I)

Regimes with small or no ELMs and high P_{ped}

a) Regimes with high P_{ped} and small ELMs (Type II ELMs : JT-60U, AUG)

modification of edge MHD plasma stability

b) Regimes with no (or infrequent) ELMs and quasi-continuous losses (EDA, QH-mode, “mixed Type I-II ELMs” in JET)

triggering of transport losses “between ELMs” $P_{ped} \leq P_{ped}^{limit}$

Regimes with high P_{ped} + small/no ELMs (II)

Mixed Type I-II in JET ←→ increased broadband MHD fluctuation at low f

T_{ped} reaches steady state between type I ELMs with increased fluctuations but

n_{ped} does NOT saturate in the Type II phases (→ end in Type I)

JET-Saibene
EPS'03

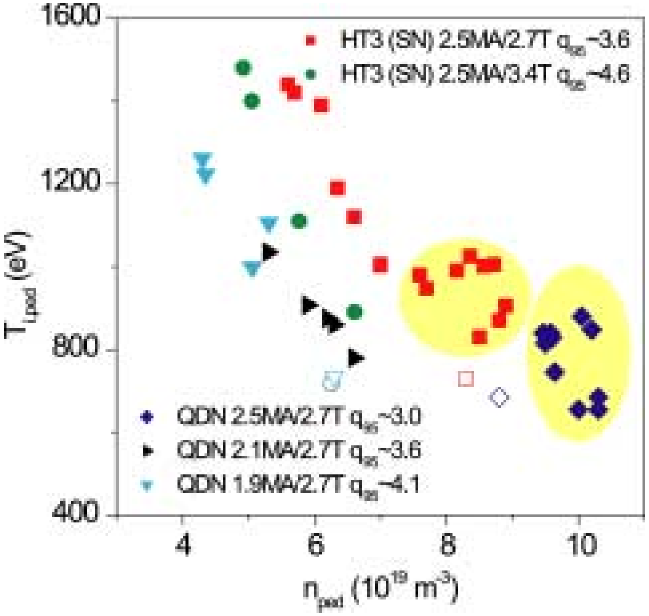

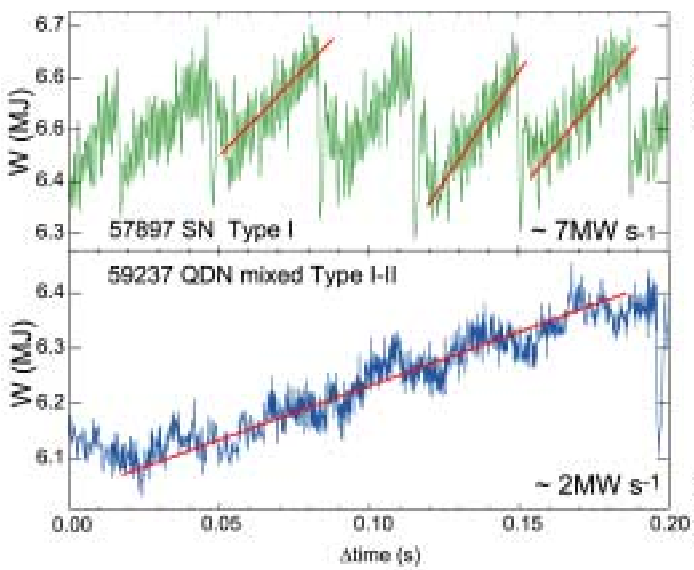

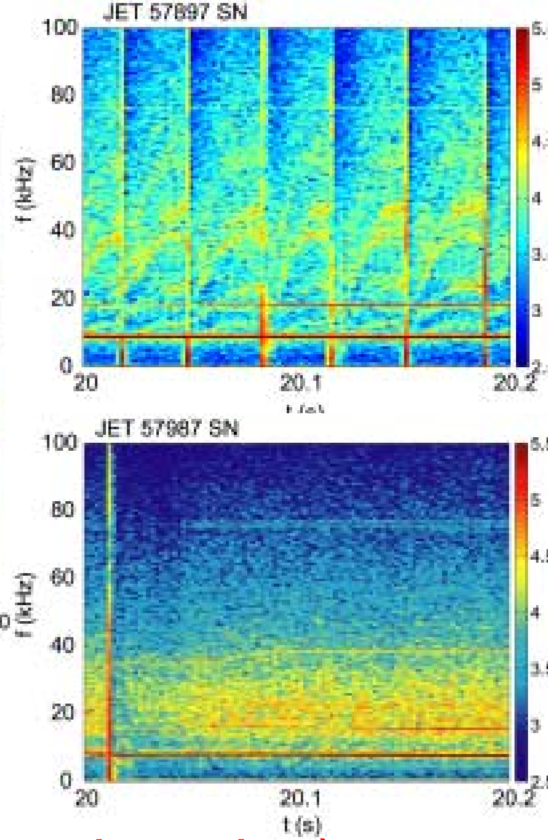

Increased Inter-ELM transport (+ washboard modes)

Regimes with high P_{ped} + small/no ELMs (III)

QH (and EDA) no-ELM regimes are associated with coherent MHD modes at the edge which lead to enhanced transport

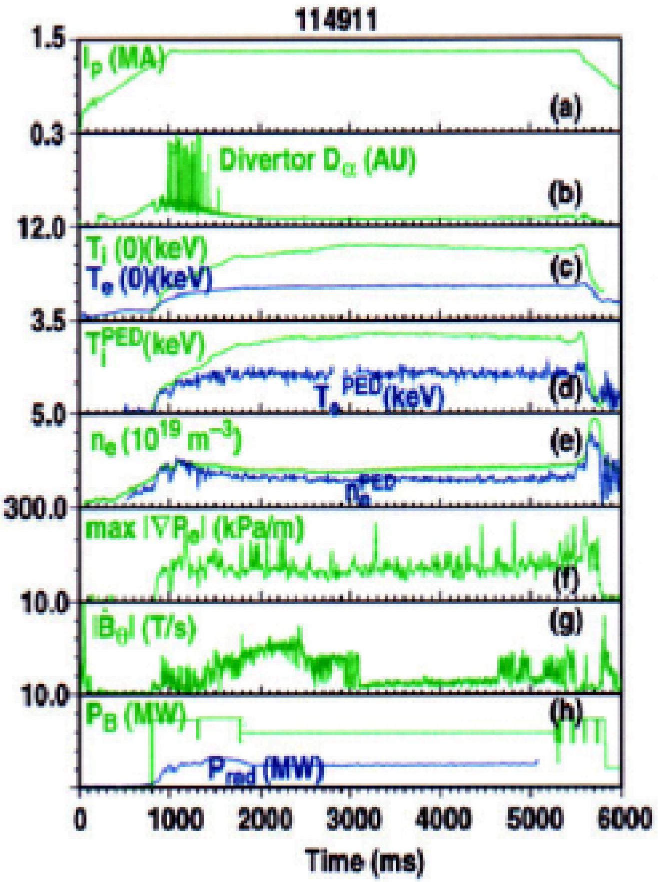

DIII-D Doyle PPCF’02, Burrell PPCF’03

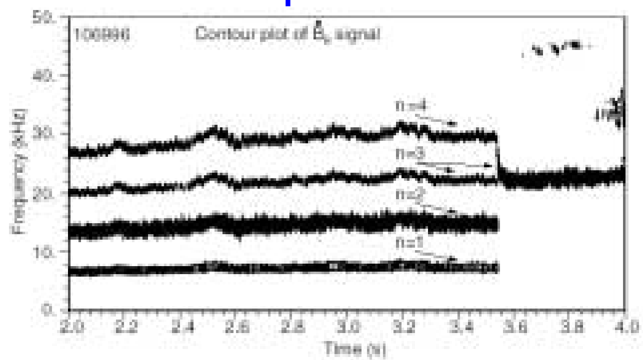

reproduced in ASDEX Upgrade

Suttrop PPCF’04

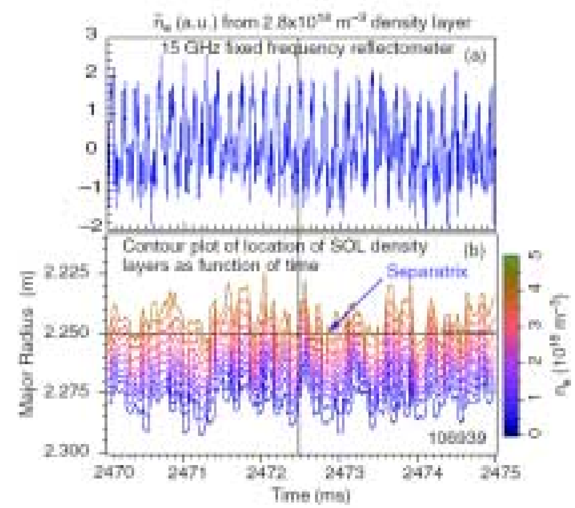

potentially interesting for next step devices but triggering of mode?

Regimes with high P_{ped} + small/no ELMs (IV)

JT-60 Type II ELM (= Grassy ELM) discharges are obtained at high δ, high β_p and high q_{95} (low ν^*_{ped})

JT-60U – Kamada PPCF'02

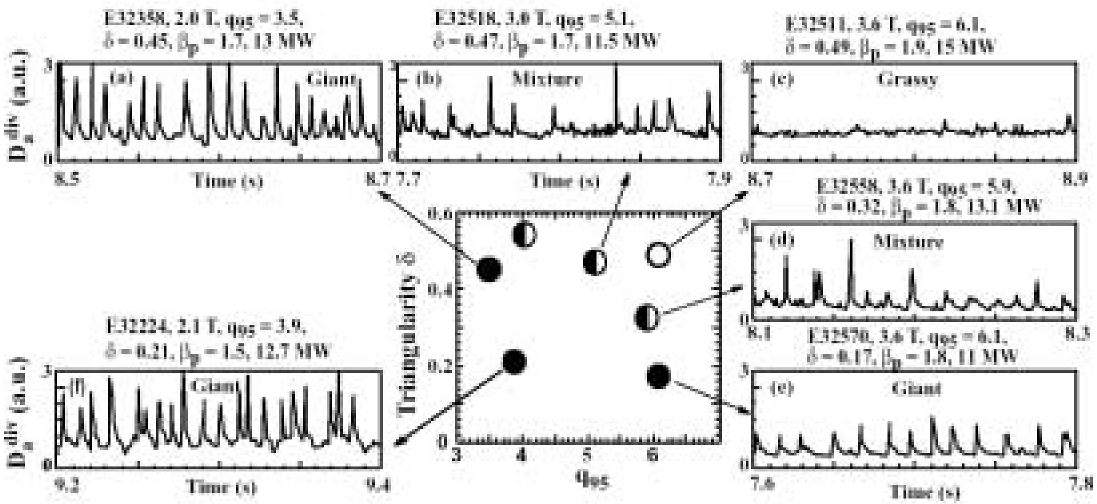

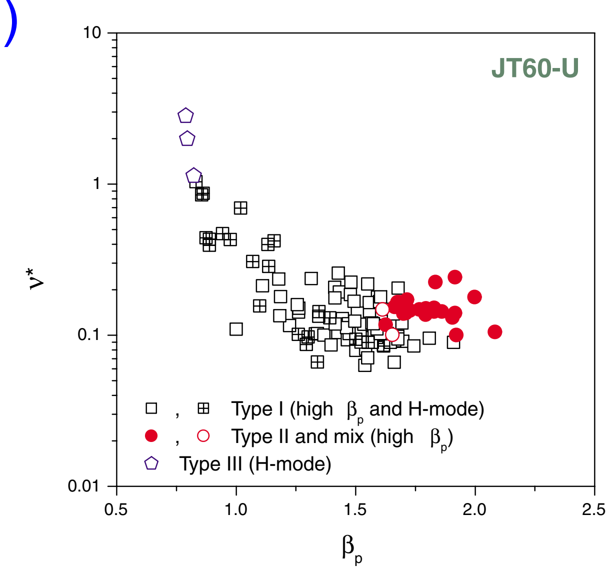

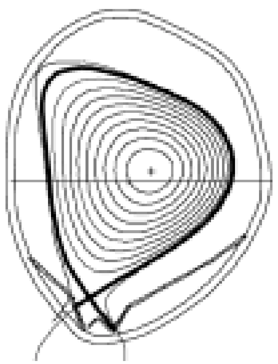

change of ELM Type because of edge stability change due to Shafranov-shift

reproduced at JET Saibene EPS'04

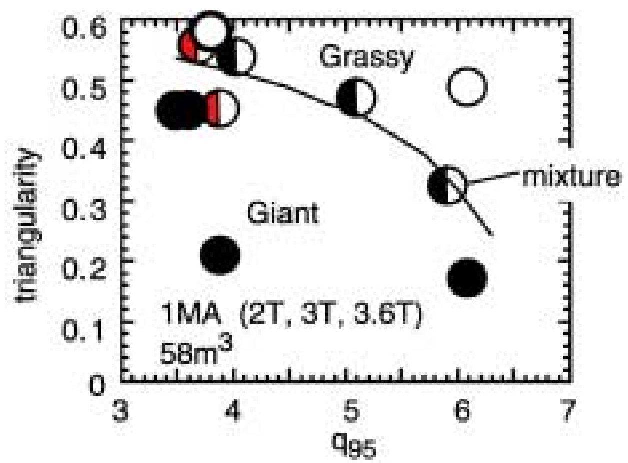

Regimes with high P_{ped} + small/no ELMs (V)

Type II ELMs in ASDEX Upgrade occur at high n_{ped} (ν^*_{ped})

ASDEX-Upgrade-Stober NF'02

● Type II ● Type III (0.35<δ<0.42, 0.8<I_p(MA)<1)

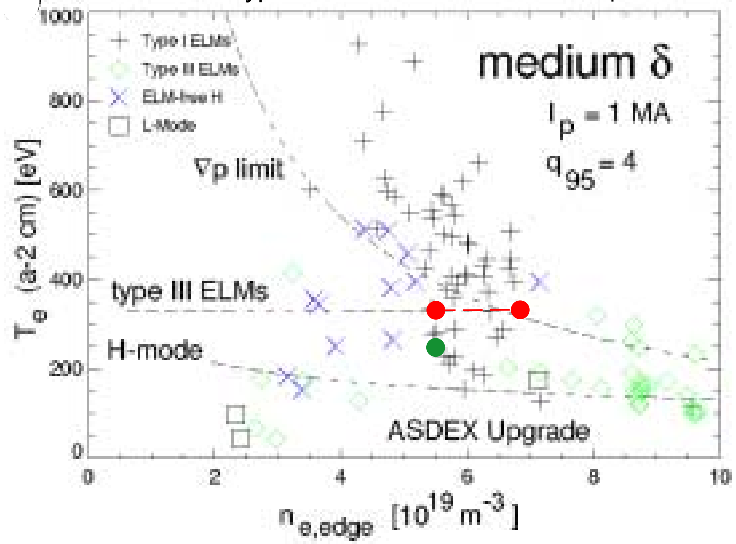

ASDEX-Upgrade-Sips NF'02

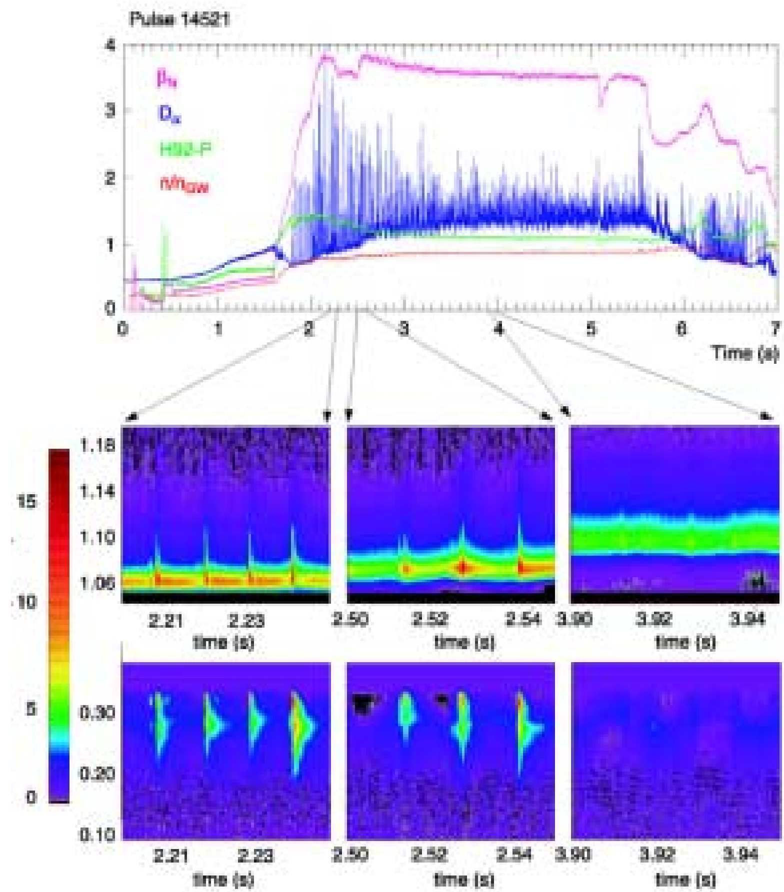

- ➢ $P_{ped}^{Type\ I} \sim P_{ped}^{Type\ II}$ transition
- ➢ Regime is robust to P_{in} ↑ (if fuelling adjusted)
- ➢ attributed to change in edge P-B stability
- ➢ compatible with high β (β_N , ν^*_{ped} interplay?)

Regimes with high P_{ped} + small/no ELMs (VI)

Type II in ASDEX-U : Quasi DN configuration

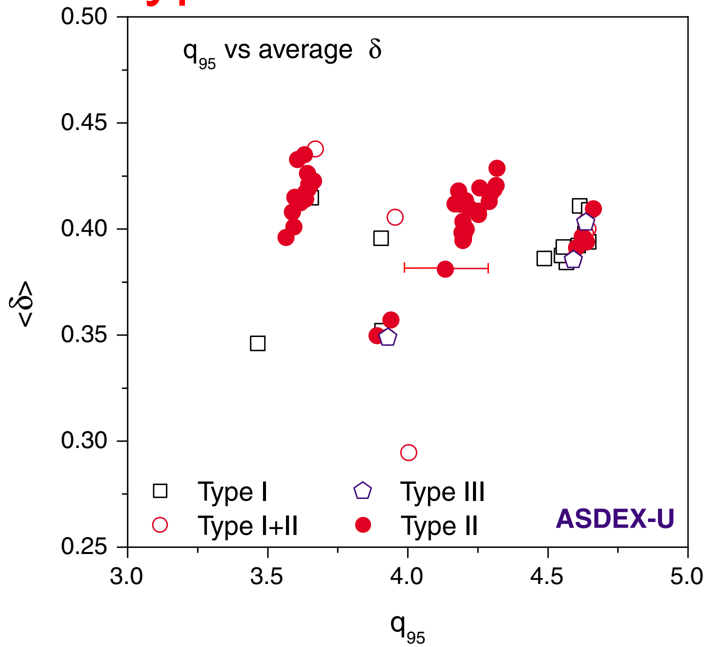

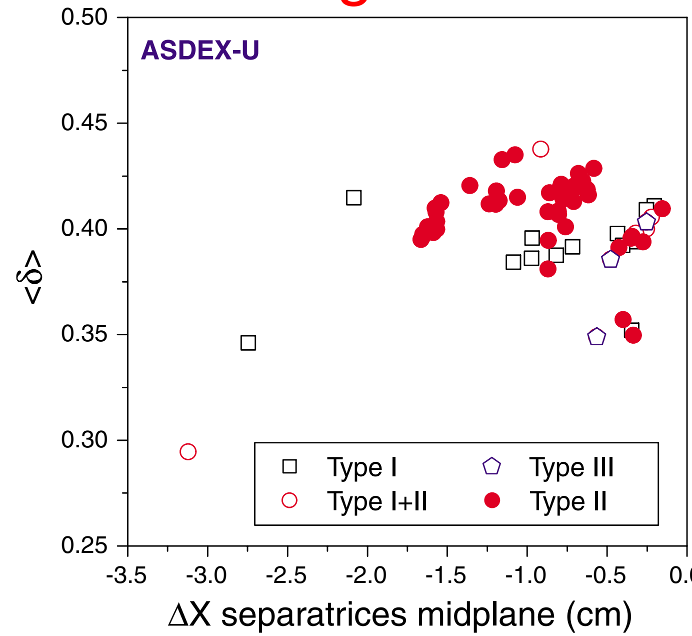

- Type II require medium/high δ and n_e
- Proximity to DN configuration is essential (no type II for ΔX_{mp}>2cm)

+ Trade-off δ/q_{95} ?

- High β not required, but compatible with the regime! (β_N~3 obtained)

not reproduced at JET Saibene EPS'03

Regimes with high P_{ped} + small/no ELMs (VII)

ASDEX Upgrade-Saarelma NF'03

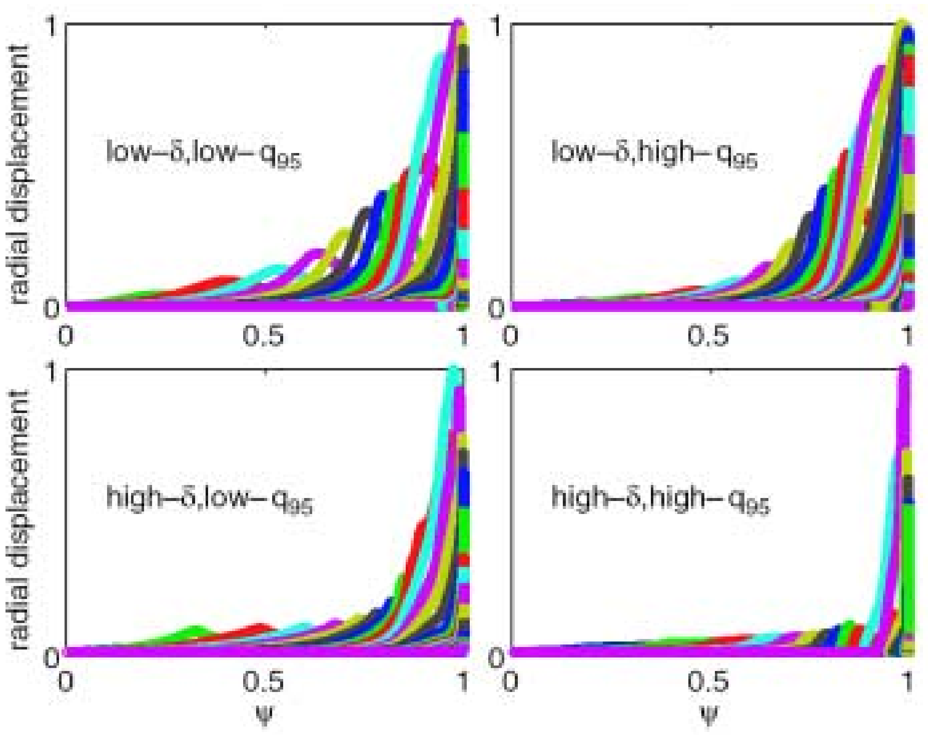

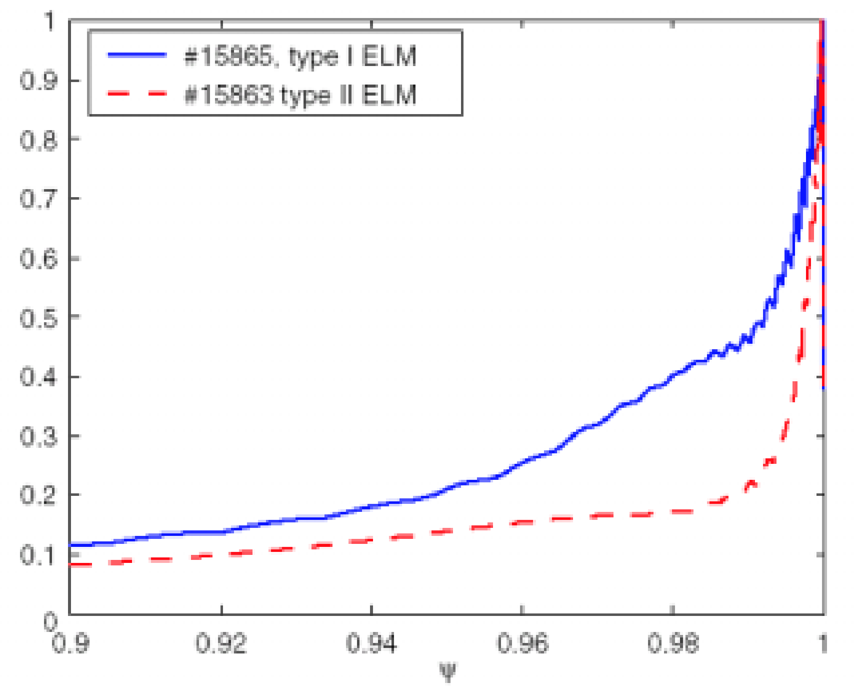

proximity to DN (#15863) leads to a sharp decrease of eigenmode width

Physics of ELM instability (V)

Growth of linear mode coincident con ELM crash (low n_e)

DIII-D-Snyder APS'01

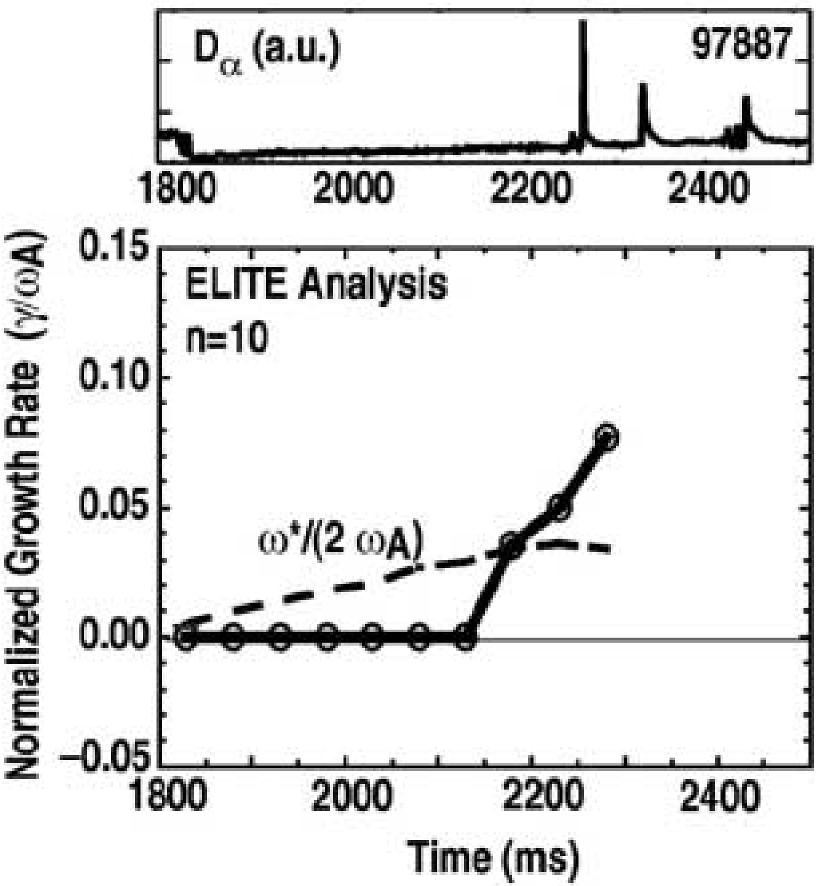

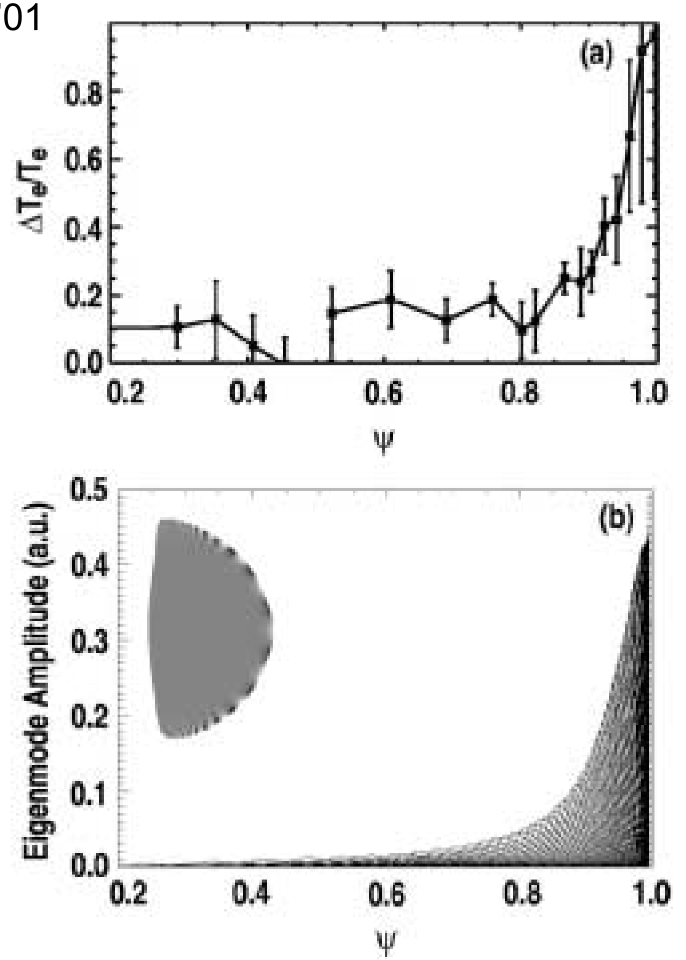

Similar results for giant ELMs in JET - Huysmans

Physics of ELM instability (IX)

Analyses of particle impact patterns on JET main wall are consistent with ballooning mode n = 12, m = 50

Between ELMs

JET-Ghendrih JNM'03

At ELMs

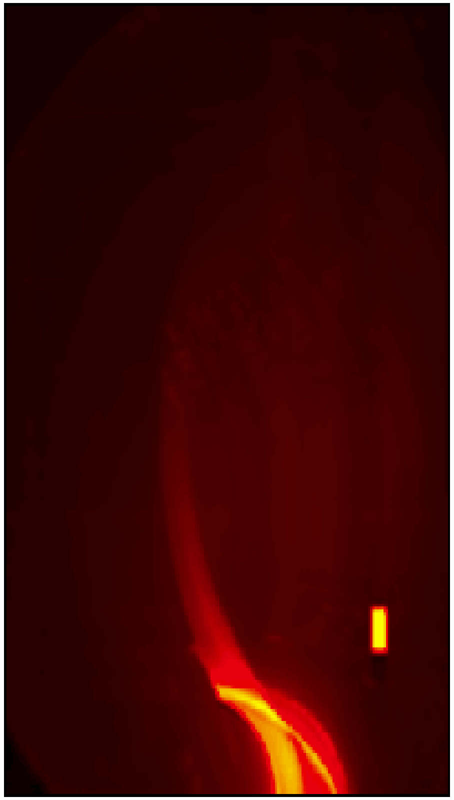

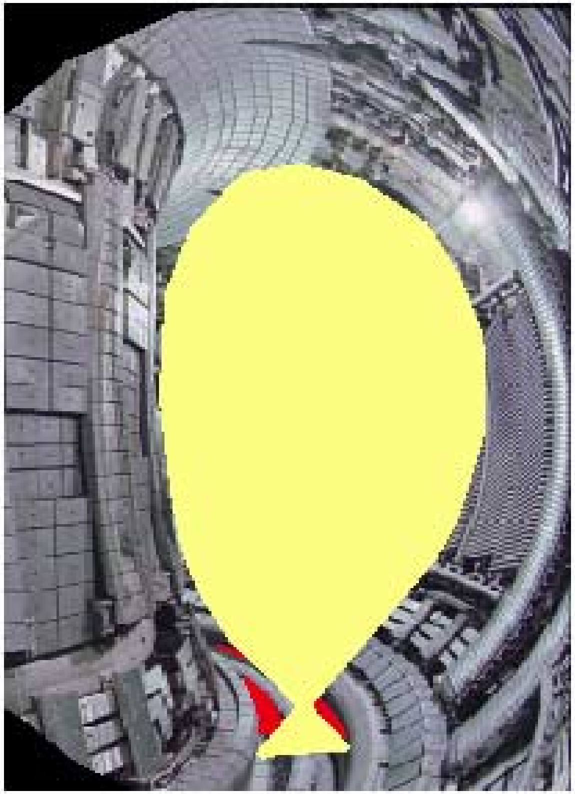

Physics of ELM instability (XIII)

JT60U-Oyama PPCF'01

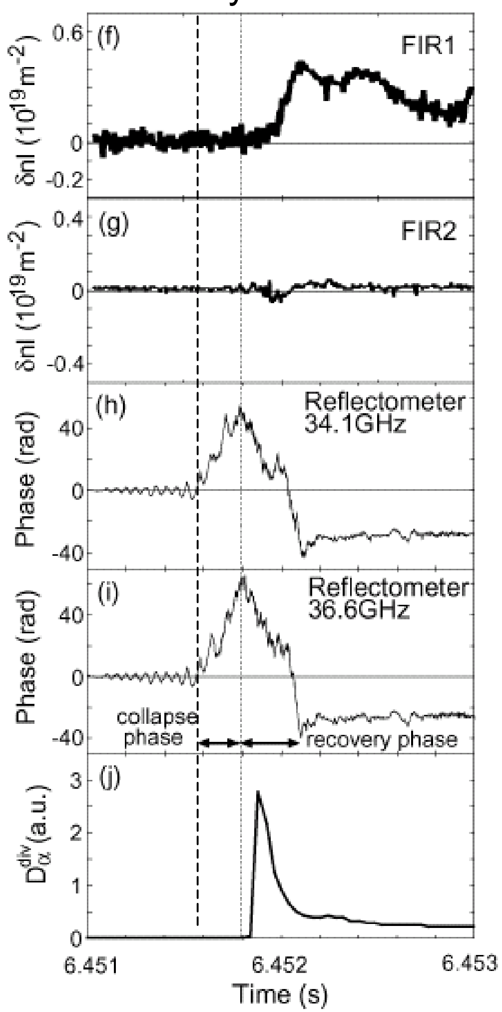

$\tau_{ELM} \sim 200\ \mu s$

DIII-D-Fenstermacher PPCF'03

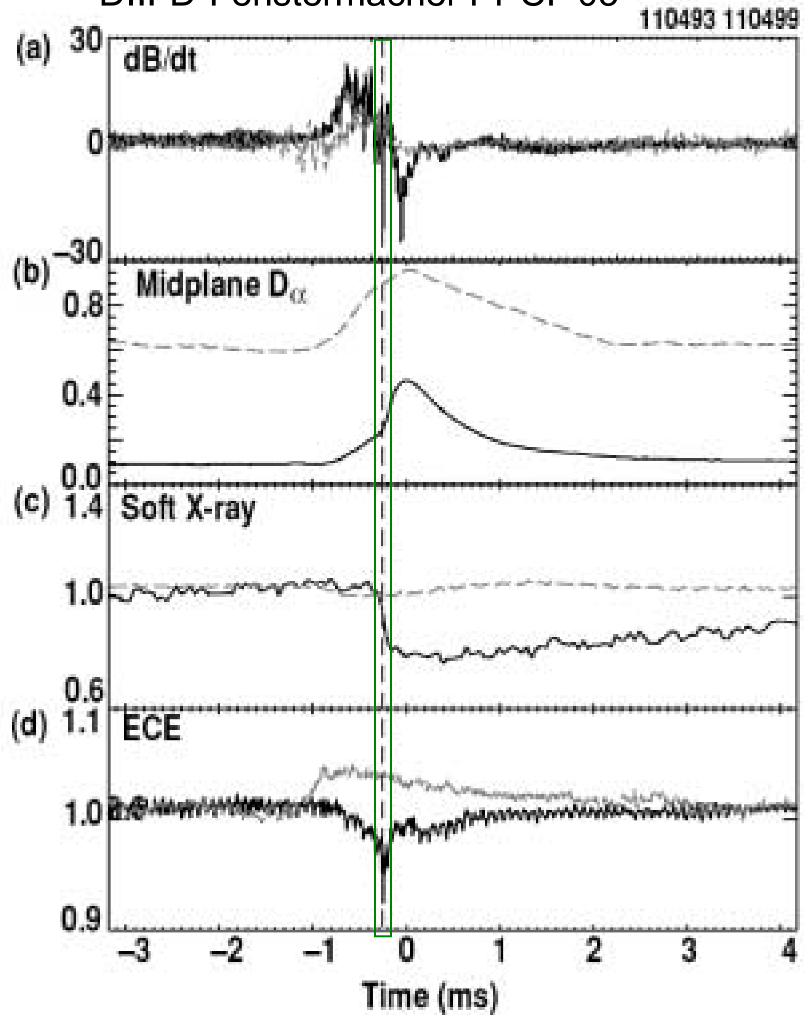

$\tau_{ELM} \sim 200\ \mu s$

Main plasma ELM energy/particle losses (XI)

ELM perturbation into edge plasma much broader than P-B modes

DIII-D-Leonard APS'02

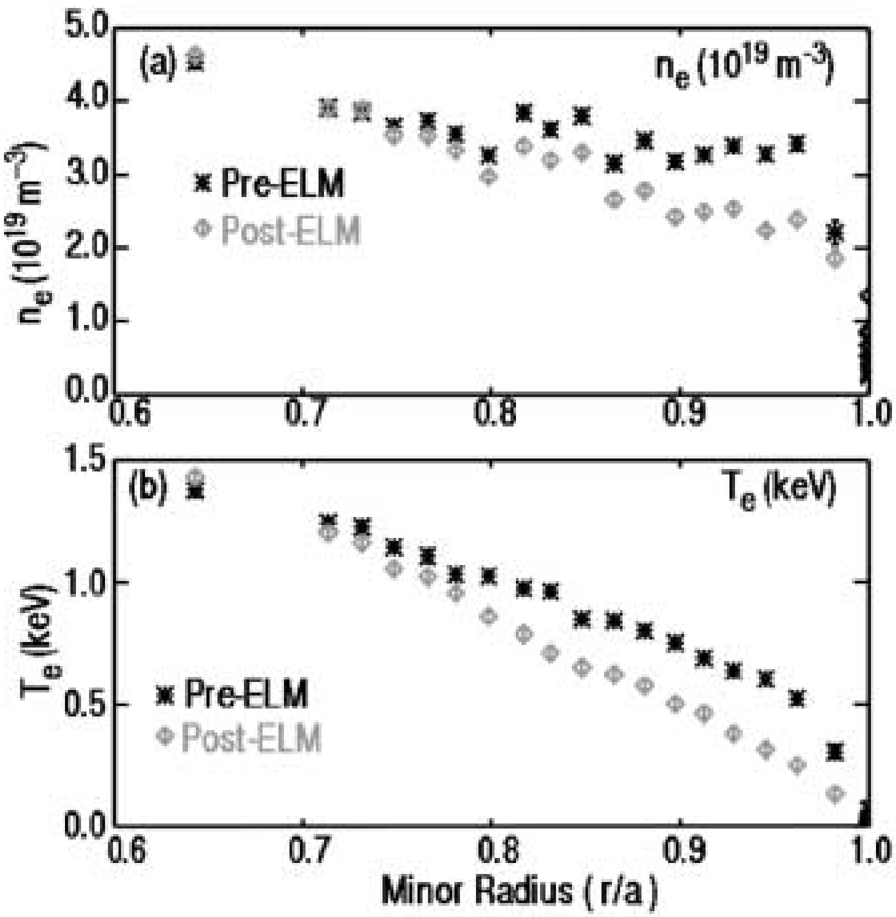

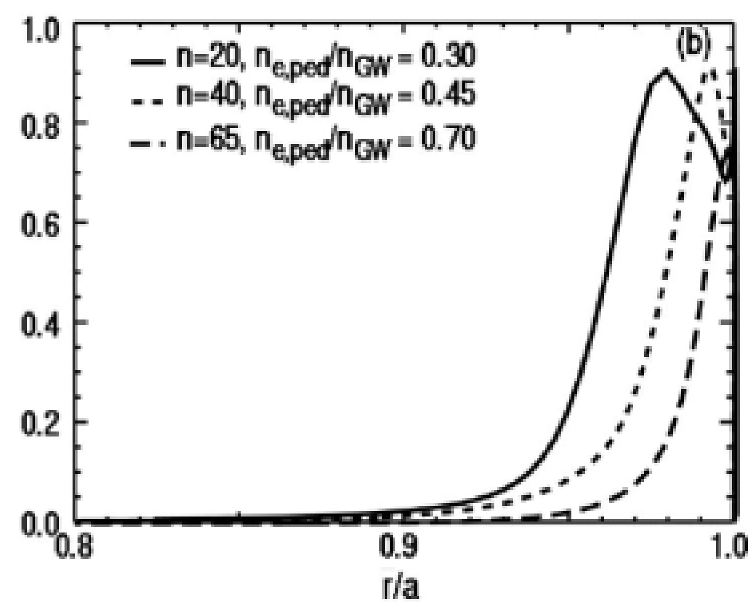

Relation between ΔW_{ELM} and P-B modes ?

ELM energy/particle fluxes to PFCs (XVII)

- $\Delta W_{ELM}/W_{ped}$ decreases with $\tau_{||}$

ITPA-Loarte PPCF'03

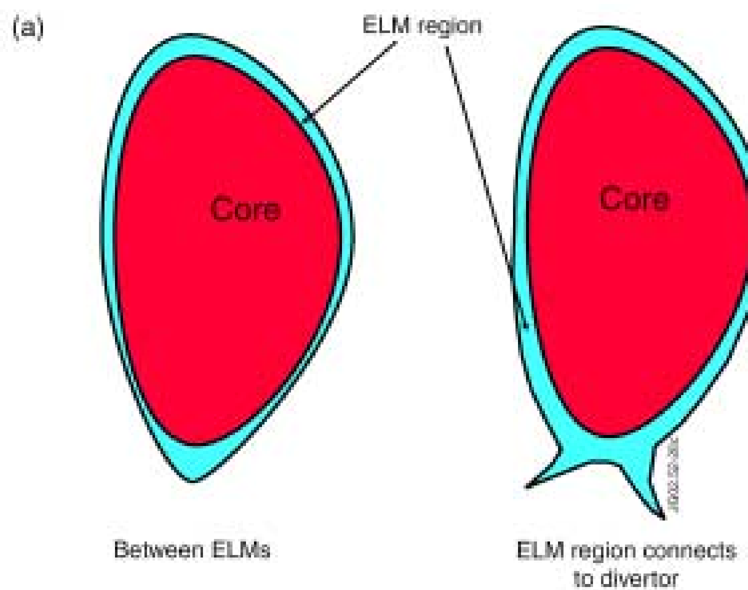

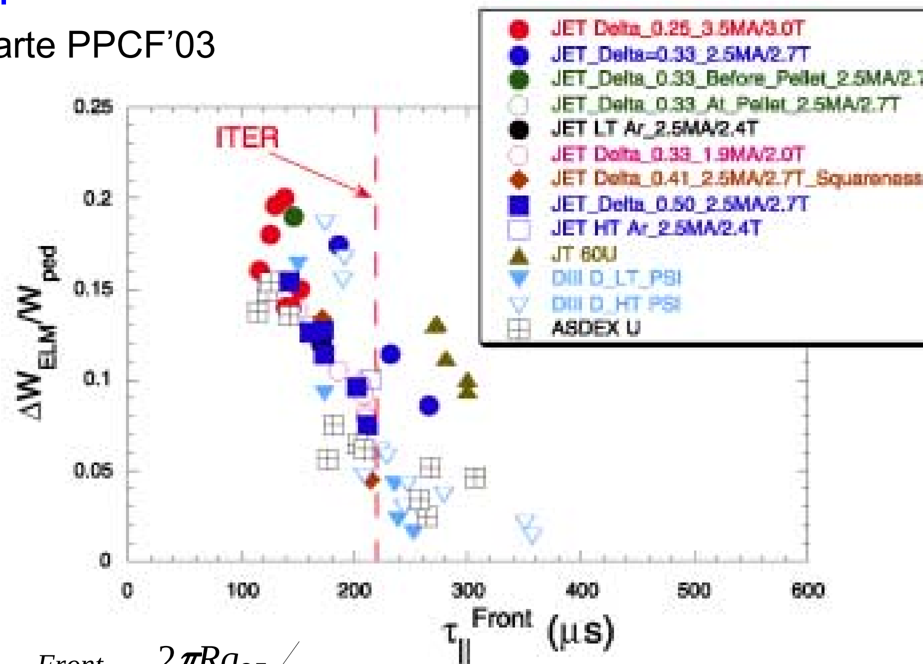

$$\tau_{||}^{Front} = \frac{2\pi R q_{95}}{c_{s,ped}}$$

Physics Model :

1) Pedestal connects to divertor for τ_{ELM}^{MHD}

2) Energy flow restricted by sheath ($\tau_{||}$) → $\Delta W_{ELM}/W_{ped} \sim (1-\exp(-\tau^{ELMMHD}/\tau_{||}))$

ELM energy/particle fluxes to PFCs (XVII)

In/Out ELM energy balance changes at ELM and with divertor/main plasma conditions

Inter-ELM

$n_{div}^{in} > n_{div}^{out}$

$T_{div}^{in} < T_{div}^{out}$

$q_{div}^{in} < q_{div}^{out}$

$\Gamma_{div}^{in} > \Gamma_{div}^{out}$

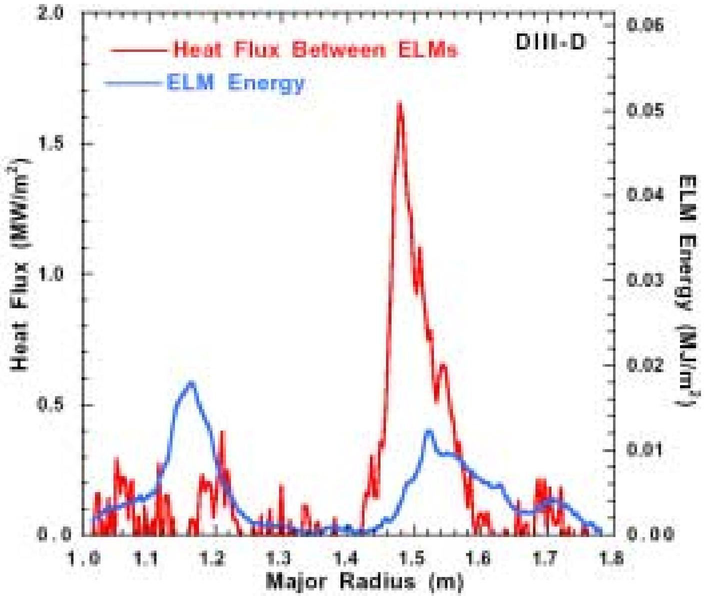

DIII-D-Leonard PSI'02, Fenstermacher PPCF'03

Energy fluxes at ELMs

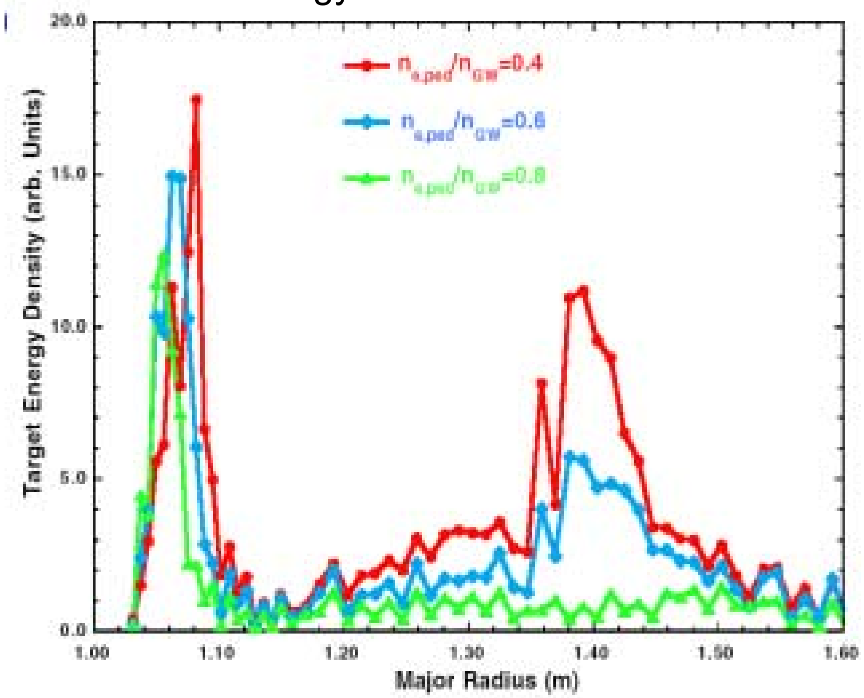

consistent with $N_{div}^{in} > N_{div}^{out}$ + sheath or changes in with energy flow with n_e

ELM energy/particle fluxes to PFCs (XVIII)

E_{ELM} > 1MJ/m² can lead to $\Gamma_C > 10^{23}$ C-atom/ELM

Poor C Retention in Divertor @ ELM
(Plasma flows out of the Divertor)

$N^{D-T}_{ITER} \sim 10^{23}$ particles

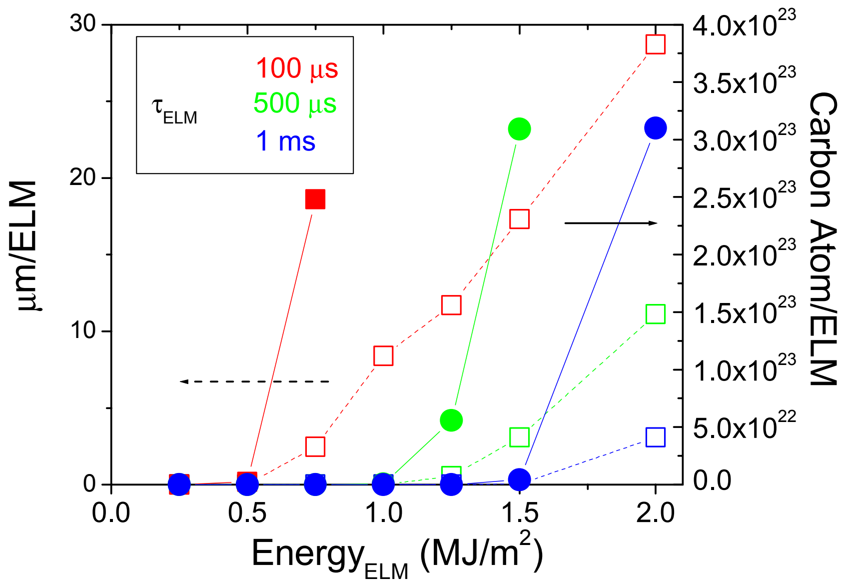

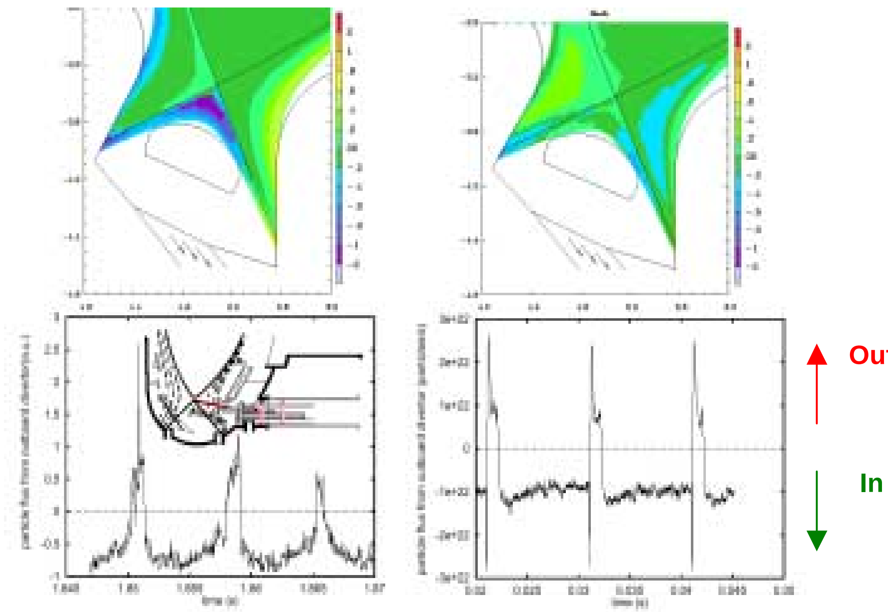

Large Proportion of Γ_C may get into Core Plasma → increase of Z_{eff} at edge

ELM energy/particle fluxes to PFCs (XIX)

Energy loss by Carbon Transient Radiation → Probably small

ADAS – M. O'Mullane

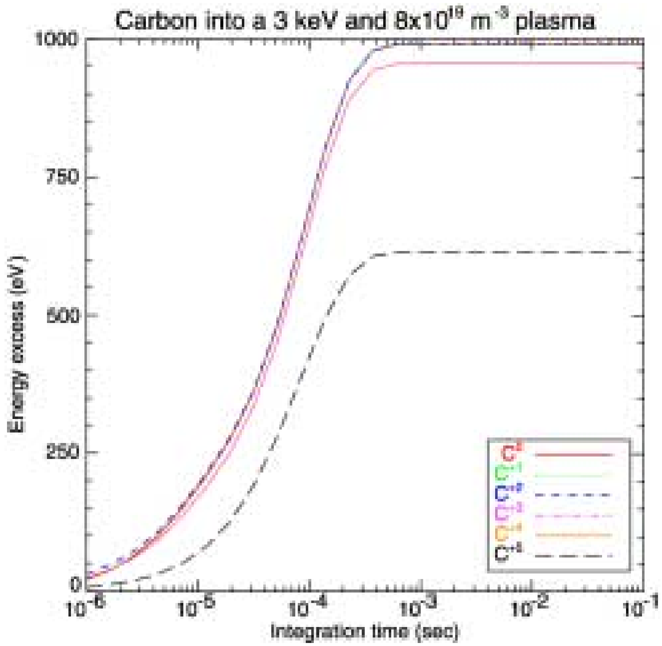

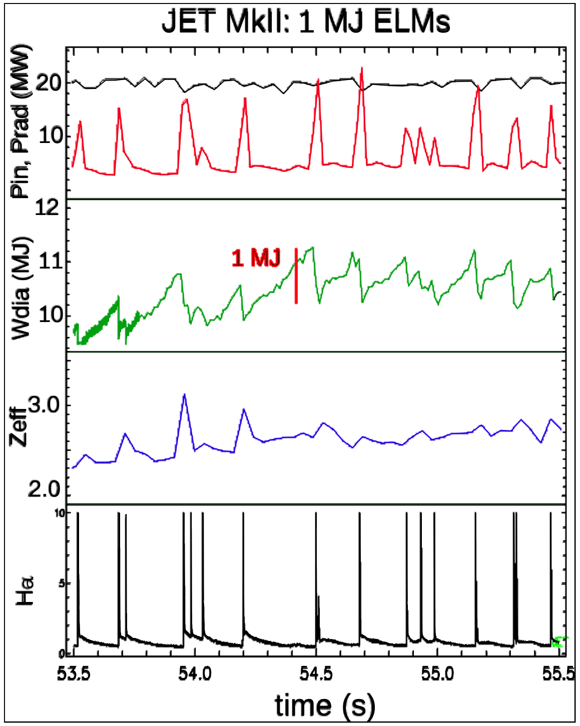

E_{ELM}^{RAD} ~ 0.5 MJ
(C. Ingesson)

W_p ~ 11 MJ
ΔW_{ELM} ~ 1 MJ

n_{ped} ~ 8 10^{19} m^{-3}
T_{ped} ~ 3 – 5 keV

- $E_{transient}^{C\text{-}radiation}$ (3 keV, 8 10^{19} m^{-3}) ~ 1 keV/atom

↓

E_{ELM}^{RAD} ~ 16 MJ << W_{plasma} (~ 350 MJ)

- JET Results agree qualitatively : Modelling/Extrapolation to ITER necessary